EXPANDING AND REFINING A MODEL FOR DENITRIFICATION IN *RHODOBACTER SPHAEROIDES* 2.4.3

A Dissertation

Presented to the Faculty of the Graduate School

of Cornell University

in Partial Fulfillment of the Requirements for the Degree of

Doctor in Philosophy

by

Angela Kay Hartsock

August 2009

EXPANDING AND REFINING A MODEL FOR DENITRIFICATION IN *RHODOBACTER SPHAEROIDES* 2.4.3

Angela Kay Hartsock, Ph.D.

Cornell University 2009

Rhodobacter sphaeroides strain 2.4.3 is a photoheterotroph of the α-proteobacteria. It is metabolically versatile and in addition to anoxygenic photosynthesis and aerobic respiration, it is capable of denitrification. The denitrification system of strain 2.4.3 has been studied in detail by our lab. Here, we expand on our model for denitrification. The genome sequence of strain 2.4.3 revealed the presence of two periplasmic nitrate reductases. Using expression and mutant studies, we show that one of these enzymes is expressed aerobically and is involved in aerobic redox homeostasis. The second enzyme is expressed under low oxygen conditions and is the nitrate reductase involved in denitrification. We provide evidence for oxygen sensitivity of the denitrification regulator NnrR in a mutant lacking the high oxygen affinity cytochrome oxidase. NnrR is a member of the FNR/CFP family of transcriptional regulators that has been shown to regulate denitrification genes in response to the denitrification intermediate nitric oxide. Using the predicted DNA binding motif of NnrR we analyzed the genome for genes potentially under NnrR control. We identified five new genes and demonstrate that expression is dependent on NnrR. One of these genes encodes pseudoazurin, which is shown to be an electron donor to nitrite reductase along with a cytochrome. Two other genes identified encode NorEF, putative additional subunits of the nitric oxide reductase enzyme complex. Inactivation of these genes decreases denitrification activity and cells show greater sensitivity to nitric oxide. We also investigated denitrification-independent nitric oxide signaling and metabolism. The Sphaeroides

Heme Protein (SHP) has been shown to have nitric oxide dioxygenase activity. Here, we show that *shp* is induced under stationary phase photo-growth and that the *shp* mutant is not impaired in growth under these conditions. Finally, we attempt to characterize a nitric oxide binding protein that may mediate signaling through a diguanylate cyclase. This may link nitric oxide into the cellular cyclic-diguanosine monophosphate signaling pathway.

BIOGRAPHICAL SKETCH

Angela Kay Hartsock was born on February 16, 1983 to Howard John and Candy Sue Hartsock in Coshocton, Ohio USA. She graduated from River View High School in Warsaw, OH in 2001. She pursued her undergraduate studies at Kenyon College of Gambier, OH, The Ohio State University of Columbus, OH, and Sydney University of Australia. In 2004 she received a Bachelors of Science degree in Microbiology from The Ohio State University.

After graduation, Angela was employed as a laboratory technician with Dr. James Shapleigh at Cornell University in Ithaca, NY. After a year she joined the lab as a graduate student, pursuing her thesis research.

This thesis is dedicated to my dad, Howard John Hartsock.

With all my love and thanks.

ACKNOWLEDGEMENTS

I would like to thank my advisor Dr. James Shapleigh. I also wish to thank the undergraduates who have worked alongside me: Anne Hammond, Tony Galinato, Mike Beckham, Colm Kellher, and Gregory Mazo. Thanks also go to my minor advisors Dr. Brian Crane and Dr. Michael Stanhope.

Special thanks go to the Department of Microbiology Undergraduate Teaching Staff. This includes Patti Butler, Doreen Dineen, Bill Ghiorse, Sue Merkel, Ereign Seacord, Barb Eaglesham, and Carole Rehkugler.

Most importantly, I would like to thank my family back home in Ohio- especially my dad and mom, my sisters, and Nick. Thank you for your love and support.

TABLE OF CONTENTS

LIST OF FIGURES

LIST OF TABLES

Chapter One

Introduction

Overview

Denitrification is a critical step in the global nitrogen cycle responsible for returning nitrogen to the atmosphere (47). In most organisms it is an alternative mode of respiration under oxygen limitation and the presence of nitrate (47). Denitrification is widespread within the bacterial world and occurs by the successive reduction of nitrate to dinitrogen gas, with each reduction step catalyzed by a specific enzyme (47). We require a better understanding of the regulatory controls and physiology of denitrification to accurately model and predict environmental parameters of the nitrogen cycle (13, 27, 37). This necessitates the development of model denitrifying organisms. Here we attempt to further establish the photoheterotroph *Rhodobacter sphaeroides* 2.4.3 as a model denitrifier. Research is undertaken to better understand the role of nitrate respiration as distinct from denitrification. Also, the regulation of denitrifying genes is examined in the context of oxygen modulating the activity of the transcriptional regulator, NnrR. In addition, the NnrR-controlled denitrification regulon is expanded to include previously unidentified members. Finally, denitrification-independent mechanisms of mitigating nitric oxide toxicity are explored.

Denitrification

The ability to respire, coupling oxidation of one substrate to reduction of another, is an important means of energy conservation in all domains of life (7). Typically, we think of respiration with oxygen as the terminal electron acceptor. However, the bacterial kingdom has shown us the diversity of options for anaerobic

respiration (26). Denitrification is the ability to respire in the absence of oxygen using nitrogen oxides (47). Denitrification proceeds by the successive reduction of nitrate to nitrogen gas (Fig. 1.1). Each reduction step is catalyzed by a dedicated enzyme.

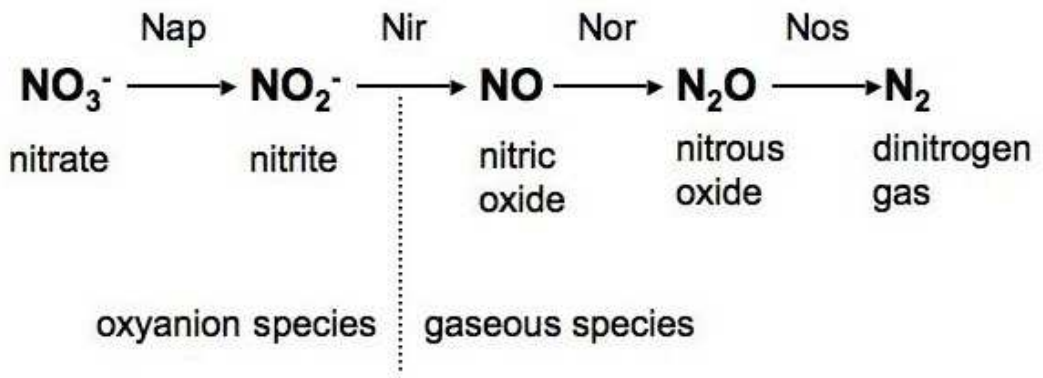

Figure 1.1: The denitrification pathway including intermediates and enzymes responsible for reduction steps. Nap is periplasmic nitrate reductase, Nir is nitrite reductase, Nor is nitric oxide reductase and Nos is nitrous oxide reductase.

Nitrate reductase reduces nitrate to nitrite. Nitrite reductase reduces nitrite to nitric oxide (NO). Nitric oxide reductase reduces NO to nitrous oxide (N_2O). And finally, nitrous oxide reductase reduces N_2O to dinitrogen gas (N_2). Denitrification enzyme activity is confined to the periplasm and the inner membrane (47). However, intermediates are freely diffusible. Importantly, denitrification is coupled to generation of a proton motive force via electron flow through the *bc*$_1$-dependent branch of the electron transport chain. This allows for ATP generation via the F_1-F_0-ATP synthase.

Denitrification is found almost exclusively in bacteria. However, there are denitrifying Archaea and Fungi (47). There is also recent evidence of denitrification in the unicellular eukaryote, *Globobulimina pseudospinescens*, a benthic foraminifer (34).

The nitrogen cycle: Denitrification is an integral part of the global nitrogen cycle (Fig. 1.2) (13, 37, 47). The global nitrogen cycle is comprised of three major nitrogen

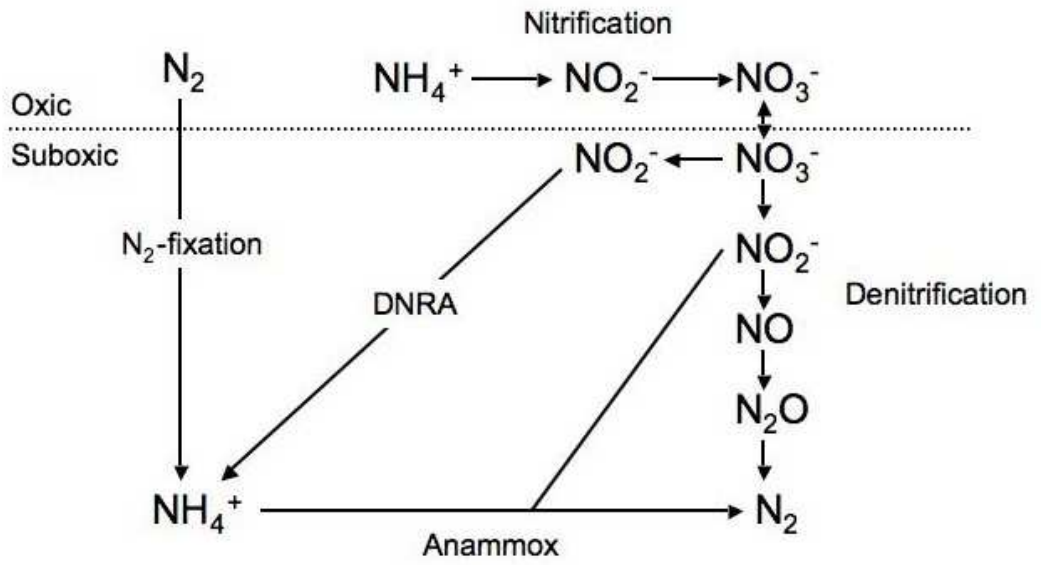

Figure 1.2: The nitrogen cycle. Nitrogen species are defined in the text. DNRA is dissimilatory nitrate reduction to ammonia.

transformations. Nitrogen fixation consumes atmospheric N_2, transforming it into ammonia to be incorporated into biomass (13, 46). This is the critical step that introduces nitrogen into the biosphere. Within the biosphere the fixed nitrogen, in the form of ammonia, is in flux with oxyanion forms of nitrogen, like nitrate and nitrite. The processes responsible for this flux are nitrification, which oxidizes ammonia to nitrate, and dissimilatory nitrate reduction, which can reduce nitrate back to ammonia (8, 13, 32). The final critical step in the nitrogen cycle is the removal of nitrogen from the biosphere by denitrification (13, 47). This completes the cycle, restoring N_2 to the atmosphere. Importantly, there is another process known as anammox that involves the anaerobic oxidation of ammonium (8, 13). This converts nitrite and ammonium to N_2, the same product as denitrification. Within the nitrogen cycle, nitrogen fixation and denitrification are critical steps. Fixation converts nitrogen from a gaseous to an aqueous phase, making it available to the biosphere. In contrast, denitrification

converts nitrogen from an aqueous form to a gaseous form, where it is no longer biologically available, except for nitrogen fixers.

Nitrogen is an essential building block of all known living organisms. On a global scale, plants and microorganisms carry out the important step of assimilating nitrogen that is then taken up by higher organisms (13). However, in most environments nitrogen is limiting, directly impacting primary productivity. During the last century, the application of fertilizers has dramatically increased bioavailable nitrogen in many soil and aquatic ecosystems (13). On one hand, this has allowed for adequate food production to support mankind. On the other hand, overloading of nitrogen has diverse and serious consequences for ecosystem health. A major consequence is an increase in primary productivity resulting in eutrophication of both terrestrial and aquatic ecosystems.

Denitrification is the major pathway affecting removal of bioavailable nitrogen and replenishment of atmospheric N_2 (13). However, denitrification can also produce significant quantities of N_2O, which is considered a greenhouse gas and contributes to ozone depletion (49). Denitrification in freshwater accounts for half of global denitrification, with terrestrial and coastal regions accounting for the remainder (13). The open ocean has a comparatively negligible contribution. Importantly, much of the nitrate denitrified in freshwater originates from land due to agricultural runoff. Attempts to calculate denitrification and nitrogen fixation capacities in both terrestrial and aquatic systems show imbalances in both (13). This suggests a need to understand more about the regulation and controls on denitrification, and furthermore nitrate respiration, in the environment.

Denitrification enzymes: The first step of denitrification is nitrate reduction, a reaction not unique to denitrification. There are three types of nitrate reductase recognized: the assimilatory group, Nas, and two dissimilatory groups, Nar and Nap

(33). The two dissimilatory types, Nar and Nap, are involved in denitrification. The major distinction between the Nar and Nap types is localization within the cell. The Nar type is localized to the inner membrane and is coupled to generation of a proton motive force (pmf) (33). In contrast the Nap type is localized to the periplasm and is not coupled to generation of a pmf (33). Our model organism has the Nap type enzyme, and so this will be the focus of this discussion.

The Nap enzyme system consists of two main subunits, NapAB, and a number of additional proteins (Table 1.1). NapA is the large subunit and contains a 4Fe-4S cluster and a bis-molybdopterin guanine dinucleotide cofactor (33). This is the active site of the enzyme responsible for nitrate reduction to nitrite. NapB is the small subunit diheme cytochrome *c* predicted to transfer electrons to the active site (33). NapC is a tetraheme *c*-type cytochrome (33). It is membrane-anchored and allows transfer of electrons from quinol to NapB. NapE and NapD are believed to be accessory proteins necessary for folding or activity (33). Nap gene clusters in the proteobacteria can be grouped into two types, those that contain *napEDABC* and those that contain *napGH* in addition to the same core of *napEDABC*. *napEDABC* is commonly found in α-proteobacteria and denitrifiers, while *napEDABCGH* is commonly found in γ-proteobacteria, some of which denitrify. Within organisms these operons can also be supplemented with additional genes. Interestingly, *R. sphaeroides* 2.4.3 has both types of Nap.

The second step of denitrification is nitrite reduction. This is an important step as it generates the first gaseous and highly toxic intermediate nitric oxide (NO) (47). Nitrite reductase (Nir) comes in two types, the copper-containing Nir and the cytochrome-containing cd_1-Nir (47). These enzymes are entirely different in terms of

Table 1.1: Enzymes discussed in the text including denitrification and NO metabolism.

Enzyme	Location	Function
periplasmic nitrate reductase (Nap)		
NapA	periplasmic	Fe-S molybdoprotein, catalytic subunit
NapB	periplasmic	diheme *c*-type cytochrome, electron transfer to NapA
NapC	membrane-anchored	tetraheme *c*-type cytochrome, electron transfer from quinol to NapB
copper-containing nitrite reductase (Nir)	periplasmic	Cu(I) center for electron transfer, Cu(II) center for active site
nitric oxide reductase (Nor)		
NorB	integral membrane	*b*-type heme and non-heme Fe binuclear active site
NorC	membrane-anchored	*c*-type heme, electron transfer to NorB
Sphaeroides Heme Protein (SHP)	periplasmic	*c*-type cytochrome with nitric oxide dioxygenase activity
diheme cytochrome *c* (DHC)	periplasmic	electron transfer to SHP
cytochrome *b*	membrane-bound	electron transfer from quinol to DHC
heme-nitric oxide and oxygen binding (H-NOX) protein	soluble intracellular	heme protein binds diatomic ligands

structure and prosthetic metal. The cd_1-Nir is prevalent in the pseudomonads while the Cu-Nir is common in a greater variety of physiological groups. Interestingly, the two types of Nir are exclusive in that each species will harbor only one type or the other. This exclusivity may be in part due to the special heme biosynthesis required for cd_1-Nir and the specific electron donor interactions required by Cu-Nir (47). Both types of Nir are periplasmic enzymes that catalyze the reduction of nitrite to NO (47). Within the Cu-Nir type, there are sub-families, blue and green, based on spectral characteristics of the Cu(II) center (47). *Rhodobacter sphaeroides* strain 2.4.3 has a green Cu-Nir, and it will be the focus here (Table 1.1).

The Cu-Nir from *R. sphaeroides* is a homotrimer containing two copper atoms per monomer (15). One copper is a Cu(I) center, while the other is a Cu(II) center (15). Importantly, the Cu(I) center is contained within a monomer, while the Cu(II) site sits at the interface between monomers, requiring ligands from both. The Cu(I) sites contained within the monomers are capable of accepting electrons from donors. The Cu(II) sites at the monomer interfaces are the active sites and receive electrons from the Cu(I) site facilitating nitrite reduction. In the general reaction mechanism, the Cu(I) site interacts with an electron donor, accepting an electron and becoming reduced (44). Nitrite is bound by a histidine residue bordering the Cu(II) center. Two residues, aspartic acid and histidine, hydrogen bond to the nitrite and donate protons for the chemical reaction (44). This results in spontaneous electron relay from the Cu(I) site to the Cu(II) site, thereby reducing nitrite and generating nitric oxide (44). Electrons for nitrite reduction are typically donated by metalloproteins, such as azurin, pseudoazurin, and various cytochromes (28, 47). The green Cu-Nir enzymes commonly interact with pseudoazurins, while blue Cu-Nir enzymes commonly interact with azurins (28).

In the next step of denitrification, NO is reduced to nitrous oxide (N_2O) by nitric oxide reductase (Nor). There are two types of Nor, the quinol oxidizing qNor, and the cytochrome *c* oxidizing cNor (48). The types are distinguished based on electron donor specificity. The qNor type directly oxidizes the quinone pool, while the cNor type utilizes a cytochrome *c* electron carrier (NorC) (48). *R. sphaeroides* has a cNor which will be the focus here, and will be simply called Nor from here forward. Nor is composed of two core subunits (Table 1.1) (48). NorB is the large subunit and is an integral membrane protein. This subunit has homology to subunit I of the cytochrome oxidase (48). NorB contains the binuclear active site of the enzyme, consisting of a heme and a non-heme Fe (48). This is the site of NO binding and subsequent two electron reduction to N_2O. NorC is the second major subunit and is a membrane-anchored periplasmic monoheme *c*-type cytochrome (48). The heme is oriented into the periplasm allowing NorC to act as a conduit for electron transfer to the active site (48). In *Paracoccus denitrificans* there are additional proteins NorE and NorF that are predicted to be a subunit III and subunit IV, respectively (4). Interestingly, NorE has homology to subunit III of the cytochrome oxidase, consistent with Nor placement in this family of enzyme (48). A mutant of *norEF* significantly decreased both Nir and Nor activities, suggesting an important role for NorEF during denitrification (4).

The last step of denitrification is the reduction of N_2O to dinitrogen gas (N_2) by nitrous oxide reductase (Nos). Nos is a soluble periplasmic enzyme and a multicopper enzyme consisting of two identical subunits (49). Each monomer contains two multinuclear Cu centers called Cu_Z and Cu_A. The Cu_A center consists of two Cu atoms bridged by two cysteine ligands and is responsible for electron transfer to the active site (49). The Cu_Z center is a tetranuclear Cu-S site with the copper atoms coordinated by histidine residues (49). The Cu_Z center is the active site of the enzyme and binds

N_2O to catalyze reduction to N_2 (49). In our organism of interest, *R. sphaeroides*, the *nos* operon is non-functional. In this case, the final product of denitrification is N_2O.

The denitrification electron transport chain. All of the denitrification enzymes together result in a series of successive reduction steps requiring electron donors. The denitrification enzymes are located in the inner membrane and periplasm and so can receive electrons from either the quinone pool or soluble periplasmic electron carriers. Figure 1.3 shows the arrangement of the enzymes and the predicted electron donors. In

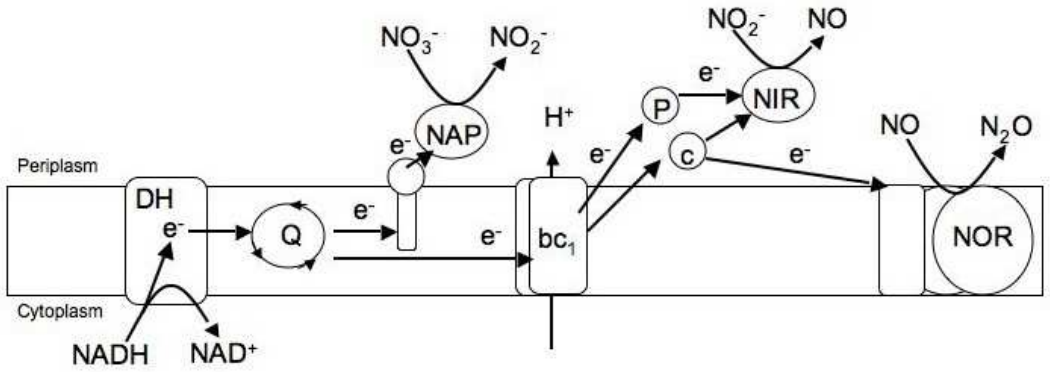

Figure 1.3: Electron flow during denitrification in *R. sphaeroides* 2.4.3. Abbreviations are as follows, DH (dehydrogenase), Q (quinone pool), bc_1 (the bc_1 complex), e^- (electron), P (pseudoazurin), c (cytochrome *c*).

short, electrons enter the chain upon the oxidation of NADH by the NADH dehydrogenase. Electrons then flow through the quinone pool. From here electrons can be transferred to Nap, allowing nitrate reduction, or they can be passed on to the bc_1-complex (33). From the bc_1-complex, electrons can be transferred to soluble electron carriers like azurins, pseudoazurins, and cytochromes. Cu-Nir has been shown to accept electrons from azurins, pseudoazurins and cytochrome *c* (47). Nor can also accept electrons from cytochrome *c* (47). The electron donors for Nos are less well defined but are likely cytochromes. Importantly, energy conservation occurs as

electrons flow through the bc_1-complex and protons are pumped across the membrane allowing ATP generation.

Regulation of Denitrification

Denitrification is found as an alternative pathway to aerobic respiration in bacteria. In the presence of oxygen, aerobic respiration is more energetically efficient. For this reason, denitrification genes are not expressed under aerobic conditions. The two major signals inducing denitrification gene expression are low oxygen and the presence of a respirable nitrogen oxide, like nitrate or nitrite (47). These two signals are integrated into a transcriptional response via a diverse set of transcriptional regulators that depend on the organism in question. An important feature of denitrification gene expression is the discontinuity between nitrate respiration, nitrite respiration to nitrous oxide, and finally nitrous oxide respiration to N_2. In fact, these processes are not obligatorily linked as evident by comparing the regulation of the reductases in question. In the simplest case, the genes encoding the reductases would be expressed coordinately by the same regulators responding to the same signals. However, it is common to see the genes for nitrate reductase controlled by one type of oxygen responsive regulator, while the genes for Nir are controlled by another type (47). In fact the only consistent overlap in regulation is at the level of Nir and Nor gene expression (47). This can be rationalized by the fact that Nir activity produces a toxic intermediate which would be efficiently respired by Nor protecting the cell from cytotoxicity. Even Nos gene expression is usually distinct from that of nitrate reductase and Nir/Nor (47).

The oxygen response. There are two oxygen-responsive regulators commonly associated with denitrification gene expression (47). One of these is an Fnr-type regulator. The second is a two-component system that is responsible for global gene

regulation in response to changes in oxygen level. In *R. sphaeroides* this two component system is known as PrrB/A, where PrrB is a sensor histidine kinase and PrrA is a response regulator (Fig. 1.4) (6). This two-component system is known by

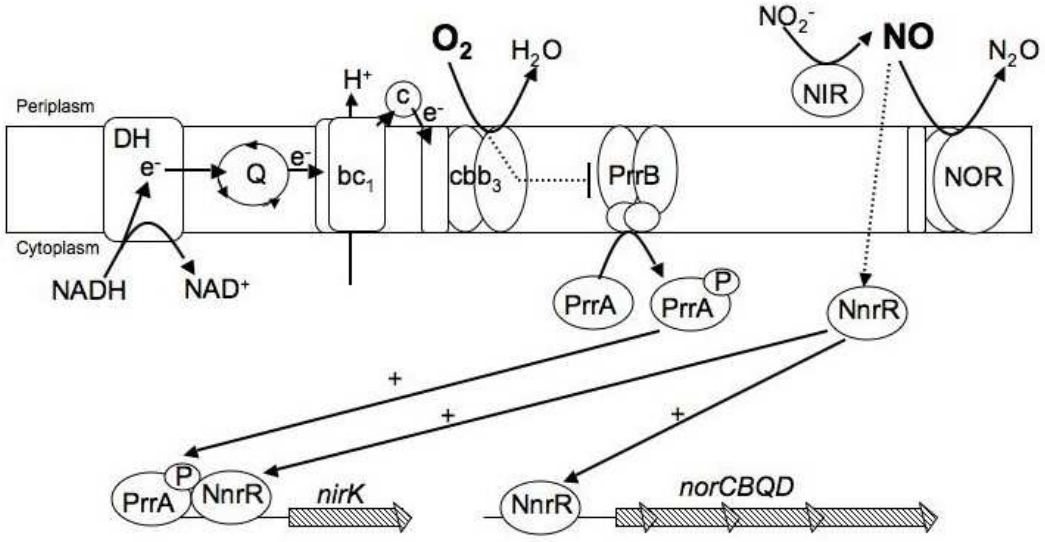

Figure 1.4: Model for denitrification gene regulation in *R. sphaeroides* 2.4.3. Regulation focuses on Nir and Nor. *nirK* encodes Nir, and *norCBQD* encodes Nor. The aerobic electron transport chain terminating in the cbb_3 cytochrome oxidase is shown on the left. The production and consumption of the NO signal by Nir and Nor, respectively, is shown on the right. Dotted lines indicate undefined signals, arrows with plus signs indicate positive regulation of the target promoter.

other names in related organisms, such as ActR/S in *Agrobacterium* and RegA/B in *Rhodobacter capsulatus* (1, 45). In *R. sphaeroides*, the signaling pathway for PrrB relies on electron flow through the aerobic electron transport chain, specifically flow through the cbb_3 cytochrome oxidase (29). Electron flow through cbb_3 results in an inhibitory signal, down-regulating the kinase activity of PrrB. As oxygen decreases and electron flow through cbb_3 decreases, the inhibitory signal is relieved, and the kinase activity of PrrB is up-regulated. This allows for phosphorylation of PrrA, which can then act as an activator of genes required under oxygen limitation (6). This includes turning on alternative metabolic programs, like denitrification, that can

supplement energy conservation. The PrrB/A system has been well studied in *R. sphaeroides* and regulates hundreds of genes involved in metabolic shifts relating to oxygen level. *nirK*, the gene encoding Nir, is regulated by PrrA, placing denitrification within the global reach of the PrrB/A system (22).

Nitrogen oxide responsive regulators. Denitrification gene expression is also regulated by the presence of respirable nitrogen oxides, like nitrate and nitrite. This is evident by the lack of *nir* and *nor* expression under low oxygen in the absence of denitrification substrate (20). This demonstrates that low oxygen alone is not sufficient to turn on denitrification, and that intermediates in denitrification play a role in expression. There are a number of denitrification specific regulators that have been identified with the central theme of NO as an activating signal (38). Experiments showed that Nir activity is required for expression of both *nir* and *nor*, implicating the product of Nir activity, NO, as the critical signal (20). In *R. sphaeroides* the NO-responsive regulator is known as NnrR (for nitrite and nitric oxide response regulator) (Fig. 1.4) (21). NnrR is a member of the Fnr-Crp family of transcriptional regulators (19). These regulators bind to target motifs via a C-terminal helix-turn-helix motif. Frequently there are small molecule signals that influence the activity of these regulators. Known signals include oxygen, carbon monoxide, and cAMP (19). There is also considerable circumstantial evidence implicating NO as the signal for a number of Fnr-Crp regulators, including NnrR (38). NnrR typically binds to target promoters at -40.5 to -43.5 from the transcript start (19).

Nitrate reduction independent of denitrification

While denitrification is generally considered to consist of the successive reduction of nitrate to N_2, in fact, these steps are not obligatorily linked. The steps of nitrate reduction and nitrous oxide reduction can be uncoupled from the rest of the

pathway (47). However, the steps of nitrite and nitric oxide reduction are coordinated. Here we will focus on the uncoupling of nitrate reduction from denitrification.

Dissimilatory nitrate reduction has been shown to serve two distinct roles in the cell. First, nitrate can be reduced to supplement energy conservation (47). This process is nitrate respiration and, either alone or in coordination with successive reduction steps, results in generation of a pmf (33). When nitrate respiration is coupled to successive reduction steps the entire process is called denitrification. In *Shewanella oneidensis*, a non-denitrifier, nitrate reduction is believed to be a dominant pathway of anaerobic respiration (9). In this organism, nitrate reduction is coupled to nitrite reduction to ammonium (9). Anaerobic growth of *E. coli*, a non-denitrifier, is also supported by nitrate reduction using both a membrane-bound and a periplasmic nitrate reductase (39). Under anaerobic conditions in the presence of nitrate and other potential terminal electron acceptors, nitrate reduction is the preferred mechanism for energy conservation (43).

The second role for nitrate reduction is as a mechanism for cellular redox homeostasis (10). During nutrient and growth rate flux, the NAD^+/NADH ratio can become imbalanced, limiting biosynthetic capabilities. In order to restore redox balance, the cell can "dump" electrons by sending them through an enzyme that is uncoupled from pmf generation. Some nitrate reductases, like the periplasmic type, are not coupled to generation of pmf and so can be used for overflow electrons (33). There is evidence for Nap playing a role in redox homeostasis in a number of organisms closely related to *R. sphaeroides* 2.4.3 (5, 10, 36). In *Paracoccus pantotrophus* there is an aerobically expressed nitrate reductase that is not utilized for denitrification (36). Instead, this enzyme is highly active during growth on reduced carbon sources when redox imbalances may occur. In *Rhodobacter sphaeroides* DSM158 and *Rhodobacter capsulatus* nitrate reduction stimulates growth under photosynthetic conditions (5, 10).

Importantly, these two bacteria are not denitrifiers so the reduction of nitrate is not being coupled to energy conservation via successive nitrogen oxide reduction steps.

Nitric Oxide Metabolism

Nitric oxide (NO) is a freely diffusible toxic intermediate of denitrification (38). NO can directly and indirectly impair cellular function (14). NO can directly bind to active site metals in key enzymes, like oxidases and reductases used for respiration. Indirectly, NO can be chemically modified to more toxic species that can damage DNA and proteins (30). During active denitrification, the presence of the Nor enzyme effectively eliminates NO, protecting the cell from cytotoxic effects. However, during non-denitrifying conditions, where *nor* is not expressed, if the cell is exposed to exogenously produced NO, there must be alternative mechanisms for NO detoxification to prevent cellular damage and inhibition of respiration.

***sphaeroides* heme protein, SHP:** SHP is an O_2-binding *c*-type cytochrome with a single high spin heme originally isolated from *R. sphaeroides* (24). SHP orthologs have been characterized from *Chromatium vinosum* and *Methylophilus methylotrophus* (12, 17). In the oxidized form of SHP the heme iron is 6-coordinate with Asparagine acting as the sixth ligand (23). In the reduced form, the asparagine no longer binds, leaving the heme open for binding diatomic species (23). Experiments have demonstrated oxygen, nitric oxide, and cyanide binding to SHP (18, 23). SHP is encoded in a three gene operon, where the two other genes code for a *b*-type cytochrome and a diheme cytochrome *c* (DHC) (Table 1.1) (11, 24). Together these proteins are predicted to form a novel electron transport chain whereby the cytochrome *b* can accept electrons from the quinone pool, pass them to DHC, which can then mediate transfer to the terminal enzyme SHP (Fig. 1.5).

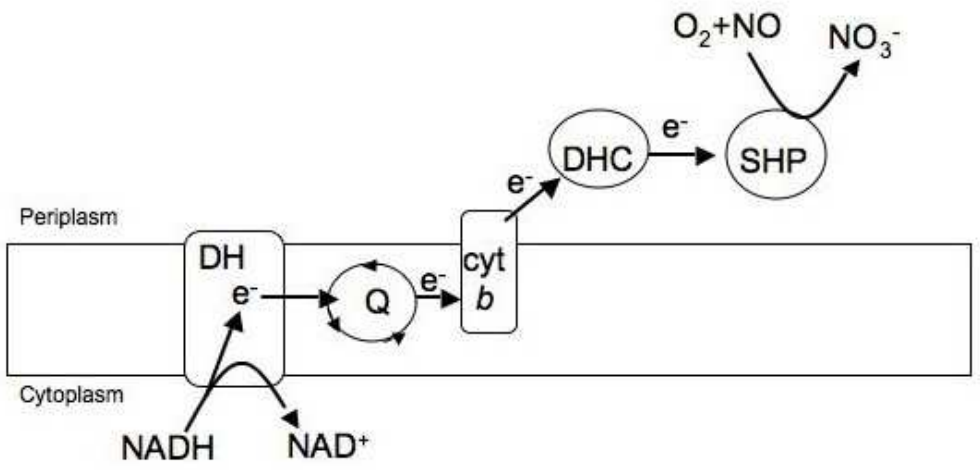

Figure 1.5: The predicted model for the SHP electron transport chain.

Recently, evidence was presented for SHP having nitric oxide dioxygenase activity (24). In vitro the oxygen-bound form of SHP can react with NO to form nitrate. Alternately, the NO-bound form of SHP can react with superoxide to also form nitrate. If this is the true enzymatic function of SHP it may constitute an aerobic pathway for NO detoxification. Importantly, the putative SHP electron transport chain is found in a diverse set of bacteria, suggesting a conserved mechanism and physiological role (11). In *R. sphaeroides* we will investigate the expression of the *shp* operon as well as viability of an *shp* mutant. This may provide a physiological context for SHP in the cell.

H-NOX (heme-nitric oxide and oxygen binding): The *hnox* gene is predicted to encode an NO-binding heme protein, based on homology to known NO-binding heme proteins of the soluble guanylate cyclase family in mammals (Table 1.1) (16). The *cdg2* gene is in an operon with *hnox* and is predicted to encode a diguanylate cyclase (DGC). DGCs are responsible for producing the second messenger, cyclic-diguanosine monophosphate, a ubiquitous signaling molecule in bacteria (35). This operon arrangement is present in many members of the α-proteobacteria, including all strains

of *R. sphaeroides*. In other bacteria, the H-NOX gene is commonly in a predicted operon with a histidine kinase or a methyl-accepting chemotaxis protein (MCP) (16). This suggests the operon structure is not accidental but reflects the potential for H-NOX to act as an NO (first messenger) signal sensor and transducer to various output domains, in this case a DGC (Fig. 1.6). Importantly, this DGC has an HNOB-A domain predicted to be associated with H-NOX domain interactions. In *Shewanella oneidensis*, where H-NOX is associated with a histidine kinase, it has been shown that the presence of NO, as an intermediate of denitrification, is sensed by H-NOX and the signal transduced to the histidine kinase, regulating its autophosphorylation activity (31). It is possible that the activity of the kinase can then regulate downstream

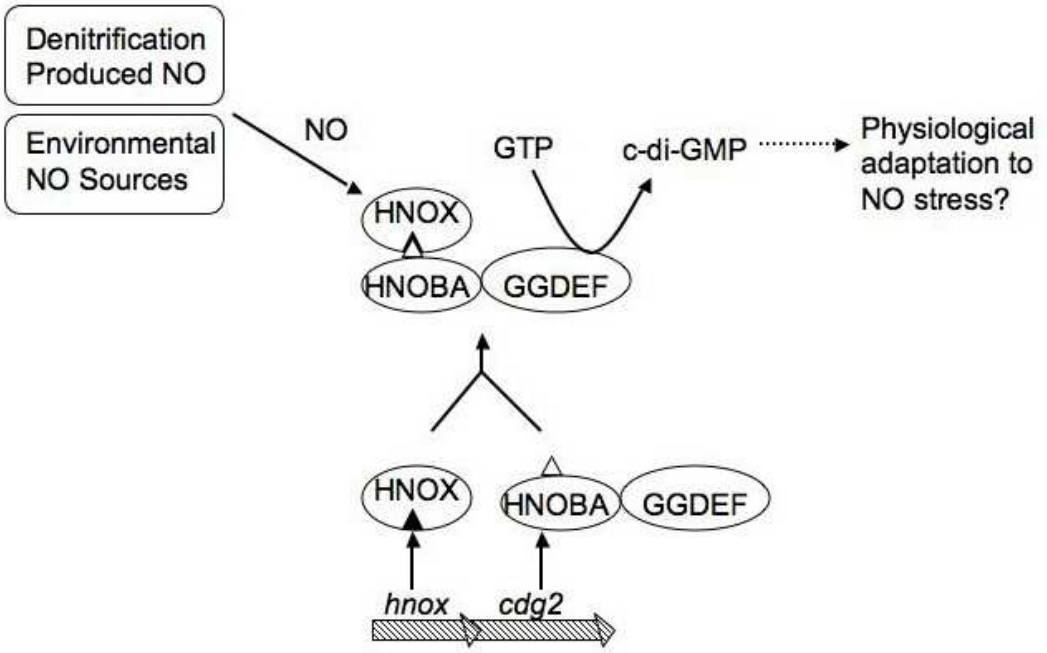

Figure 1.6: The predicted H-NOX signaling pathway. HNOB-A is a domain associated with the H-NOX domain. GGDEF is the domain responsible for diguanylate cyclase activity. c-di-GMP is cyclic diguanosine monophosphate, the product of diguanylate cyclase activity.

transcriptional events leading to adaptation to a low-oxygen, nitrate- or nitrite-rich environment. In other organisms, primarily obligate anaerobes, H-NOX is associated with MCPs (3). For these organisms, it has been suggested that NO is sensed as a toxic signal which results in taxis away from the signal. These studies have suggested two potential roles for H-NOX, that of sensing endogenous NO production as a sign of denitrification, and sensing environmental NO as a toxic molecule to be avoided (3). Among the α-proteobacteria, not all species/strains that have the H-NOX gene associated with a DGC gene are capable of denitrification, suggesting that the response to NO may not be specific for physiological adaptation to denitrification, but may be a response to NO toxicity. In *R. sphaeroides* we will investigate the H-NOX protein as a player in NO sensing and physiological adaptations to NO stress.

Rhodobacter sphaeroides

Rhodobacter sphaeroides 2.4.3, our model organism, is a photoheterotrophic α-proteobacteria. *R. sphaeroides* is metabolically complex and can grow under a diverse set of environmental and culture conditions. It is best known as a model organism for anoxygenic photosynthesis and is of interest for bioenergy and bioremediation applications (2, 40). *R. sphaeroides* is adaptable and can transition efficiently from aerobic respiration in the presence of oxygen to anoxygenic photosynthesis in the absence of oxygen. Some strains, like 2.4.3, are capable of denitrification and have integrated nitrogen oxide respiration into their low oxygen and anaerobic metabolism.

Denitrification is up regulated in response to decreasing oxygen tension by the PrrBA two component system (22). In addition, a second layer of regulation occurs in response to the presence of respirable nitrogen oxides via NnrR (41). To facilitate this transition, NnrR is expressed at a low constitutive level throughout growth. As

background levels of Nir activity produce small quantities of NO, this can activate NnrR and lead to full expression of denitrification genes (Fig. 1.4).

Currently, of the four sequenced strains of *R. sphaeroides*, only strain 2.4.3 is a full denitrifier. However, the other strains still code for some features of nitrogen oxide metabolism (Table 1.2). Strain 2.4.1 retains Nap and Nor but lacks Nir. Strain

Table 1.2: Presence of the denitrification enzymes across the four sequenced strain of *R. sphaeroides*. +, indicates present, -, indicates absent.

R. sphaeroides **strain**	***napKEFDABC "onap"***	***napFDAGHBC "rnap"***	***nirK***	***norBCQD***
2.4.3	+	+	+	+
KD131	-	-	+	+
2.4.1	+	-	-	+
2.4.9	-	-	-	+

2.4.9 lacks Nap and Nir, but has Nor. Finally, strain KD131 lacks Nap, but has Nir and Nor. The common theme is retention of Nor in all strains. This suggests that NO may be present in *Rhodobacter*'s preferred niche and furthermore, that Nor is an effective mechanism for ridding the cell of NO. Also, Nap is present in two out of the four strains suggesting that nitrate respiration may be advantageous, even though Nap in the absence of the rest of the denitrification pathway would provide no energetic benefit. Interestingly, KD131 could use denitrification for energy conservation as it has both Nir and Nor, but we would not predict NO_2^- to be in abundance in the environment, restricting the energetic potential.

Research Synopsis by Chapter

Over the past decade our lab has identified and characterized many of the key players in denitrification in *Rhodobacter sphaeroides* 2.4.3. However, the availability of the genome sequence has allowed us to expand and refine our model. Open questions addressed in the following chapters are as follows:

In Chapter 2, we study two distinct nitrate reductases (Nap) encoded in the 2.4.3 genome. Our null hypothesis is that these enzymes, which have the same enzymatic function, do not act in unique physiological roles within the cell. Experiments show that one Nap is required for denitrification, while the second plays no role. This refutes our hypothesis, supporting the alternative, that these enzymes have unique physiological roles. Studies show that endogenous electron flow to the second Nap enzyme is favored under conditions where the cells are likely to be experiencing redox imbalances. Further supporting our alternative hypothesis, the Nap specific to denitrification is not utilized under conditions of aerobic redox imbalance.

Chapter 3 focuses on the potential for oxygen to influence the activity of the denitrification transcriptional regulator NnrR. In a mutant lacking the high affinity cytochrome oxidase denitrification does not occur. Our hypothesis is that the denitrification regulators PrrA and NnrR are functional. A series of experiments are presented that show NnrR to be non-functional, refuting our hypothesis. Utilizing informative mutants and manipulated O_2 culture conditions, an alternative hypothesis is presented implicating O_2 as an inhibitory signal to NnrR.

Chapter 4 investigates the NnrR regulon in strain 2.4.3. A genome search for the predicted conserved NnrR binding site identified six additional genes with this site within their promoter. We hypothesize these genes are regulated by NnrR. Expression studies show that five of these genes require NnrR for expression, supporting our original hypothesis for these genes. This expands the NnrR regulon by five members.

Two of the new members were linked to a role in denitrifying physiology. One gene encodes a pseudoazurin, which is shown to be an electron donor to Nir. Together with cytochrome c_2, these are the two major electron donors to Nir. The second characterized member of the regulon is NorEF, encoded by the *norEF* operon. These proteins are predicted to play a role in Nor activity. We also compare the NnrR regulons across the sequenced strains of *R. sphaeroides* to gain insight into how the regulon changes as the capacity for denitrification changes.

In chapter 5 the focus turns to denitrification-independent NO metabolism. Genome comparison reveals that all strains of *R. sphaeroides* retain Nor, presumably because NO is a frequently encountered toxin. However, Nor activity is confined to denitrifying conditions which are characterized by low oxygen and the presence of NO. This leaves unfilled niches for other NO defense mechanisms, specifically during aerobic growth. Strain 2.4.1 of *R. sphaeroides* encodes the SHP protein. We investigated expression of the *shp* operon and find that expression is induced under anaerobic growth conditions and is repressed by the presence of Nir, suggesting NO may be an inhibitory signal for expression. The expression pattern does not correlate with the proposed enzymatic function, raising interesting questions about the physiological role of SHP (24).

Chapter 6 continues the focus on denitrification-independent NO metabolism with a study of the H-NOX NO sensory protein. H-NOX is a heme protein that may serve as a link between NO signaling and cyclic diguanosine monophosphate signaling in bacteria. We characterize the phenotypes of knockout and overexpression strains of *hnox*. In addition, we attempt to purify the H-NOX protein and a diguanylate cyclase, which is predicted to interact with H-NOX.

Finally, the appendix contains a short study of aerobic respiration in the pathogen *Brucella neotomae*. This includes expression of the major oxidases and establishment of a functional cytochrome *c* maturation system.

REFERENCES

1. **Baek, S., A. Hartsock, and J. Shapleigh.** 2008. *Agrobacterium tumefaciens* C58 uses ActR and FnrN to control nirK and nor expression. J. Bacteriol. **190:**78-86.

2. **Bai, H. J., Z. M. Zhang, G. E. Yang, and B. Z. Li.** 2008. Bioremediation of cadmium by growing *Rhodobacter sphaeroides*: kinetic characteristic and mechanism studies. Bioresour. Technol. **99:**7716-22.

3. **Boon, E. and M. Marletta.** 2005. Ligand discrimination in soluble guanylate cyclase and the H-NOX family of heme sensor proteins. Current Opinion in Chemical Biology **9:**441-446.

4. **de Boer, A., J. van der Oost, W. Reijnders, H. Westerhoff, A. Stouthamer, and R. van Spanning.** 1996. Mutational analysis of the nor gene cluster which encodes nitric-oxide reductase from *Paracoccus denitrificans*. Eur. J. Biochem. **242:**592-600.

5. **Ellington, M. J., D. J. Richardson, and S. J. Ferguson.** 2003. *Rhodobacter capsulatus* gains a competitive advantage from respiratory nitrate reduction during light-dark transitions. Microbiology (Reading, Engl.) **149:**941-8.

6. **Eraso, J., J. Roh, X. Zeng, S. Callister, M. Lipton, and S. Kaplan.** 2008. Role of the global transcriptional regulator PrrA in *Rhodobacter sphaeroides* 2.4.1: combined transcriptome and proteome analysis. J. Bacteriol. **190:**4831-48.

7. **Falkowski, P. G. and L. V. Godfrey.** 2008. Electrons, life and the evolution of Earth's oxygen cycle. Philos Trans R Soc Lond, B, Biol Sci **363:**2705-16.

8. **Francis, C. A., J. M. Beman, and M. M. Kuypers.** 2007. New processes and players in the nitrogen cycle: the microbial ecology of anaerobic and archaeal ammonia oxidation. ISME J **1:**19-27.

9. **Gao, H., Z. K. Yang, S. Barua, S. B. Reed, M. F. Romine, K. H. Nealson, J. K. Fredrickson, J. M. Tiedje, and J. Zhou.** 2009. Reduction of nitrate in *Shewanella*

oneidensis depends on atypical NAP and NRF systems with NapB as a preferred electron transport protein from CymA to NapA. ISME J 1-11.

10. **Gavira, M., M. Roldan, F. Castillo, and C. Moreno-Vivian.** 2002. Regulation of nap gene expression and periplasmic nitrate reductase activity in the phototrophic bacterium *Rhodobacter sphaeroides* DSM158. Journal of Bacteriology **184:**1693-702.

11. **Gibson, H., C. Mowat, C. Miles, B. Li, D. Leys, G. Reid, and S. Chapman.** 2006. Structural and functional studies on DHC, the diheme cytochrome c from *Rhodobacter sphaeroides*, and its interaction with SHP, the *sphaeroides* heme protein. Biochemistry **45:**6363-71.

12. **Gray, G. O., D. F. Gaul, and D. B. Knaff.** 1983. Partial purification and characterization of two soluble c-type cytochromes from *Chromatium vinosum.* Arch. Biochem. Biophys. **222:**78-86.

13. **Gruber, N. and J. N. Galloway.** 2008. An Earth-system perspective of the global nitrogen cycle. Nature **451:**293-6.

14. **Hughes, M. N.** 2008. Chemistry of nitric oxide and related species. Methods Enzymol. **436:**3-16.

15. **Jacobson, F., H. Guo, K. Olesen, M. Okvist, R. Neutze, and L. Sjolin.** 2005. Structures of the oxidized and reduced forms of nitrite reductase from *Rhodobacter sphaeroides* 2.4.3 at high pH: changes in the interactions of the type 2 copper. Acta Crystallogr. D Biol. Crystallogr. **61:**1190-8.

16. **Iyer, L., V. Anantharaman, and L. Aravind.** 2003. Ancient conserved domains shared by animal soluble guanylyl cyclases and bacterial signaling proteins. BMC Genomics **4:**5.

17. **Klarskov, K., D. Leys, K. Backers, H. Costa, H. Santos, Y. Guisez, and J. Van Beeumen.** 1999. Cytochrome c" from the obligate methylotroph *Methylophilus*

methylotrophus, an unexpected homolog of sphaeroides heme protein from the phototroph Rhodobacter sphaeroides. Biochim. Biophys. Acta **1412:**47-55.

18. **Klarskov, K., G. Van Driessche, K. Backers, C. Dumortier, T. Meyer, G. Tollin, M. Cusanovich, and J. Van Beeumen.** 1998. Ligand binding and covalent structure of an oxygen-binding heme protein from *Rhodobacter sphaeroides*, a representative of a new structural family of c-type cytochromes. Biochemistry **37:**5995-6002.

19. **Korner, H., H. Sofia, and W. Zumft.** 2003. Phylogeny of the bacterial superfamily of Crp-Fnr transcription regulators: exploiting the metabolic spectrum by controlling alternative gene programs. FEMS Microbiol. Rev. **27:**559-92.

20. **Kwiatkowski, A. and J. Shapleigh.** 1996. Requirement of nitric oxide for induction of genes whose products are involved in nitric oxide metabolism in *Rhodobacter sphaeroides* 2.4.3. J. Biol. Chem. **271:**24382-8.

21. **Kwiatkowski, A., W. Laratta, A. Toffanin, and J. Shapleigh.** 1997. Analysis of the role of the nnrR gene product in the response of *Rhodobacter sphaeroides* 2.4.1 to exogenous nitric oxide. J. Bacteriol. **179:**5618-20.

22. **Laratta, W., P. Choi, I. Tosques, and J. Shapleigh.** 2002. Involvement of the PrrB/PrrA two-component system in nitrite respiration in *Rhodobacter sphaeroides* 2.4.3: evidence for transcriptional regulation. J. Bacteriol. **184:**3521-9.

23. **Leys, D., K. Backers, T. Meyer, W. Hagen, M. Cusanovich, and J. Van Beeumen.** 2000. Crystal structures of an oxygen-binding cytochrome c from *Rhodobacter sphaeroides*. J. Biol. Chem. **275:**16050-6.

24. **Li, B. R., J. L. Anderson, C. G. Mowat, C. S. Miles, G. A. Reid, and S. K. Chapman.** 2008. *Rhodobacter sphaeroides* haem protein: a novel cytochrome with nitric oxide dioxygenase activity. Biochem. Soc. Trans. **36:**992-5.

25. **Liu, H. P., S. Takio, T. Satoh, and I. Yamamoto.** 1999. Involvement in denitrification of the napKEFDABC genes encoding the periplasmic nitrate reductase system in the denitrifying phototrophic bacterium *Rhodobacter sphaeroides* f. sp. denitrificans. Biosci. Biotechnol. Biochem. **63:**530-6.

26. **Lovley, D. R. and J. D. Coates.** 2000. Novel forms of anaerobic respiration of environmental relevance. Curr. Opin. Microbiol. **3:**252-6.

27. **Mulholland, P. J., A. M. Helton, G. C. Poole, R. O. Hall, S. K. Hamilton, B. J. Peterson, J. L. Tank, L. R. Ashkenas, L. W. Cooper, C. N. Dahm, W. K. Dodds, S. E. Findlay, S. V. Gregory, N. B. Grimm, S. L. Johnson, W. H. McDowell, J. L. Meyer, H. M. Valett, J. R. Webster, C. P. Arango, J. J. Beaulieu, M. J. Bernot, A. J. Burgin, C. L. Crenshaw, L. T. Johnson, B. R. Niederlehner, J. O'Brien, J. D. Potter, R. W. Sheibley, D. J. Sobota, and S. M. Thomas.** 2008. Stream denitrification across biomes and its response to anthropogenic nitrate loading. Nature **452:**202-5.

28. **Murphy, L. M., F. E. Dodd, F. K. Yousafzai, R. R. Eady, and S. S. Hasnain.** 2002. Electron donation between copper containing nitrite reductases and cupredoxins: the nature of protein-protein interaction in complex formation. J. Mol. Biol. **315:**859-71.

29. **Oh, J., I. Ko, and S. Kaplan.** 2004. Reconstitution of the *Rhodobacter sphaeroides* cbb3-PrrBA signal transduction pathway in vitro. Biochemistry **43:**7915-23.

30. **Patel, R. P., J. McAndrew, H. Sellak, C. R. White, H. Jo, B. A. Freeman, and V. Darley-Usmar.** 1999. Biological aspects of reactive nitrogen species. Biochim. Biophys. Acta **1411:**385-400.

31. **Price, M., L. Chao, and M. Marletta.** 2007. *Shewanella oneidensis* MR-1 H-NOX Regulation of a Histidine Kinase by Nitric Oxide. Biochemistry **46:**13677-13683.

32. **Prosser, J. I. and G. W. Nicol.** 2008. Relative contributions of archaea and bacteria to aerobic ammonia oxidation in the environment. Environ. Microbiol. **10:**2931-41.

33. **Richardson, D. J., B. C. Berks, D. A. Russell, S. Spiro, and C. J. Taylor.** 2001. Functional, biochemical and genetic diversity of prokaryotic nitrate reductases. Cell Mol. Life Sci. **58:**165-78.

34. **Risgaard-Petersen, N., A. M. Langezaal, S. Ingvardsen, M. C. Schmid, M. S. Jetten, d. C. Op, J. W. Derksen, E. Pina-Ochoa, S. P. Eriksson, L. P. Nielsen, N. P. Revsbech, T. Cedhagen, van der Zwaan, G.J.** 2006. Evidence for complete denitrification in a benthic foraminifer. Nature **443:**93-6.

35. **Ryjenkov, D., M. Tarutina, O. Moskvin, and M. Gomelsky.** 2005. Cyclic diguanylate is a ubiquitous signaling molecule in bacteria: insights into biochemistry of the GGDEF protein domain. J. Bacteriol. **187:**1792-8.

36. **Sears, H. J., P. J. Little, D. J. Richardson, B. C. Berks, S. Spiro, and S. J. Ferguson.** 1997. Identification of an assimilatory nitrate reductase in mutants of *Paracoccus denitrificans* GB17 deficient in nitrate respiration. Arch. Microbiol. **167:**61-6.

37. **Seitzinger, S.** 2008. Nitrogen cycle: out of reach. Nature **452:**162-3.

38. **Spiro, S.** 2007. Regulators of bacterial responses to nitric oxide. FEMS Microbiol. Rev. **31:**193-211.

39. **Stewart, V., P. J. Bledsoe, L. L. Chen, and A. Cai.** 2009. Catabolite repression control of napF (periplasmic nitrate reductase) operon expression in *Escherichia coli* K-12. Journal of Bacteriology **191:**996-1005.

40. **Tavano, C. L. and T. J. Donohue.** 2006. Development of the bacterial photosynthetic apparatus. Curr. Opin. Microbiol. **9:**625-31.

41. **Tosques, I., J. Shi, and J. Shapleigh.** 1996. Cloning and characterization of nnrR, whose product is required for the expression of proteins involved in nitric oxide metabolism in *Rhodobacter sphaeroides* 2.4.3. J. Bacteriol. **178:**4958-64.

42. **Tosques, I., A. Kwiatkowski, J. Shi, and J. Shapleigh.** 1997. Characterization and regulation of the gene encoding nitrite reductase in *Rhodobacter sphaeroides* 2.4.3. J. Bacteriol. **179:**1090-5.

43. **Unden, G. and J. Bongaerts.** 1997. Alternative respiratory pathways of *Escherichia coli*: energetics and transcriptional regulation in response to electron acceptors. Biochim. Biophys. Acta **1320:**217-34.

44. **Wijma, H. J., L. J. Jeuken, M. P. Verbeet, F. A. Armstrong, and G. W. Canters.** 2006. A random-sequential mechanism for nitrite binding and active site reduction in copper-containing nitrite reductase. J. Biol. Chem. **281:**16340-6.

45. **Wu, J. and C. E. Bauer.** 2008. RegB/RegA, a global redox-responding two-component system. Adv. Exp. Med. Biol. **631:**131-148.

46. **Zehr, J. P., B. D. Jenkins, S. M. Short, and G. F. Steward.** 2003. Nitrogenase gene diversity and microbial community structure: a cross-system comparison. Environ. Microbiol. **5:**539-54.

47. **Zumft, W.** 1997. Cell biology and molecular basis of denitrification. Microbiol. Mol. Biol. Rev. **61:**533-616.

48. **Zumft, W. G.** 2005. Nitric oxide reductases of prokaryotes with emphasis on the respiratory, heme-copper oxidase type. J. Inorg. Biochem. **99:**194-215.

49. **Zumft, W. G. and P. M. Kroneck.** 2007. Respiratory transformation of nitrous oxide (N2O) to dinitrogen by Bacteria and Archaea. Adv. Microb. Physiol. **52:**107-227.

Chapter Two

Physiological roles for two periplasmic nitrate reductases in *Rhodobacter sphaeroides* 2.4.3

Summary

The metabolically versatile purple bacterium *Rhodobacter sphaeroides* 2.4.3 is a denitrifier that has operons encoding two periplasmic nitrate reductase enzymes. We hypothesize that these two enzymes play different roles in the cell, with one being a respiratory enzyme while the other is involved in redox homeostasis. One operon is expressed aerobically and repressed under low oxygen, while the second is expressed anaerobically. Mutants of the nitrate reductases also have different phenotypes. When the aerobic nitrate reductase is absent, there is no detectable aerobic nitrate reduction, but cells can respire nitrate anaerobically. In contrast, when the anaerobic nitrate reductase is absent, aerobic nitrate reduction is detectable but anaerobic nitrate reduction is impaired. There is no cellular aerobic nitrate reductase activity in liquid culture but there is high activity in cells grown on solid media, revealing additional regulatory controls on nitrate reduction. Cells were grown on different carbon sources where growth on more reduced carbon sources required greater Nap activity. This is consistent with a role for the aerobic nitrate reductase in redox homeostasis. These results show that one of the nitrate reductases is specific for respiration and denitrification, while the other may play a role in redox homeostasis during aerobic growth.

Introduction

Nitrate reduction is widespread in the bacterial kingdom where it is used for both assimilatory and dissimilatory processes (11, 22). Assimilatory processes include

nitrate reduction to ammonia for biosynthesis. Dissimilatory processes include denitrification, the respiration of nitrate to nitrogen gas, and ammonification, the respiration of nitrate to ammonia. This makes the reduction of nitrate an important reaction within the global nitrogen cycle. Nitrate is present in many terrestrial and aquatic ecosystems in excess due to agricultural runoff of nitrate-based fertilizer (12). Understanding the regulation and physiological roles of nitrate reductases in diverse organisms will allow more accurate modeling and predictions of nitrate fate in the environment. Like the diverse processes utilizing nitrate reduction, the enzymes required are physiologically distinct (11, 22). There are 3 broad types of nitrate reductase recognized: the assimilatory group, Nas, and two dissimilatory groups, Nar and Nap. These enzymes differ in their localization with the cell. Nas is cytoplasmic, Nar is membrane-bound, and Nap is periplasmic (22). Environmental surveys for the dissimilatory Nap and Nar type genes demonstrate an almost equal representation of both groups (2). This suggests that Nap type enzymes are playing a significant role in the environment. This chapter focuses on distinct physiological roles for Nap enzymes within a single organism.

Nap is a two-subunit enzyme that utilizes a tetraheme cytochrome for quinol oxidation. Like the other types of nitrate reductase, Nap has a molybdenum cofactor as the site of nitrate reduction. These enzymes are commonly the first step in a multi-step nitrogen oxide reduction pathway. While Nap turnover is not associated with generation of a proton motive force (pmf), coupling nitrate reduction to further reduction steps, as in denitrification, results in pmf generation via the bc_1-dependent branch of the electron transport chain (11). This indirectly couples some Nap enzymes to growth and energy conservation. Other Nap enzymes are not coupled to further reduction steps, resulting in no obvious energy conservation. These Nap enzymes have instead been shown to aid the cell in redox homeostasis (11). Bacteria growing in

heterogeneous environments or on reduced carbon sources likely encounter flux in growth substrate and terminal oxidant resulting in redox imbalances. The presence of an uncoupled nitrate reductase could act as an outlet for excess electrons, balancing NAD^+/NADH pools within the cell.

In *Paracoccus pantotrophus* there is an aerobically expressed Nap that is not utilized for denitrification (23). Instead, this enzyme is highly active during growth on reduced carbon sources. Furthermore, protein film voltammetry using the purified heterodimer shows redox values consistent with a role in redox balancing (9). The reduction potential of 0.1V is lower than that of the respiratory nitrate reductase (Nar) from this organism, which is used for denitrification. This suggests Nap activity requires higher ubiquinol/ubiquinone ratios, which would occur when electron flow into the chain exceeds electron transfer to a terminal oxidant. In the closely related organisms, *Rhodobacter sphaeroides* DSM158 and *Rhodobacter capsulatus*, Nap has been shown to stimulate growth under photosynthetic conditions in the presence of nitrate (5, 10). During photosynthetic growth the cells may require a sink for excess reducing equivalents. Importantly, these organisms are not denitrifiers, so they cannot be using Nap for energetic purposes.

In our laboratory we study the model organism *Rhodobacter sphaeroides*, a photoheterotroph of the α-proteobacteria. Genome sequencing of four strains has revealed diversity in nitrate reduction ability. Strain 2.4.3 has two distinct operons encoding Nap enzymes, strain 2.4.1 has only one of these operons, while strain 2.4.9 and KD131 have none. These strains also vary in their capacity for denitrification. 2.4.3 is a denitrifier, while 2.4.1 and 2.4.9 are partial denitrifiers lacking nitrite reductase, and KD131 lacks nitrate reductase but retains nitrite and nitric oxide reductases. The lack of correlation between the presence of Nap and the ability to denitrify suggests a role for Nap outside of respiration. Here we exploit the fact that

strain 2.4.3 has two Nap enzymes by investigating the potential for these two enzymes to have distinct physiological roles.

Materials and Methods

Bacterial strains and culture conditions. Three strains of *Rhodobacter sphaeroides* were used in this study. Strain 2.4.3 is a denitrifier and our model system. Strains 2.4.1 and 2.4.9 are partial denitrifiers used for comparison to strain 2.4.3. Derivatives of these strains are listed in Table 2.1. *Rhodobacter* strains were grown in Sistrom's medium at 30°C and, when necessary, antibiotics were added at the following concentrations: kanamycin 25μg/mL, tetracycline 1μg/mL, streptomycin 50μg/mL. Flask culture conditions have been previously described (29). For denitrifying growth KNO_3 was added to 10mM. For photosynthetic culture, 15mL serum vials were filled and sealed. The vials were then incubated ~12 inches from 2 incandescent 75W bulbs at room temperature with vigorous shaking. For microaerobic plate growth, plates were incubated in Gas-Pak jars with a headspace that was alternately vacuumed and N_2 replaced for 3 cycles.

Escherichia coli strain DH5-α or JM109 was used for cloning and transformation purposes, and strain S17-1 or S17-1λ*pir* was used for bi-parental conjugations. *E. coli* was cultured in Luria-Bertani medium (18) at 32°C and, when necessary, antibiotics were added at the following concentrations: ampicillin 100μg/mL, kanamycin 25μg/mL, tetracycline 10μg/mL, streptomycin 25μg/mL.

Construction of plasmids and strains. Chromosomal DNA was isolated from 2.4.3 using the Puregene DNA Isolation Kit. All oligonucleotide primers were purchased from Integrated DNA Technologies (IDT). In most cases, restriction sites were added to the 5' end of primers to facilitate cloning, and these are underlined in primer

Table 2.1: Strains and plasmids used in this study.

Strains or plasmid	Genotype or Description	Reference or source
Strains		
DH5αF'	Host for *E. coli* cloning: F' 80 *lacZm15 redA endA1 gyrA96 thi-1hsdR17* ($r_k m_v$) *supE44 relA1 deoR* (*lacZYA–argF*)*U169*	
JM109	Host for *E. coli* cloning:	
S17-1	For conjugational transfer of plasmids: *recA thi pro hasdRM*$^+$ *RP4:*2-Tc:*Mu:*Km:TnZ	
S17-1λ*pir*	For conjugational transfer of plasmids:	
2.4.3	Wild-type strain of *Rhodobacter sphaeroides*	ATCC17025
2.4.1	Wild-type strain of *Rhodobacter sphaeroides*	Type strain
2.4.9	Wild-type strain of *Rhodobacter sphaeroides*	ATCC17023?
prrA	*prrA::aph*, 2.4.3 derivative, Km^R	(17)
fnrL	2.4.3 with insertional inactivation of *fnrL*	(14)
Δ*ccoN*	2.4.3 with ΩSm/Sp in *ccoN*, deletion mutant	Hartsock, Shapleigh
rnap	2.4.3 with insertional inactivation of *rnapA*, Km^R	this study
onap	2.4.3 with insertional inactivation of *onapA*, Tc^R	this study
rnap/*onap*	2.4.3 with inactivation of both *rnap* and *onap*, Km^R/Tc^R	this study
fnrX	2.4.3 with insertional inactivation of gene 3486, Tc^R	this study
qsrR	2.4.3 with insertional inactivation of gene 0408, Tc^R	this study
Plasmids		
pUC19	Used for cloning in *E. coli* DH5-α (Ap^R)	(31)
pRK415	Broad-host-range plasmid (Tc^R)	(15)
pSUP202-1	Mobilizable suicide vector (Tc^R, Ap^R, Cm^R)	(24)
pKOK-6	Source of *lacZ*-Km cassette (Tc^R, Km^R, Ap^R)	(16)
pJP5603	Mobilizable suicide vector (Km^R)	(21)
pRNAPZ	pRK415 with the *rnap* promoter fused to *lacZ*, transcriptional reporter (Tc^R, Km^R)	this study
pONAPZ	pRK415 with the *onap* promoter fused to *lacZ*, transcriptional reporter (Tc^R, Km^R)	this study
pRNAPKO	pJP5603 with *napA* internal region (*rnap*) (Km^R)	this study
pONAPKO	pSUP202-1 with *napA* internal region (*onap*) (Tc^R)	this study
pFNRXKO	pSUP202-1 with *fnrX* internal region (Tc^R)	this study
pQSRRKO	pSUP202-1 with *qsrR* internal region (Tc^R)	this study

sequences. PCR, restriction digests, and ligations were done according to standard protocols. Plasmid isolation was done by the alkaline lysis method (18). Transformations were done using the TSS method (3). Plasmids are listed in Table 2.1.

***lacZ* expression fusions.** Expression fusions were constructed for the *rnap* operon (Rsph17025_3218-3224) and the *onap* operon (Rsph17025_3986-3992). For the *rnap* fusion, the predicted promoter was amplified using primers (5'-CCCGAATTCCCATGACATCGACACCGAC-3') and (5'-CCCGTCGACCAGGATCCGCAGAAGGTG-3'). This region corresponds to 896 bases upstream of the operon start. This amplicon was cloned into pUC19 via EcoRI and SalI and verified by sequencing. The promoter was cloned into the broad host-range vector pRK415. The *lacZ* cassette of pKOK-6 was cloned via PstI and orientation was confirmed. This construct was transformed into *E. coli* S17-1 and subsequently conjugated into *Rhodobacter* strains. The predicted *onap* promoter was amplified using primers (5'-GCGGAATTCACTATCTCGTGGTCGGCC-3') and (5'-GCGCTGCAGCAGGAACGGCCAGATCAC-3'). This corresponds to 682 bases upstream of the operon start. The amplicon was cloned into pUC19 via EcoRI and PstI and verified by sequencing. The promoter was cloned into pRK415 and the *lacZ* cassette of pKOK-6 was cloned via PstI. This construct was then transformed into *E. coli* S17-1 and subsequently conjugated into *Rhodobacter* strains.

Mutant strains. The *onap* mutant was generated by homologous recombination using the suicide vector pSUP202-1. First, an internal region of *napA* was amplified using primers (5'-CGCGAATTCAGTGGACGATCTGGGAGG-3') and (5'-CGGCTGCAGAGCGAGAAGGGCGAATTG-3'). This amplicon was cloned into pUC19 and verified by sequencing. The gene fragment was then cloned into the suicide plasmid pSUP202-1 via EcoRI and PstI. The final construct was transformed

into *E. coli* S17-1 and conjugated into *R. sphaeroides* 2.4.3. The gene disruption was confirmed by PCR using primers flanking the crossover region.

The *rnap* mutant was generated by homologous recombination using the suicide vector pJP5603. First, an internal region of *napA* was targeted for amplification using primers (5'-AACATGGCCGARATGCAYCC-3') and (5'-CCSCGSACRTGCTGGTTGAASCC-3'). These primers are degenerate because at the time the genome sequence of 2.4.3 was unavailable, and these primers were based on *napA* sequence from strain 2.4.1. This amplicon was cloned into pUC19 via HincII and verified by sequencing. The gene fragment was then cloned into pJP5603 via BamHI and HindIII. The final construct was verified and transformed into *E. coli* S17-1λ*pir*. This strain was used for conjugation with *R. sphaeroides* 2.4.3. Gene disruption was verified by PCR.

The double *onap/rnap* mutant was generated by starting with the *rnap* mutant and conjugating in the construct to generate the *onap* disruption. This mutant was verified by PCR.

The gene at locus 3486 encodes the Fnr-type regulator that was targeted as a potential regulator of *rnap*. This gene was inactivated by insertional inactivation. A central region of the gene, not including either end, was amplified using primers (5'-CATCTGCAGAGATCGTGGACTTCCAGG-3') and (5'-CACGAATTCGAGAGCGGGCAGGCATAG-3'). This amplicon was cloned into pUC19 via EcoRI and PstI and verified by sequencing. The gene fragment was then moved into the suicide vector pSUP202-1 via EcoRI and PstI. The final construct was transformed into *E. coli* S17-1 and then conjugated into strain 2.4.3 to generate the mutant. Inactivation of the gene was verified by PCR using primers flanking the open reading frame. The *rnap*::*lacZ* construct was then conjugated into the mutant to test *rnap* expression.

The gene at locus 0408 encodes the luxR-type regulator targeted as a potential regulator of *onap*. This gene has been designated as *qsrR* in strain 2.4.1 (13). A central region of the gene was amplified using primers (5'-CACCTGCAGCTTCTCAACGAGACCTTC-3') and (5'-CACGAATTCCACAGGGCCGCACCAAG-3'). The amplicon was cloned into pUC19 via EcoRI and PstI and verified by sequencing. The fragment was then cloned into pSUP202-1 via EcoRI and PstI. The final construct was transformed into *E. coli* S17-1 and then conjugated into strain 2.4.3, generating the mutant. Inactivation of the gene was verified by PCR using primers flanking the open reading frame. The *onap::lacZ* construct was then conjugated into the mutant to test *onap* expression.

Enzyme assays. Gene expression was measured via β-galactosidase activity as previously described (18). Activity was determined based on three independently grown cultures. In all cases, expression was monitored throughout growth, and representative values for growth phases of interest were averaged. Error bars represent one standard deviation.

Nitrate reductase activity was measured using methyl viologen as an artificial electron donor (26). This is a colorimetric assay, which detects nitrite as the product of nitrate reduction. Nitrate (500μM) is added to cells along with the artificial electron donor, and the reaction is timed. In this case all reactions were terminated at the same time. Activity was based on three independently grown cultures. Error is represented as one standard deviation.

Nitrate was measured in media using the szechrome reaction (Polysciences, Inc). Samples of cells were taken at various time points and diluted 20-fold. Szechrome reagent was then added, and the absorbance recorded at 570nm. When nitrate was no longer detectable, the assay was repeated without culture dilution to confirm the absence of nitrate. A nitrate standard curve was generated to convert

absorbance values to concentrations. The correlation between absorbance and concentration was linear over the range of concentrations relevant to this study.

Nitrite was detected as an indication of endogenous Nap activity under aerobic conditions. For liquid culture, 50μL of cells were used for assays. For solid media, plugs of agar were sampled using the blunt end of a 200μL pipet tip, melted in 100uL of H_2O and then 50uL used for assays. Phosphate buffer (0.9mL), sulfanilic acid (1.0mL), and azo dye (1.0mL) were added. Nitrite levels correlate with the absorbance at 540nm. In aerobic liquid culture there was no nitrite produced, so this was considered zero Nap activity.

Results

Comparison of the two *nap* operons. A comparison of the *nap* operons from sequenced bacterial genomes reveals significant heterogeneity in operon composition (22). A common feature of almost all *nap* operons is the presence of *napDABC*. This correlates with the importance of these gene products in enzyme function. NapA is the catalytic subunit, and NapB and NapC are heme-containing subunits involved in electron transfer (11). Other genes present in *nap* operons have less defined functions, including roles in assembly and transport of Nap components to the periplasm. *R. sphaeroides* strain 2.4.3 has two distinct *nap* operons. One of these operons is located on a large plasmid (pRSPA02) from gene number 3986-3992 and includes 7 genes as follows, *napKEFDABC*. This operon is most similar to *nap* operons from closely related organisms, like *Paracoccus pantotrophus*, that utilize this enzyme for redox homeostasis (23). For this reason, the operon has been designated as *onap* with the "o" standing for "overflow" in reference to a role for this enzyme in electron overflow and redox homeostasis. The *onap* operon includes the core genes *napDABC*, common to all Nap enzymes, and in addition *napKEF*. *napK* and *napE* encode integral membrane

proteins of unknown function, while *napF* encodes a soluble cytoplasmic [4Fe-4S] protein (11).

The second *nap* operon is located on chromosome II from gene number 3218-3224 and includes 7 genes as follows, *napFDAGHBC*. This gene content of this operon is similar to *nap* operons from γ-proteobacteria, including several denitrifying *Shewanella* species and the non-denitrifying *E. coli*. In these organisms, Nap has been shown to support anaerobic growth (11). For this reason, the operon has been designated *rnap* with the "r" standing for "respiration" in reference to an energetic role for this enzyme. In addition to *napDABC*, this operon has *napFGH*. *napG* encodes a soluble predicted [4Fe-4S] protein of unknown localization (11). *napH* encodes a membrane protein with four transmembrane helices that has motifs possibly involved in metal binding (11).

Importantly, the two *nap* operons in 2.4.3 are not paralogous but seem to be distinct in origin. As similar Nap enzymes in other organisms are known to have distinct physiological roles, by analogy we would predict oNap to be involved in redox homeostasis, while rNap is involved in denitrification. We first investigated the expression pattern of both the *onap* and *rnap* operons. If these enzymes have distinct physiological roles, we would expect regulation of the operons to also be distinct.

Expression of the *rnap* operon. Expression of the *rnap* operon was assessed using a *lacZ* transcriptional fusion. In liquid culture, expression increased 16-fold with decreasing oxygen tension and was nitrate independent (Fig. 2.1). There are two well-studied global oxygen-responsive regulators in 2.4.3, the two-component system PrrBA and FnrL (8, 32). Expression did not change in mutant backgrounds for both PrrA and FnrL suggesting an alternative mechanism of oxygen-dependent regulation (Fig. 2.1). An analysis of the *rnap* promoter region reveals an Fnr-type site

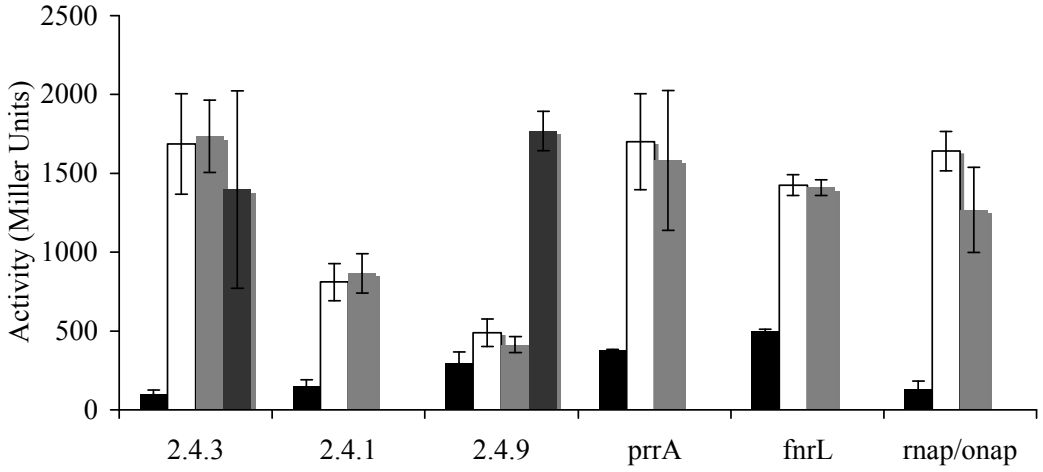

Figure 2.1: Expression of *rnap* measured by β-galactosidase activity. Black bars represent oxic conditions, white bars represent micro-oxic, light grey represent micro-oxic plus 12mM KNO_3, and dark grey represent micro-oxic plus 1mM KNO_2.

(5'- TTGATATGGATCAA-3') at -80 upstream of the translation start. In *R. sphaeroides* there are a number of Fnr-type regulators, aside from FnrL, that could potentially mediate oxygen-dependent regulation. We took advantage of the fact that each sequenced strain of *R. sphaeroides* harbors an overlapping, as well as a unique, set of Fnr-type regulators. We investigated expression of *rnap* in strains 2.4.1 and 2.4.9 to determine if the pattern of regulation is conserved across the strains, implying a conserved mechanism. In 2.4.1 the expression pattern was similar to 2.4.3, with a 5-fold increase in expression with decreasing oxygen tension. However, in 2.4.9 expression was no longer strongly induced with decreasing oxygen (Fig. 2.1). Expression was induced by nitrite under low oxygen. However, in 2.4.3 nitrite did not induce expression. Furthermore, nitrate added to the cultures is reduced to nitrite during growth, but the absence of nitrate reductase ability in a double *onap*/*rnap* mutant, resulting in the inability to make nitrite, did not change expression (Fig. 2.1). We suggest that regulation in 2.4.9 is non-native and an artifact. This brings us back to the idea of an Fnr-type regulator that is present in 2.4.3 and 2.4.1, where regulation is

conserved, and absent in 2.4.9. An analysis of the suite of Fnr-type regulators in 2.4.3 led to gene 3486 which is present with high identity (88%) in 2.4.1, and is less conserved in 2.4.9 (68%). This regulator was inactivated by Campbell insertion, and *rnap* expression was assessed. In the 3486 mutant background, *rnap* was expressed at wild-type levels under aerobic (186±3 Units), microaerobic (1973±111 Units) and denitrifying (2040±60 Units) conditions with no significant change in level of expression. This eliminates this Fnr-type regulator as the regulator of *rnap* making it possible that one of the other Fnr-type regulators controls *rnap*.

Expression of *rnap* was also investigated under photosynthetic conditions, on plates, and with varying carbon sources (data not shown). In all cases expression followed the same oxygen-dependent pattern, with no significant changes in expression level.

Expression of the *onap* operon. Expression of the *onap* operon was also assessed using a *lacZ* transcriptional fusion. In the dark in liquid culture *onap* expression decreased modestly during the transition from aerobic (1000 Units) to microaerobic growth (700 Units). This could suggest oxygen-dependent repression that is masked by residual β-galactosidase. Consistent with this, a 7-fold increase in expression was observed when cells were transitioned from photoanoxic conditions to fully oxic conditions (Fig. 2.2). A similar trend in expression was observed for strains 2.4.1 and 2.4.9, suggesting a conserved mechanism of regulation.

Expression was also monitored on plate media where the same trend in expression was observed for strains 2.4.3, 2.4.1, and 2.4.9 (Fig. 2.3). Aerobic expression was at least 8-fold higher than microaerobic expression. Expression was nitrate independent; however, the maximal level of expression under aerobic conditions was reduced by nitrate in strain 2.4.3. Interestingly, expression on aerobic plates was also significantly higher than expression in aerobic liquid culture by at least

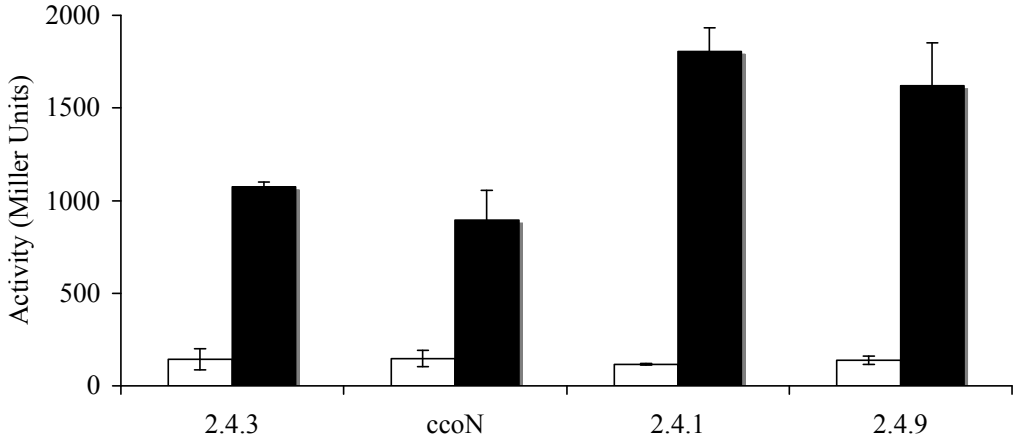

Figure 2.2: Expression of *onap* in liquid culture as measured by β-galactosidase activity. White bars represent cultures growing photosynthetically under anaerobic conditions. Black bars represent cultures that were transitioned to fully aerobic conditions.

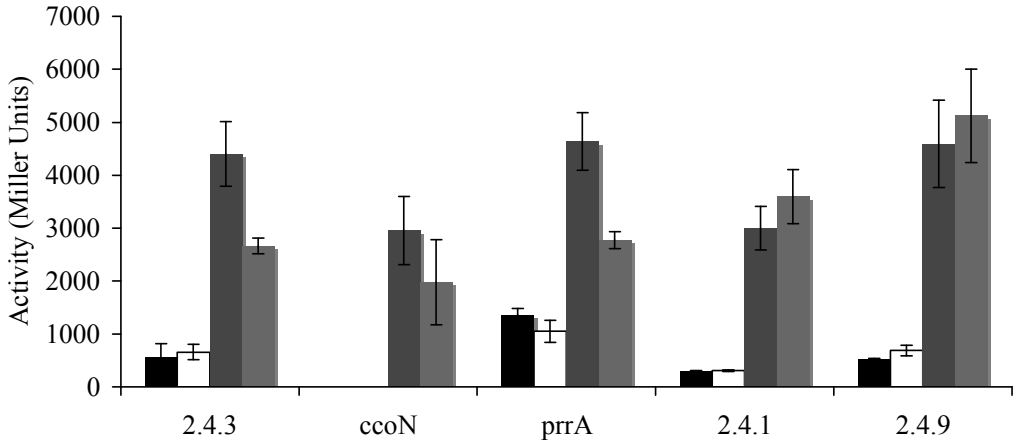

Figure 2.3: Expression of *onap* on solid plate culture as measured by β-galactosidase activity. Black bars are micro-oxic plates, white bars are micro-oxic plates supplemented with 10mM KNO_3, dark grey bars are oxic plates, and light grey bars are oxic plates with 10mM KNO_3. Note, there are no micro-oxic values for *ccoN* because this mutant cannot grow under low oxygen conditions.

4 fold. Regulatory control is most likely exerted by the PrrBA two component regulatory system, which mediates oxygen-responsive regulation in all three strains. In strain 2.4.1, microarray studies demonstrated the *onap* operon to be repressed by PrrA-P under low oxygen, and repression was relieved upon a transition to aerobic growth (1). The expression pattern in strain 2.4.3 is consistent with this mechanism of regulation.

To confirm PrrA-dependent regulation, expression was assessed in a PrrA mutant background on solid media and liquid media. On solid media under low oxygen, repression was partially relieved, resulting in a 3-fold increase over wild-type expression (Fig. 2.3). In liquid culture there was no significant difference between *onap* expression in wild-type versus *prrA* (data not shown). In addition, expression was assessed in a Δ*ccoN* mutant background. This mutant lacks the cbb_3-cytochrome oxidase, relieving the inhibitory signal to PrrB and resulting in constitutive PrrA-P in the cell (20). This may allow aerobic repression of the *onap* operon. On solid media, Δ*ccoN* had 65% of wild-type expression somewhat consistent with higher levels of PrrA-P under aerobic conditions (Fig. 2.3). In liquid culture, during anoxic photogrowth *onap* was expressed at low levels, and expression increased to levels comparable to wild-type during aerobic growth (Fig. 2.2). This is in contrast to what we would predict based on higher PrrA-P levels.

Aerobic *onap* expression on solid media is significantly higher than in liquid culture, presenting somewhat of a paradox. Studies have shown plate culture to be oxygen limiting as colony growth progresses. In fact, *Rhodobacter* has been shown to down regulate the low oxygen affinity oxidase and up regulate the high oxygen affinity oxidase during plate culture consistent with oxygen limitation (personal communication). Our model for *onap* regulation would suggest that as oxygen becomes limiting PrrA-P would repress *onap*. The fact that we observe the opposite

suggests the signal cascade controlling *onap* may be more complex and furthermore, that there may be a physiological requirement for Onap in this condition. As cells accumulate on the plates, *onap* could be regulated in a cell density dependent manner. A recent study of the quorum sensing regulon of *R. sphaeroides* 2.4.1 linked the regulator QsrR to expression of a number of redox proteins including nitrate reductase (13). Here we insertionally inactivated the homolog of *qsrR* in strain 2.4.3 and observed the effect on *onap* expression.

On solid media in the *qsrR* background, *onap* expression was identical to wild-type with expression high under aerobic conditions (3250±55 Units) and repressed under low oxygen (1350±25 Units). Expression was also identical to wild-type under photoanoxic conditions (206±12 Units) and in aerobic liquid culture (887±33 Units). It is possible that QsrR does not directly influence *onap* expression but instead influences Onap activity. However, *qsrR* has similar Nap activity to wild-type under all conditions tested.

In *Paracoccus pantotrophus onap* expression is up-regulated during growth on reduced carbon sources (7). We do not see this trend in strain 2.4.3 or 2.4.1 during growth on malate, succinate, and butyrate. Strain 2.4.3 is expressed at 3217±240 Units on malate, at 440±611 Units on succinate, and at 2111±91 Units on butyrate. Strain 2.4.1 is expressed at 4341±17 Units on malate, at 3001±409 Units on succinate, and at 2259±33 Units on butyrate. Expression is not significantly different between carbon sources and thus does not correlate with the oxidation state of the substrate.

Mutant studies. The expression studies suggest two differing physiological roles for the Naps of 2.4.3. Onap is expressed predominantly under oxic conditions, suggesting a possible link to aerobic redox homeostasis, while Rnap is expressed under low-oxygen and is presumably the major nitrate reductase used for energetic purposes.

Mutants were made in both Naps, as well as a double mutant, to study their physiological roles under varying growth conditions.

Aerobic planktonic growth. *onap* is maximally expressed aerobically and therefore is presumably assembled and functional under this condition. However, when nitrate is added to aerobically growing wild-type cells, it is not reduced to nitrite, suggesting the enzyme is present but is not linked into a functioning electron transport chain. To circumvent this problem, methyl viologen is used as an artificial electron donor, uncoupling Nap activity from endogenous electron transport. In this case, wild-type cells show significant reduction of nitrate to nitrite (Table 2.2). Because denitrification

Table 2.2: Nap activity in aerobic cultures.

Strain	Nap Present	A540nm	%wt Nap Activity
2.4.3	Onap, Rnap	0.17±0.008	100%
onap	Rnap	0.03±0.009	<20%
rnap	Onap	0.20±0.007	100%
onap/rnap	None	0	0%

is not induced aerobically, any nitrite produced is not further respired, allowing us to detect nitrite as a direct measurement of Nap activity. In contrast to wild-type, *onap* has <20% of wild-type Nap activity under aerobic conditions. In comparison, *rnap* has wild-type levels of Nap activity, and *onap/rnap* has no detectable Nap activity. This demonstrates that Onap is not only expressed aerobically but is the predominant Nap present in aerobic cells.

Aerobic colony (non-planktonic) growth. One of the observations from the expression studies was the paradox concerning elevated *onap* expression during plate culture. The Nap mutants were grown under aerobic conditions on plates with added nitrate to verify if nitrate reduction is taking place. Consistent with the expression results, 2.4.3 accumulated significant amounts of nitrite in the media (Fig. 2.4). *onap*

did not accumulate significant levels of nitrite, while *rnap* accumulated levels comparable to wild-type. Furthermore, methyl viologen Nap assays showed that *onap* cells had very low Nap activity while *rnap* had wild-type levels of Nap activity. These studies have elucidated a condition where *onap* is highly expressed and functioning in the cell. This is in contrast to highly aerated planktonic growth where *onap* is highly expressed, but there is no detectable nitrate reduction. This may represent a condition where the cells require an electron sink for redox balancing. If that is the case, different carbon sources may influence the need for redox balancing.

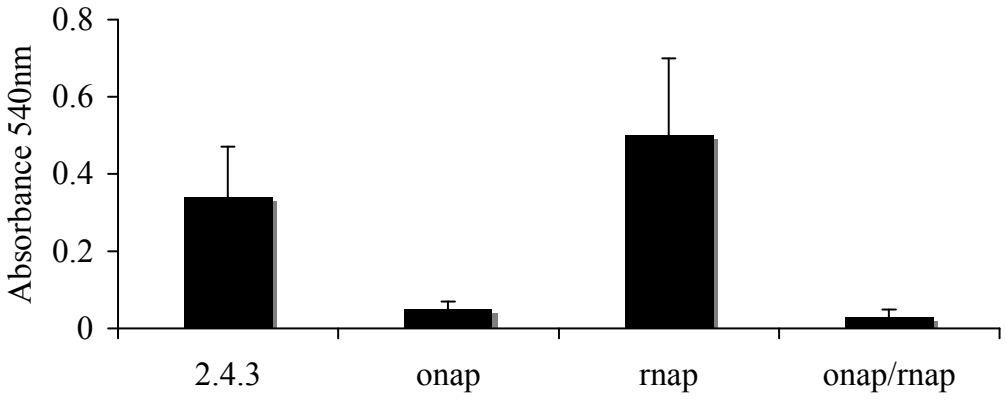

Figure 2.4: Nap activity detected by the production of nitrite on aerobic culture plates.

Growth on different carbon sources. Strains 2.4.3 and 2.4.1 were grown on different carbon sources with nitrate in the media. Strain 2.4.1 has only oNap and therefore may display Nap activity in these conditions, serving as a comparison to 2.4.3. If Nap activity is required for redox balancing this will result in nitrite production and the amount of nitrite may correlate with the requirement for redox balancing. The carbon sources used were malate, succinate, butyrate, lactate, and pyruvate. In general, we considered malate as an oxidized C-source, succinate as our baseline C-source, and butyrate as the more reduced C-source. Lactate was also compared to pyruvate as the

more reduced to oxidized source, respectively, with both being more reduced than succinate.

Based on the genome sequences of strains 2.4.3 and 2.4.1, they should have the same capabilities for growing on the selected C-sources. However, 2.4.3 grows noticeably slower on pyruvate and butyrate, regardless of the presence or absence of nitrate, and malate, but only in the presence of nitrate. After successive culturing on each respective C-source, growth could be modestly enhanced on both butyrate and pyruvate, but strain 2.4.3 continued to grow slowly on malate with nitrate amendment. In contrast, strain 2.4.1 grew robustly on all C-sources, with only slight defects on butyrate and pyruvate. The unexplained differences in C-source preference makes the comparison of oNap activity between the strains informative. The results with 2.4.3 can be compared to 2.4.1 to verify the phenotype is Nap-dependent and not a result of poor growth.

Both 2.4.3 and 2.4.1 accumulate more nitrite when grown on butyrate versus succinate versus malate (Table 2.3). This correlates with the oxidation state of the C-sources. Strain 2.4.3 also accumulates a modest amount of nitrite when grown on pyruvate and lactate, with no significant difference in amount. In contrast, 2.4.1 accumulates a modest amount of nitrite when grown on pyruvate but no nitrite when grown on lactate (Table 2.3). Interestingly, both 2.4.3 and 2.4.1 accumulate high amounts of nitrite when a succinate culture is used to inoculate lactate media (data not shown). This may indicate that Nap is important when the cell switches between these

Table 2.3: Nitrite produced during growth on different carbon sources. Where the level of nitrite is represented on a scale of low (-) to high (+++).

Strain	Malate	Succinate	Butyrate	Pyruvate	Lactate
2.4.3	-	+	+++	+/-	+/-
2.4.1	-	+/-	+++	+/-	-

two C-sources. However, when aerobic cells in liquid culture are switched from succinate to lactate, no nitrite accumulates, suggesting the phenotype may be specific to C-source transitions during non-planktonic growth.

Denitrifying growth. The expression of *rnap* correlates with denitrification genes suggesting Rnap is the major nitrate reductase during denitrification. In fact, the *rnap* mutant had impaired ability to reduce nitrate under low oxygen denitrifying conditions (Fig. 2.5). The disappearance of nitrate in the culture was monitored using the szechrome reaction for detection of nitrate. Importantly, these cultures are started aerobically, and so the first 15-20 hours represents aerobic growth. The amount of nitrate reduced by *rnap* was 50% of that reduced by wild-type cells in the same conditions for the same culture duration. While the cells are not efficiently reducing nitrate, there is some nitrate reduction due to oNap as seen by comparison to *onap/rnap* where nitrate levels stay high throughout the culture duration. Eventually, oNap activity will reduce the available nitrate; however, it takes at least twice as long as wild-type, and in some cases the nitrate is never completely reduced. A comparison of wild type and *onap* shows the same rate of nitrate reduction, consistent with oNap not playing a major role in denitrification. Furthermore, under completely anaerobic dark conditions from the start of culture, where growth depends strictly on denitrification, *rnap* and the double *nap* mutant are unable to grow while wild-type and *onap* grow normally.

Photosynthetic growth under high light. When cultures of 2.4.3 are grown under low oxygen and high light, significant amounts of nitrite accumulate in the media as growth progresses. To determine the Nap responsible for this nitrite production we grew wild-type, *onap*, *rnap*, and *onap/rnap* under these conditions. The wild-type and *onap* cultures produced high amounts of nitrite while the *rnap* and *onap/rnap* cultures had significantly less nitrite accumulation. This suggests rNap is the predominant

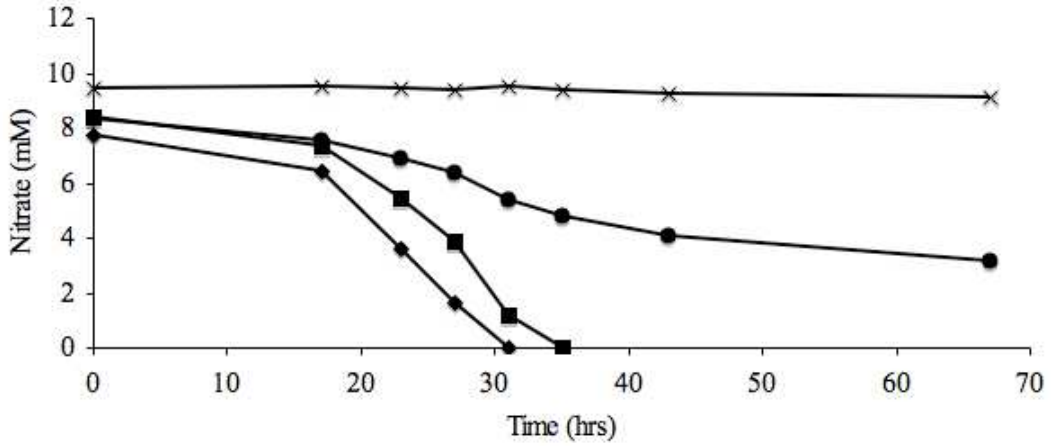

Figure 2.5: Reduction of nitrate over time in denitrifying cultures. (×) *onap/rnap* double mutant, (●) *rnap* mutant, (■) *onap* mutant, (◆) wild-type.

nitrate reductase. By following nitrite reductase activity in wild-type, we see that denitrification commences early in the growth curve, but as the pH increases during photosynthetic growth nitrite reductase activity diminishes, and nitrite begins to accumulate (data not shown). During photogrowth the pH increases from 7.0 to >9.0 before growth ceases. This suggests rNap is less sensitive to high pH than nitrite reductase and continues to reduce nitrate after denitrification ceases. In *rnap* there is a modest amount of nitrite produced by oNap that accumulates slowly over the course of the experiment. However, the amount of nitrite is 10-fold less than that produced by rNap. It is possible that there is some advantage to continuing to reduce nitrate when denitrification ceases. To test this, wild-type and *onap/rnap* were co-cultured under photosynthetic conditions with and without nitrate. After growth, cells were plated on media for wild-type and *onap/rnap* as well as on media to select for *onap/rnap*. The CFU/mL for the two strains were then compared to gauge fitness of *onap/rnap* in this condition. Both in the presence and absence of nitrate, wild-type and *onap/rnap* were found at approximately equal numbers. This suggests nitrate reduction is not conferring a significant advantage in these conditions.

Discussion

R. sphaeroides 2.4.3 has two operons encoding distinct periplasmic nitrate reductases. One of these, *onap*, encodes a Nap predicted to be involved in redox homeostasis. The *onap* operon is expressed maximally in the presence of oxygen, and expression is repressed when oxygen decreases. Expression is controlled in part by the PrrBA two-component system. However, regulation may be more complicated as expression on plates is significantly higher than expression in liquid culture. This increase in expression on plates does not correlate with our predictions on the activity of PrrBA under these conditions (20). Specifically, we predict that as cells accumulate, oxygen becomes limiting, increasing levels of PrrA-P, and repressing *onap* expression. Even in liquid culture, there is no strict correlation between the predicted presence or absence of PrrA-P and repression of *onap*. In the *prrA* background, if PrrA is the only repressor of *onap*, we would predict *onap* expression to remain high under low oxygen. However, while expression is higher than in wild-type, there is still a reduction in expression level that is independent of PrrA. In the Δ*ccoN* background, PrrA-P levels have been shown to be high under aerobic conditions (19). However, *onap* is only modestly repressed aerobically in Δ*ccoN* on plates, and not repressed at all in aerobic liquid culture. The expression of *onap* seems to be more complicated and likely requires other regulators. This is consistent with *onap* regulation in *Paracoccus pantotrophus*. In this organism *onap* is expressed aerobically and repressed under low oxygen (20). However, there is also a level of regulation linked to the oxidation state of the carbon source used for growth. When *P. pantotrophus* is grown on reduced carbon sources, like butyrate, expression increases. In fact, experiments have demonstrated the presence of alternative promoters in the region upstream of *onap* (6). One of these promoters is required for the oxygen dependent regulation, while the

second promoter is active during growth on reduced carbon sources. While we do not see any change in expression with different C-sources, there is the potential for other signals and regulators to play a role in *onap* expression. Regulation of *onap* was not carbon source dependent, but was influenced by growth planktonically versus non-planktonically. This led us to consider the potential for a quorum sensing regulator, QsrR, to regulate *onap* as suggested from strain 2.4.1 (13). In fact, we found no evidence for regulation, but this does not rule out the potential for cell density dependent regulation as there are other quorum sensing regulators in the 2.4.3 genome.

The *onap* mutant eliminated methyl viologen-dependent Nap activity in aerobic cultures consistent with oNap being the predominant aerobic Nap. oNap was also found to be responsible for the Nap activity detected during aerobic plate culture. Interestingly, there are some similarities between plate culture and a natural mode of bacterial growth, the biofilm. In both instances motility is limited, and cell accumulation results in steep gradients of nutrients and oxygen (25). On plates, there would be gradients of nutrients from the surface of the agar and oxygen from the atmosphere. Under these dynamic conditions, Onap may be useful in redox homeostasis. Nitrate reduction, as a means of redox balancing during biofilm growth, may also apply to plate culture of *R. sphaeroides*. Importantly, oNap activity on plates is not specific to strain 2.4.3 but is also found in strain 2.4.1, which has oNap. Furthermore, the activity of oNap on plates correlates with the oxidation state of the carbon source. All of these experiments together support a role for oNap in redox homeostasis especially during heterogeneous plate culture. In aerobic liquid culture, the rapid mixing may allow efficient and balanced respiration obviating the need for redox balancing via nitrate reduction.

The second operon, *rnap*, encodes a Nap involved in anaerobic respiration. Expression of *rnap* is low aerobically, where oxygen is the preferred terminal oxidant,

and increases as oxygen decreases and alternative terminal electron acceptors are required. It is likely that *rnap* is regulated in response to oxygen by an Fnr-type regulator, as the promoter contains a perfect Fnr binding site. In *E. coli*, *rnap* is expressed under low oxygen conditions with regulation mediated by Fnr (4). However, in *E. coli* there is evidence of nitrate dependent regulation as well as catabolite repression regulation (27). We were unsuccessful in identifying the specific regulator, but all of our experiments suggest that an oxygen-responsive Fnr is the primary regulatory control on the *rnap* operon.

The *rnap* mutant was unable to grow strictly by denitrification, suggesting that while oNap is present at some amount, it is not sufficient to complement for the lack of rNap. Furthermore, in low oxygen liquid culture, *rnap* consumed nitrate significantly more slowly than wild-type and *onap*. It is not clear from these experiments whether oNap can function efficiently during denitrification. An assessment is complicated by the fact that *onap* expression is repressed under denitrification conditions. It is possible that if *onap* were highly expressed it could complement for rNap. Or, it is possible that the redox poise of rNap and oNap differ, and under denitrifying conditions electron transfer to oNap is less efficient than that to rNap. In *Paracoccus pantotrophus*, where oNap is used for aerobic redox homeostasis, there is a membrane-bound nitrate reductase (Nar) that is used for denitrification (30). It is possible that the oNap of *P. pantotrophus* does not operate efficiently during denitrification. However, in *R. sphaeroides* IL106 there is an *onap*-type operon that is expressed under both aerobic conditions, presumably for redox homeostasis, as well as under anaerobic conditions, where it supports denitrification (28). This could be a case where an oNap-type enzyme is optimized to function in both roles.

It is not unusual for organisms to have multiple types of nitrate reductase. This suggests these enzymes are not one-size-fits-all. Instead, they may be tailored to the

different physiological needs for nitrate reduction. Among Nap enzymes, some of this specificity may be conferred by the accessory genes found in different operons or by differences in the core subunits NapABC (11). This makes *R. sphaeroides* 2.4.3 a good model system for studying two distinct Nap enzymes in an identical metabolic background. If oNap is tailored for redox homeostasis, the enzyme prosthetic groups may have lower reduction potentials. This would require more reduced cellular conditions for efficient electron transfer to Nap. In contrast, a respiratory Nap would most often be functioning during balanced metabolism and therefore may be fine-tuned to higher reduction potentials. This would allow rapid electron transfer to Nap from a more oxidized quinone pool, as would be present during balanced denitrifying growth. This study has demonstrated distinct physiological roles for oNap and rNap, making *R. sphaeroides* 2.4.3 an excellent system for further study on the enzymological features possibly constraining Nap physiological function.

REFERENCES

1. **Arai, H., J. H. Roh, and S. Kaplan.** 2008. Transcriptome dynamics during the transition from anaerobic photosynthesis to aerobic respiration in *Rhodobacter sphaeroides* 2.4.1. J. Bacteriol. **190:**286-299.

2. **Bru, D., A. Sarr, and L. Philippot.** 2007. Relative abundances of proteobacterial membrane-bound and periplasmic nitrate reductases in selected environments. Appl. Environ. Microbiol. **73:**5971-4.

3. **Chung, C. T., S. L. Niemela, and R. H. Miller.** 1989. One-step preparation of competent *Escherichia coli*: transformation and storage of bacterial cells in the same solution. Proc. Natl. Acad. Sci. U. S. A. **86:**2172-2175.

4. **Darwin, A. J. and V. Stewart.** 1995. Nitrate and nitrite regulation of the Fnr-dependent aeg-46.5 promoter of *Escherichia coli* K-12 is mediated by competition between homologous response regulators (NarL and NarP) for a common DNA-binding site. Journal of Molecular Biology **251:**15-29.

5. **Ellington, M. J., D. J. Richardson, and S. J. Ferguson.** 2003. *Rhodobacter capsulatus* gains a competitive advantage from respiratory nitrate reduction during light-dark transitions. Microbiology (Reading, Engl.) **149:**941-8.

6. **Ellington, M. J., W. L. Fosdike, R. G. Sawers, D. J. Richardson, and S. J. Ferguson.** 2006. Regulation of the nap operon encoding the periplasmic nitrate reductase of *Paracoccus pantotrophus*: delineation of DNA sequences required for redox control. Arch. Microbiol. **184:**298-304.

7. **Ellington, M. J., K. K. Bhakoo, G. Sawers, D. J. Richardson, and S. J. Ferguson.** 2002. Hierarchy of carbon source selection in *Paracoccus pantotrophus*: strict correlation between reduction state of the carbon substrate and aerobic expression of the nap operon. J. Bacteriol. **184:**4767-74.

8. **Eraso, J., J. Roh, X. Zeng, S. Callister, M. Lipton, and S. Kaplan.** 2008. Role of the global transcriptional regulator PrrA in *Rhodobacter sphaeroides* 2.4.1: combined transcriptome and proteome analysis. J. Bacteriol. **190:**4831-48.

9. **Gates, A. J., D. J. Richardson, and J. N. Butt.** 2008. Voltammetric characterization of the aerobic energy-dissipating nitrate reductase of *Paracoccus pantotrophus*: exploring the activity of a redox-balancing enzyme as a function of electrochemical potential. Biochem. J. **409:**159-68.

10. **Gavira, M., M. Roldan, F. Castillo, and C. Moreno-Vivian.** 2002. Regulation of nap gene expression and periplasmic nitrate reductase activity in the phototrophic bacterium *Rhodobacter sphaeroides* DSM158. J. Bacteriol **184:**1693-702.

11. **Gonzalez, P. J., C. Correia, I. Moura, C. D. Brondino, and J. J. Moura.** 2006. Bacterial nitrate reductases: Molecular and biological aspects of nitrate reduction. Journal of Inorganic Biochemistry **100:**1015-23.

12. **Gruber, N. and J. N. Galloway.** 2008. An Earth-system perspective of the global nitrogen cycle. Nature **451:**293-6.

13. **Hwang, W., K. E. Lee, J. K. Lee, B. C. Park, and K. S. Kim.** 2008. Genes of *Rhodobacter sphaeroides* 2.4. 1 Regulated by Innate Quorum-sensing Signal, 7, 8-cis-N-(Tetradecenoyl) Homoserine Lactone. J. Microbiol. Biotechnol. **18:**219-227.

14. **Jain, R. and J. Shapleigh.** 2001. Characterization of nirV and a gene encoding a novel pseudoazurin in *Rhodobacter sphaeroides* 2.4.3. Microbiology (Reading, Engl.) **147:**2505-15.

15. **Keen, N. T., S. Tamaki, D. Kobayashi, and D. Trollinger.** 1988. Improved broad-host-range plasmids for DNA cloning in gram-negative bacteria. Gene **70:**191-197.

16. **Kokotek, W. and W. Lotz.** 1989. Construction of a lacZ-kanamycin-resistance cassette, useful for site-directed mutagenesis and as a promoter probe. Gene **84:**467-471.

17. **Laratta, W., P. Choi, I. Tosques, and J. Shapleigh.** 2002. Involvement of the PrrB/PrrA two-component system in nitrite respiration in *Rhodobacter sphaeroides* 2.4.3: evidence for transcriptional regulation. J. Bacteriol. **184:**3521-9.

18. **Maniatis, T., E. F. Fritsch, and J. Sambrook.** 1982. Molecular Cloning: a laboratory manual. Cold Spring Harbor Laboratory Press, Cold Spring Harbor, NY.

19. **O'Gara, J., J. Eraso, and S. Kaplan.** 1998. A redox-responsive pathway for aerobic regulation of photosynthesis gene expression in *Rhodobacter sphaeroides* 2.4.1. J. Bacteriol. **180:**4044-50.

20. **Oh, J., I. Ko, and S. Kaplan.** 2004. Reconstitution of the *Rhodobacter sphaeroides* cbb3-PrrBA signal transduction pathway in vitro. Biochemistry **43:**7915-23.

21. **Penfold, R. J. and J. M. Pemberton.** 1992. An improved suicide vector for construction of chromosomal insertion mutations in bacteria. Gene **118:**145-6.

22. **Richardson, D. J., B. C. Berks, D. A. Russell, S. Spiro, and C. J. Taylor.** 2001. Functional, biochemical and genetic diversity of prokaryotic nitrate reductases. Cell Mol. Life Sci. **58:**165-78.

23. **Sears, H. J., G. Sawers, B. C. Berks, S. J. Ferguson, and D. J. Richardson.** 2000. Control of periplasmic nitrate reductase gene expression (napEDABC) from *Paracoccus pantotrophus* in response to oxygen and carbon substrates. Microbiology (Reading, Engl.) **146 (Pt 11):**2977-85.

24. **Simon, R., U. Priefer, and Pühler, A.** 1983. A broad host range mobilization system for in vivo genetic engineering: transposon mutagenesis in gram negative bacteria. Bio/Technology **1:**784-791.

25. **Stewart, P. S.** 2003. Diffusion in biofilms. J. Bacteriol **185:**1485-91.

26. **Stewart, V. and J. Parales.** 1988. Identification and expression of genes narL and narX of the nar (nitrate reductase) locus in *Escherichia coli* K-12. J. Bacteriol **170:**1589-97.

27. **Stewart, V., P. J. Bledsoe, L. L. Chen, and A. Cai.** 2009. Catabolite repression control of napF (periplasmic nitrate reductase) operon expression in *Escherichia coli* K-12. J. Bacteriol. **191:**996-1005.

28. **Tabata, A., I. Yamamoto, M. Matsuzaki, and T. Satoh.** 2005. Differential regulation of periplasmic nitrate reductase gene (napKEFDABC) expression between aerobiosis and anaerobiosis with nitrate in a denitrifying phototroph *Rhodobacter sphaeroides* f. sp. denitrificans. Arch. Microbiol. **184:**108-16.

29. **Tosques, I., J. Shi, and J. Shapleigh.** 1996. Cloning and characterization of nnrR, whose product is required for the expression of proteins involved in nitric oxide metabolism in *Rhodobacter sphaeroides* 2.4.3. J. Bacteriol. **178:**4958-64.

30. **Wood, N. J., T. Alizadeh, S. Bennett, J. Pearce, S. J. Ferguson, D. J. Richardson, and J. W. Moir.** 2001. Maximal expression of membrane-bound nitrate reductase in *Paracoccus* is induced by nitrate via a third FNR-like regulator named NarR. J. Bacteriol. **183:**3606-13.

31. **Yanisch-Perron, C., J. Vieira, and J. Messing.** 1985. Improved M13 phage cloning vectors and host strains: nucleotide sequences of the M13mp18 and pUC19 vectors. Gene **33:**103-19.

32. **Zeilstra-Ryalls, J. and S. Kaplan.** 1995. Aerobic and anaerobic regulation in *Rhodobacter sphaeroides* 2.4.1: the role of the fnrL gene. J. Bacteriol. **177:**6422-31.

Chapter Three

Evidence for oxygen inhibition of NnrR in *Rhodobacter sphaeroides* 2.4.3

Summary

Rhodobacter sphaeroides 2.4.3 is unable to denitrify in the absence of a functional high affinity aerobic cytochrome oxidase. Here we attempt to rationalize how denitrification can be linked to activity of an aerobic cytochrome oxidase by establishing the potential for oxygen inhibition of the denitrification regulator NnrR. A mutant in the high affinity oxidase, Δ*ccoN*, is unable to denitrify and does not express the denitrification enzymes Nir and Nor. If *nir* is expressed constitutively in this background, growth ceases, and *nor*, which is NnrR-dependent, is not expressed. However, if oxygen levels are artificially reduced to levels potentially below that of the high affinity oxidase, denitrification is wild-type in the Δ*ccoN* background. In addition, co-culture experiments show that a strain carrying the high affinity oxidase allows Δ*ccoN* to denitrify. Attempts were made to isolate an oxygen-insensitive NnrR variant; however, they were unsuccessful.

Introduction

Denitrification is the dissimilatory reduction of nitrogen oxides to gaseous end products (29). This process is utilized as an alternative respiratory mode in hypoxic and anoxic conditions and is typically secondary to aerobic respiration in the presence of oxygen. Denitrification is widespread in the biological world with members of the microbial eukaryotes, fungi, archaea, and bacteria able to exploit nitrogen oxides (23, 29). Within the bacterial world, denitrification is known to be induced via an up regulation of denitrification genes in response to low oxygen and the presence of respirable nitrogen oxides (29). The denitrification cascade follows by the sequential

reduction of nitrate or nitrite to nitrous oxide or dinitrogen gas. An obligate intermediate in this cascade is nitric oxide, produced upon nitrite reduction (29). Nitric oxide is the first gaseous intermediate and is highly toxic, thus the step of nitrite reduction commits the cells to completing the cascade by reducing nitric oxide to nitrous oxide. The critical nature of nitrite reduction is manifest in the pattern of gene regulation in many denitrifying organisms. It is not unusual for the gene or genes encoding nitrite reductase to be the pivotal point in gene regulation with multiple regulators acting (1, 3, 5, 13). In addition, the production of NO is believed to act directly as a signal for transcriptional regulators of denitrification genes (25). In *Agrobacterium tumefaciens* the gene encoding nitrite reductase, *nirK*, has two levels of regulation. First, *nirK* is regulated by ActR, a global transcriptional regulator, and then by NnrR, a denitrification specific regulator (1).

In our laboratory, we study *Rhodobacter sphaeroides* strain 2.4.3 as a model for denitrification in an anoxygenic photoheterotroph. Strain 2.4.3 has a copper nitrite reductase, encoded by *nirK*, and a nitric oxide reductase (2, 27). Previously, NnrR was established as an NO-responsive Fnr/Crp-type transcriptional regulator that regulates the genes involved in denitrification including *nirK* (11, 26). In addition, we have evidence of *nirK* regulation by the global two-component response regulatory system PrrAB, ActRS orthologs (13).

The PrrBA two-component system is well studied in *Rhodobacter sphaeroides* (6). PrrB is the histidine sensor kinase, and PrrA is the response regulator. The PrrBA system takes its signals from the redox state of the aerobic electron transport chain, namely via activity of the high oxygen affinity cbb_3 cytochrome oxidase (19). As electron flow through the chain decreases, concomitant with oxygen levels, the kinase activity of PrrB is up regulated. In turn, PrrA is phosphorylated and activates or represses hundreds of genes involved in the transition from aerobic to anaerobic

growth (6). The genes include those involved in photosynthesis, nitrogen fixation, carbon fixation, and denitrification to name a few. Research involving the interplay between the *cbb*$_3$ oxidase and PrrBA has established some general trends in signaling (17, 19). Importantly, the *cbb*$_3$ oxidase is required for inhibiting the kinase activity of PrrB. In the absence of a functional *cbb*$_3$ oxidase, PrrB constitutively phosphorylates PrrA, uncoupling the regulatory system from oxygen levels and allowing activation or repression of genes normally regulated under low oxygen conditions (17).

Currently, our model of denitrification gene regulation places *nirK* under NnrR and PrrA control in 2.4.3 (13, 26). However, previous studies showed conflicting results concerning the contribution of PrrA to *nirK* regulation. Specifically, in the absence of PrrA, *nirK* is not expressed, as expected due to PrrA being a required transcriptional activator of *nirK* (13). However, in the absence of the *cbb*$_3$ oxidase, where we predict high levels of phosphorylated PrrA due to up-regulated PrrB kinase activity, *nirK* is not expressed (13). Here we consider the regulation of *nirK* and undertake experiments to integrate these results into a model mechanism for *nirK* regulation involving both PrrA and NnrR.

Materials and Methods

Bacterial Strains and Culture Conditions. Two strains of *Rhodobacter sphaeroides* were used in this study. Strain 2.4.3 (ATCC 17025) was used as the model denitrifying strain, and the type strain 2.4.1 (ATCC 17023) was used as a non-denitrifying comparison. Mutants of these strains used in this study are listed in Table 3.1. *Rhodobacter* was cultured in Sistrom's medium at 32°C, and, when necessary, media was amended with 12mM KNO_3 to support denitrifying growth (15). Flask culture conditions have been previously described (26). Relevant antibiotics were

Table 3.1 Strains and plasmids used in this study.

Strains or plasmid	Genotype or Description	Reference/ Source
Strains		
DH5αF'	*E. coli* cloning host: F' 80 *lacZm15 redA endA1 gyrA96 thi-1hsdR17* ($r_k m_v$) *supE44 relA1 deoR* (*lacZYA–argF*)*U169*	
S17-1	For conjugal transfer of plasmids: *recA thi pro hasdRM*$^+$ *RP4:*2-Tc:*Mu:*Km:TnZ	
2.4.3	Wild-type strain of *Rhodobacter sphaeroides*	ATCC17025
2.4.1	Wild-type strain of *Rhodobacter sphaeroides*	Type strain
prrA	*prrA::aph*, 2.4.3 derivative, Km^R	(13)
ΔccoN	2.4.3 derivative with ΩSm/Sp in *ccoN*, deletion mutant	this study
Plasmids		
pUC19	Used for cloning in *E. coli* DH5-α (Ap^R)	(28)
pRK415	Broad-host-range plasmid (Tc^R)	(8)
pBBR1MCS-5	Broad-host-range plasmid (Gm^R)	(10)
pSUP202-1	Mobilizable suicide vector (Tc^R, Ap^R, Cm^R)	(24)
pKOK-6	Source of *lacZ*-Km cassette (Tc^R, Km^R, Ap^R)	(9)
pHP45Ω	Source of *aadA*$^+$-Sm^R cassette (Ap^R, Sm^R)	(22)
pNir-298	pRK415 with *nirK-lacZ* containing 298 base pairs of the *nirK* promoter (Tc^R, Km^R)	(13)
pNir-201	pRK415 with *nirK-lacZ* containing 201 base pairs of the *nirK* promoter (Tc^R, Km^R)	this study
pNir-184	pRK415 with *nirK-lacZ* containing 184 base pairs of the *nirK* promoter (Tc^R, Km^R)	this study
pNir-119	pRK415 with *nirK-lacZ* containing 119 base pairs of the *nirK* promoter (Tc^R, Km^R)	this study
pNir-111	pRK415 with *nirK-lacZ* containing 111 base pairs of the *nirK* promoter (Tc^R, Km^R)	this study
pNir-93	pRK415 with *nirK-lacZ* containing 93 base pairs of the *nirK* promoter (Tc^R, Km^R)	this study
pNir-84	pRK415 with *nirK-lacZ* containing 84 base pairs of the *nirK* promoter (Tc^R, Km^R)	(13)
pNir-62	pRK415 with *nirK-lacZ* containing 62 base pairs of the *nirK* promoter (Tc^R, Km^R)	this study
ccoNKO	pSUP202-1 with *ccoN*:: Ω*aadA*$^+$ (Tc^R, Sm^R)	this study
pUI2803H303A	pRK415 with *ccoNOQP*, *ccoN* mutation H303A (Tc^R)	(18)
pWLNIR	pRK415 with *prrnB'-nirK* fusion (Tc^R)	(13)

added at the following concentrations: tetracycline, 1.0 μg/mL; kanamycin, 25 μg/mL; streptomycin, 50 μg/mL; and gentamicin 20 μg/mL. *Escherichia coli* DH5-α was used for molecular cloning and transformations. *Escherichia coli* S17-1 was used for biparental matings. All *E. coli* cultures were grown in Luria-Bertani medium, and liquid cultures were grown at 32°C with aeration (16). When necessary, antibiotics were added at the following concentrations: ampicillin, 100 μg/mL; tetracycline, 10 μg/mL; streptomycin, 25 μg/mL; and kanamycin, 25 μg/mL.

Construction of Plasmids and Strains. Strains and plasmids used in this study are listed in Table 3.1. For PCR reactions, chromosomal DNA was isolated from strain 2.4.3 using the Puregene DNA Isolation Kit. All oligonucleotide primers were purchased from Integrated DNA Technologies (IDT) and are listed in Table 3.2.

Table 3.2: Oligonucleotide sequences

Oligonucleotide	Sequence (5' to 3')
nirK-201	CAGGGTACCGTTCCGGCCAACTGACCTC
nirK-184	CAGGTACCCTCGCACCCGCCGCCAATG
nirK-174	CAGGGTACCCCGCCAATGGCAC
nirK-119	CAGGTACCGTGCGACGCAGGGCCCTTG
nirK-111	GCGGTACCAGGGCCCTTGTTTTACAG
nirK-101	GCGGTACCGTTTTACAGGGTGCGAC
nirK-93	CGGGTACCGGGTGCGACATTTGCGAC
nirK-61	CGTGGTACCTGCCGGCGCTTGTTG
nirKlacZR	GACGGATCCATAGTCGCCCTCATGCAC
nirKlacZR2	GCAGGATCCAAGGGCGGAGGCACGA
ccon1-F	CGACTGCAGTCATCCGCTACGGTGTGGTG
ccon1-R	GCGGATCCGGTGACGATGAAGGCAAG
ccon2-F	GCGGATCCCATCGGCCATGTGCATTC
ccon2-R	CGGAATTCTGTAGCACATGATCAGCG

Plasmid isolation was done by the alkaline lysis method (16). Standard methods were used for restriction digests, ligations, and biparental conjugations. Transformations were done using the TSS chemical method (4).

Truncation lacZ fusions. To study the regulation of *nirK*, a series of promoter truncations were made to identify critical regions. For each expression fusion, the appropriate promoter region was amplified by PCR and subsequently cloned into pUC19 via BamHI and KpnI. This construct was confirmed by sequencing. The promoter region was then moved into the broad host range plasmid pRK415 via BamHI and KpnI. The *lacZ* cassette was added via PstI and originates from pKOK-6, which contains a *lacZ* cassette carrying a kanamycin resistance gene. These constructs were verified for orientation of the *lacZ* cassette using restriction digest mapping. The construct was then transformed into S17-1 and subsequently conjugated into 2.4.3 or relevant mutant background by biparental conjugations. For truncations the number refers to the number of base pairs upstream of the start of translation. The -201 truncation was made using primers nirk-201 and nirKlacZ, the -184 with nirK-184 and nirKlacZ, the -174 with nirK-174 and nirKlacZ, the -119 with nirK-119 and nirKlacZ, the -111 with nirK-111 and nirKlacZ, the -101 with nirK-101 and nirKlacZ, the -93 with nirK-93 and nirKlacZ, and the -61 with nirK-61 and nirKlacZ. The primer sequences are listed in Table 3.2, and primers were designed with the appropriate restriction site at the 5' end.

Δ*ccoN* mutant construct. A mutant of 2.4.3 lacking the cbb_3 oxidase was made by deleting *ccoN*, which encodes the catalytic subunit. This was achieved by double homologous recombination, with insertion of a streptomycin cassette. To allow for a double crossover event, two flanking regions of *ccoN* were amplified using the primer pairs ccon1-F/ccon1-R and ccon2-F/ccon2-R. Amplicons were cloned together into pUC19, ccon1 by PstI/BamHI and ccon2 by BamHI/EcoRI. A streptomycin resistance cassette was inserted via the BamHI site; this utilized the $aadA^+$ cassette from pHP45Ω. The entire construct was then moved into the suicide vector pSUP202-1 by EcoRI and PstI. This construct was moved into S17-1 and conjugated into 2.4.3.

Transconjugants were selected on streptomycin, subsequently screened to confirm tetracycline sensitivity, and the insertion in *ccoN* verified by PCR.

***nirK* overexpression construct.** For overexpression of *nirK*, an existing overexpression construct (pWLNIR) fusing *prrnB'* and *nirK* was moved into a new vector background, pBBR1-MCS5, by HindIII and EcoRI.

Enzyme assays. Relative gene expression levels for the *lacZ* fusions were measured as a function of β-galactosidase activity (16). Activity was determined based on three independent cultures, and values were averaged. Error bars represent one standard deviation. For experiments where expression was with respect to a specific growth phase, activity values were consistently representative of the growth phase based on optical density measurements.

Nir activity was determined using a colorimetric Nir assay (13). Activity was determined for at least three independently grown cultures. Values were averaged, and error bars represent one standard deviation.

Special culture conditions. For denitrifying growth at high rpm, flasks were grown as previously described (26, 27) at approximately 250 rpm. For denitrifying growth at low rpm, flasks were grown in the dark on a bench-top rotary shaker at approximately 50 rpm. For photo-denitrifying at high rpm, flasks were grown in a bench-top water bath shaker next to an incandescent light source. For photo-denitrifying growth at low rpm, flasks were grown on a bench-top rotary shaker next to an incandescent light source.

Oxygen Experiments. This experiment was used to determine the impact of headspace oxygen levels on denitrification. Cells were grown in 125mL serum vials as follows. Solid media slants were made in serum vials using 15mL culture media, poured while the vial was sitting at an angle. Cells were then inoculated onto the slants. Vials were sealed and evacuated for 40 seconds using a vacuum pump. The

vials were then flushed with N_2 gas for 45 seconds. Vials were equilibrated to atmospheric pressure using a water filled syringe to allow trapped gas to bubble through without allowing atmospheric exchange. Leaving the gas escape syringe in place, the desired amount of atmospheric air was added back using a gas tight syringe. Finally, the gas escape syringe was removed, and the vials were incubated at 32°C in the dark. For each percent oxygen headspace, the following volumes of air were added back: 2% (11.1mLs), 1% (7.4mLs), 0.5% (3.7mLs), 0.3% (2.5mLs), 0.2% (1.2mLs), 0.1% (0.73mLs), 0.05% (0.36mLs), and 0% (no add back). The atmospheric control (20% oxygen) was vacuumed and N_2 flushed and then allowed to equilibrate with atmospheric air.

Mutagenesis. To generate random NnrR mutants, UV mutagenesis was used (20). UV mutagenesis was done on Δ*ccoN* carrying a plasmid with the *nor* promoter fused to a kanamycin resistance gene (*aph*). If NnrR becomes active (oxygen insensitive), kanamycin resistance should be conferred. This was used as a selection for mutants. Secondly, mutagenesis was done on Δ*ccoN* carrying a plasmid that constitutively expressed *nirK*. This strain seems to produce toxic levels of NO, if NnrR becomes active it should allow for growth of this strain in the presence of nitrate. Finally, spontaneous mutants were also screened for using selective culturing conditions.

Results and Discussion

***nirK* promoter truncations.** Initially, the regulation of *nirK* was investigated by a series of promoter truncations. Previous research showed wild-type expression from a 298 base pair promoter and abrogated expression from an 84 base pair promoter (13). This suggests critical regulatory elements in the promoter region spanning from -84 to -298 upstream of *nirK*. Importantly, the NnrR binding site is at -62 and is not affected by the -84 truncation, suggesting additional regulation occurring upstream of NnrR.

Our previous studies implicated PrrA as one additional regulator of *nirK* (13). In this study, each promoter truncation was fused to *lacZ*, and expression was monitored in the wild-type background under denitrifying conditions. Expression decreased with decreasing promoter length (Fig. 3.1). These results highlight a significant region in

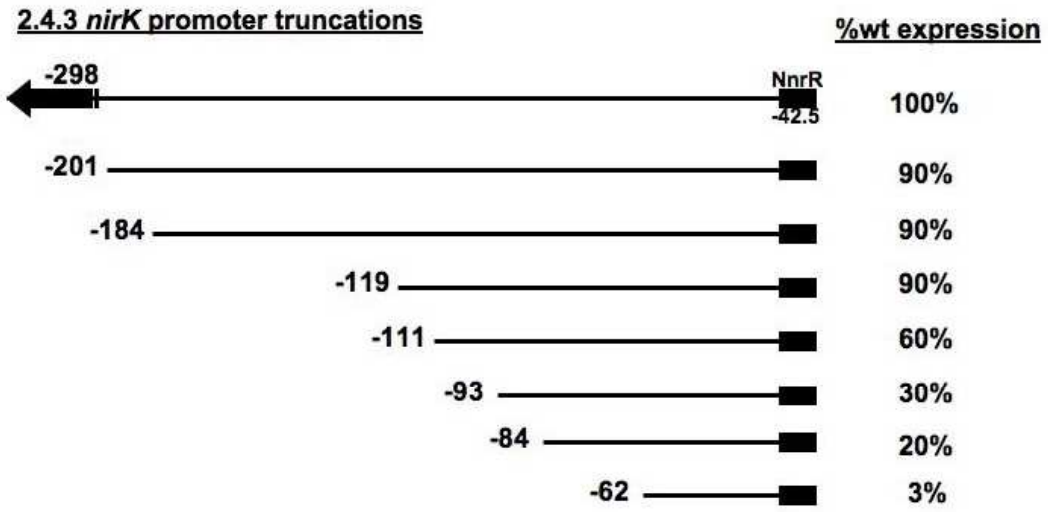

Figure 3.1: Expression from various *nirK* promoter truncations. Expression was measured as β-galactosidase activity and converted to % expression from a full length promoter (-298). The promoters are depicted up to the NnrR binding site, which is at -42.5bp from the translation start.

the promoter, where from –119 to -84 there is a significant loss in *nirK* expression. This suggests a potential regulatory element in this region. While it is difficult to predict PrrA binding sites due to low site consensus, within this region there are putative PrrA binding sites. Our current model of *nirK* regulation consists of transcriptional activation by PrrA-P, binding in the -80 to -120 region, and by NnrR binding at -62.

***nirK* expression.** Based on our model for *nirK* regulation and previous research on the PrrBA system, we sought to extend our study by investigating *nirK* expression in a *ccoN* mutant background. *ccoN* encodes the catalytic subunit of the cbb_3 cytochrome

oxidase which acts as a key signal to the PrrBA system (19). *Rhodobacter* encodes two terminal oxidases for aerobic respiration, a low affinity aa_3 oxidase and the high affinity cbb_3 oxidase. *ccoN* was inactivated by insertion of a streptomycin resistance cassette, resulting in deletion of 700 bases from the middle of the open reading frame. In the Δ*ccoN* background, *nirK* was not induced under any condition, or from any promoter truncation (data not shown). This result was previously observed with a distinct *ccoN* mutant (13). A new mutant was made for these studies as the original disruption of *ccoN* was via a single homologous recombination event (13), and this insertion was unstable and subject to reversion. In a mutant lacking a functional cbb_3-cytochrome oxidase, PrrA is predicted to be constitutively phosphorylated resulting in active PrrA under all growth conditions (17). For *nirK*, this should result in normal expression. The *ccoN* mutation does result in elevated aerobic pigmentation, characteristic of *ccoN* mutants in strain 2.4.1 (17). This indicates the mutation is impacting gene expression in 2.4.3 as seen in 2.4.1. Also, Δ*ccoN* is impaired in aerobic growth at low oxygen tension, consistent with lack of the high affinity cbb_3 oxidase. This led us to consider why *nirK* is unexpressed in the Δ*ccoN* background.

To understand *nirK* regulation, we must consider the multiple factors playing an indirect role in expression. First, *nirK* regulation is controlled indirectly by nitrate reductase expression and activity. Nitrate reductase is up-regulated by an unknown mechanism in response to decreasing oxygen levels (Hartsock and Shapleigh, unpublished). Nitrate reductase is required for production of nitrite, the substrate for Nir. Basal levels of *nirK* expression result in a small amount of functional Nir that can catalyze the reduction of nitrite to NO (27). NO then acts as a signal for NnrR, which up-regulates *nirK* along with the other denitrification genes (11). Because nitrate reduction does not take place aerobically, we would not predict *nirK* to be expressed aerobically in Δ*ccoN* even though PrrA is active. We would, however, predict that as

oxygen decreases, nitrate reductase will become active, and the signal cascade for NnrR activation will take place. Then NnrR, along with the constitutively active PrrA, would result in normal expression. We do not see this predicted result. We hypothesize that some factor of the unique physiology of Δ*ccoN* is influencing denitrification gene expression. To better understand this phenomenon, we characterized the Δ*ccoN* mutant in more detail.

Characterization of *ΔccoN*. When Δ*ccoN* was grown under standard denitrifying conditions, nitrite accumulated to high levels, and Nir activity was at basal background levels (Fig. 3.2). This is in contrast to wild-type, where nitrite is efficiently respired and never accumulates to significant levels, if it accumulates at all (13). Growth of Δ*ccoN* was also characterized under photo-denitrifying conditions. Cells were inoculated into aerobic stoppered flasks where they respired oxygen until

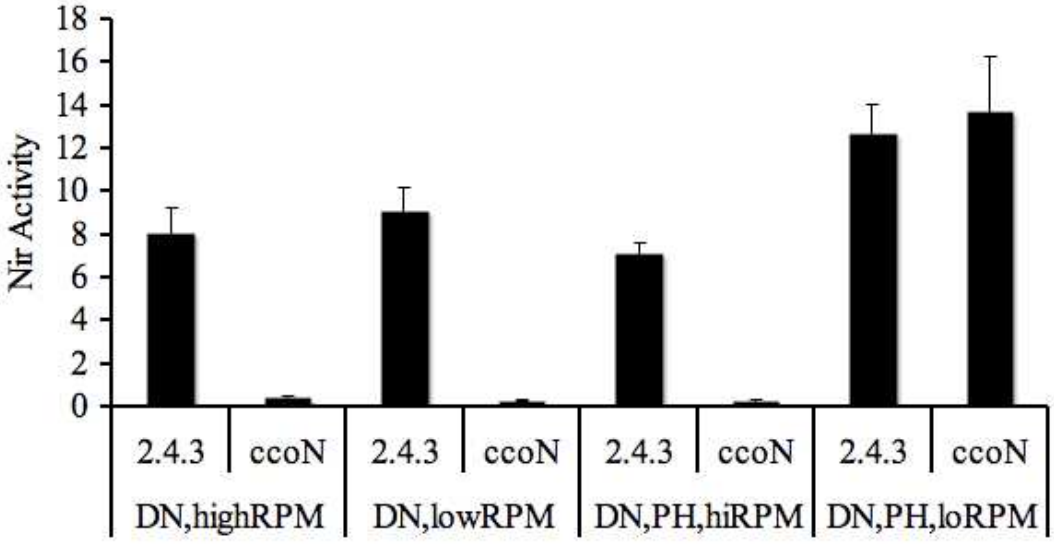

Figure 3.2: Nir activity of 2.4.3 versus Δ*ccoN*. Conditions are abbreviated below each data set and are as follows: DN is denitrifying low oxygen conditions, PH is photogrowth, hiRPM is vigorous shaking, loRPM is slow/minimal shaking.

depletion, at which point denitrification and anoxygenic photosynthesis can commence. This condition may be informative as it allows robust growth, via photosynthesis, after the aerobic growth phase. Typically under non-photosynthetic dark conditions, growth of Δ*ccoN* will begin to taper off post aerobic phase. If Δ*ccoN* encounters some energetic barrier after the depletion of oxygen and then cannot efficiently transition to denitrification, the ability to transition to robust photogrowth may restore the ability to denitrify. Our experiments show that photo-denitrifying growth with rapid mixing does not allow for Nir activity (Fig. 3.2). Nitrite accumulates to high levels despite the robust growth.

Unexpectedly, the rate of culture mixing did influence Nir activity under photo conditions. In the light, cultures that were gently mixed had wild-type levels of Nir activity at very low optical densities, while those in the dark at the same rate of mixing and optical density had no activity. This could be explained by the fact that the environment in the flask is stratified. Oxygen diffusion may be sufficiently limited from the surface of the liquid such that anaerobic conditions are experienced in the bottom of the flask, and the presence of light allows photosynthetic growth and denitrification. Together, these results show that in most conditions in Δ*ccoN*, the respiratory nitrate reductase is functional, allowing reduction of nitrate to nitrite upon decreasing oxygen tension. This suggests the block in denitrification is occurring at the level of Nir activity or *nirK* expression.

To investigate the potential for Nir activity in Δ*ccoN*, YSW35+nirK was conjugated into Δ*ccoN*. YSW35+nirK is a plasmid carrying the *nirK* ribosome binding site and open reading frame under *prrnB'* control. This results in constitutive expression of *nirK* and uncouples Nir activity from *nirK* expression. In Δ*ccoN* with constitutive *nirK* expression, the presence of nitrate severely inhibits aerobic growth (Fig. 3.3), and *nor* is not expressed (data not shown). Nir is present and functional as

evidenced by reduction of nitrite using methyl viologen as an electron donor (Fig. 3.4). Methyl viologen-dependent activity is 10-fold higher in this strain than in Δ*ccoN*; however, whole cell activity using endogenous electron donors is at basal levels perhaps due to NO toxicity. The nitrate dependent growth inhibition suggests that nitrate is being reduced to nitrite and then further reduced to NO by the constitutive presence of Nir. The lack of *nor* expression results in no Nor enzyme to further reduce the toxic NO, leading to growth inhibition.

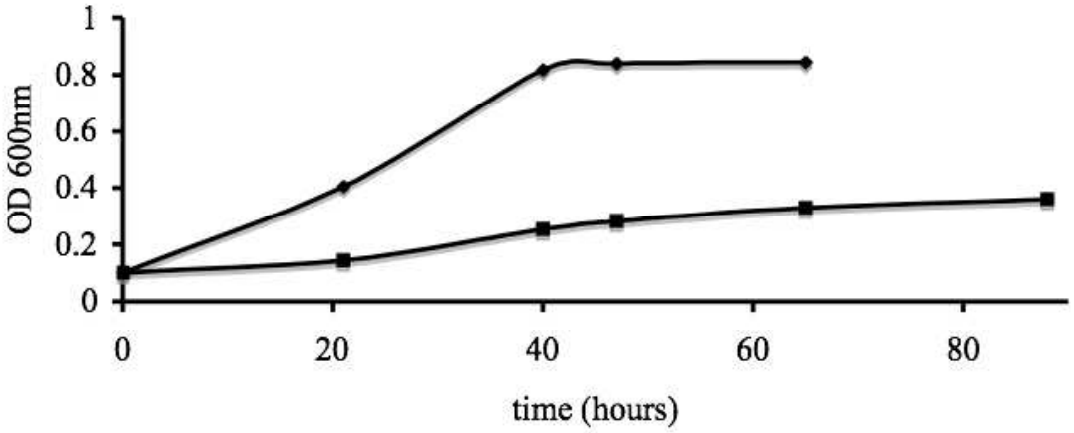

Figure 3.3: Growth curve of Δ*ccoN* with constitutively expressed *nirK* under low oxygen (◆) and under low oxygen with nitrate (■).

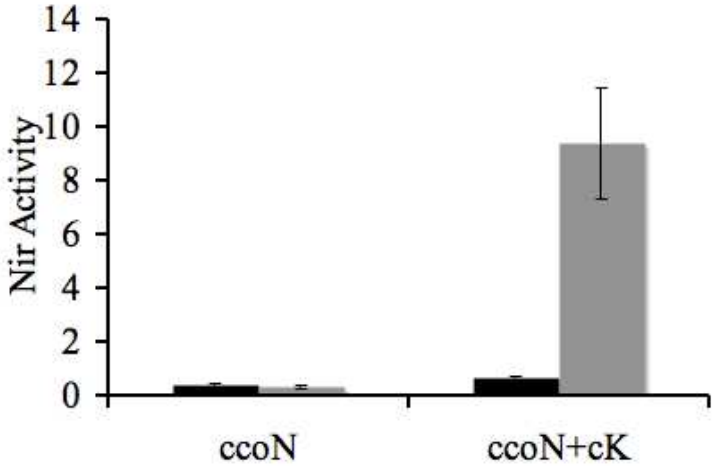

Figure 3.4: Nir activity of Δ*ccoN* versus Δ*ccoN* with constitutively expressed *nirK* (cK). Black bars represent whole cell endogenous Nir activity. Grey bars represent methyl viologen dependent Nir activity.

Importantly, NO, the signal for NnrR, is predicted to be present, yet the denitrification regulon is not induced. Previously, we have observed induction of denitrification in the absence of Nor (2). Together with the previous experiment, this shows that both *nirK* and *nor* are not expressed in Δ*ccoN*, even in the presence of Nir and NO. Regulation of *nirK* and *nor* overlaps via the shared regulator NnrR. This led us to consider whether NnrR activity is impaired in Δ*ccoN*. One possible mechanism for inhibition of NnrR is by oxygen. Δ*ccoN* is lacking the high oxygen affinity oxidase; therefore, the mutant may not be capable of respiring oxygen down to the same level as wild-type cells. We hypothesize that above a certain oxygen threshold, NnrR, even in the presence of the NO-based activating signal, is non-functional.

In *Bradyrhizobium japonicum*, which has the same two terminal oxidases as *Rhodobacter*, the high affinity cbb_3 oxidase is required for living in the practically anoxic root nodule environment (21). Studies of the oxygen affinity of the aa_3 versus the cbb_3 show that the cbb_3 has an apparent K_m for oxygen of 7nM, while that of the aa_3 is 8-fold higher (21). This suggests the cbb_3 operates efficiently at a very low range of oxygen concentration, and it is possible that NnrR is only functional within that range.

Oxygen experiments. To investigate the correlation between oxygen level and denitrification in Δ*ccoN*, a series of experiments was carried out in sealed vials with different established headspace oxygen concentrations. Wild-type 2.4.3 could grow under atmospheric (20%) oxygen down to 0% oxygen (Fig. 3.5). Wild-type cells began to denitrify at approximately 1% oxygen and below. In contrast, Δ*ccoN* grew from atmospheric oxygen down to 2%, and from 0.1% down to zero, but could not grow between 0.2% and 1% oxygen (Fig. 3.5). Importantly the growth below 0.2% was nitrate dependent, suggesting growth by denitrification. Furthermore,

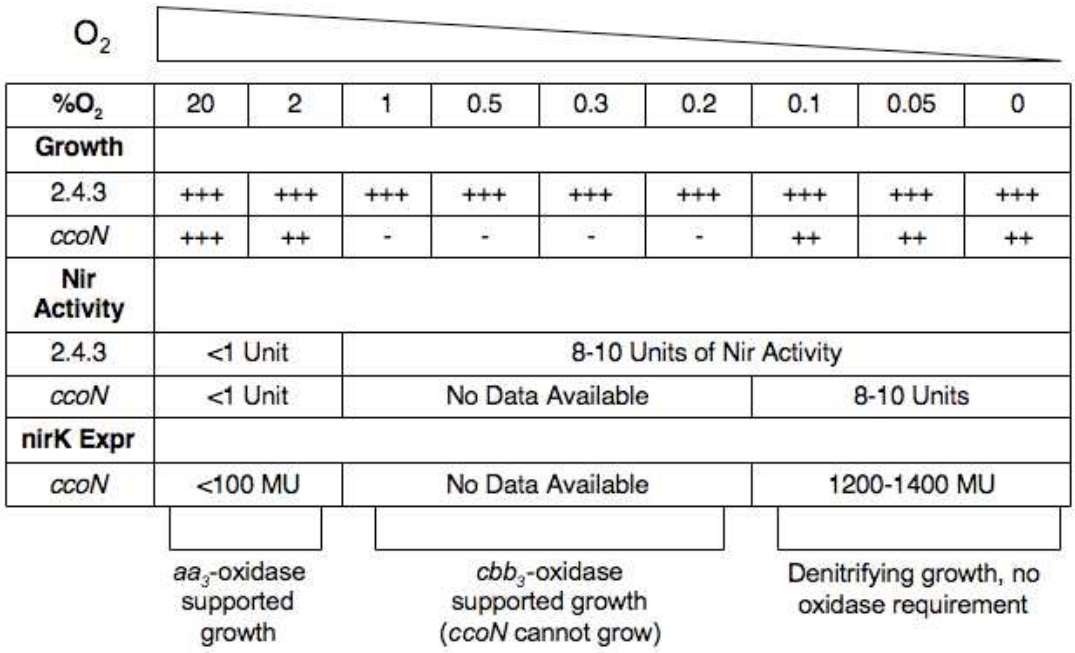

Figure 3.5: Effect of oxygen concentration on the growth and denitrification of wild-type versus Δ*ccoN*. Growth is signified by "+" signs where wild-type growth is set to "+++" and Δ*ccoN* growth is relative. *nirK* expression values in Miller Units (MU) are from a *lacZ* fusion.

these cells had wild-type levels of Nir activity. In agreement with these results, *nirK* and *nor* were expressed at wild-type denitrifying levels from 0.2% oxygen down to 0% oxygen. This suggests a gap in the transition of Δ*ccoN* cells from aerobic to denitrifying growth. Initially, the cells can respire using the low-affinity aa_3 cytochrome oxidase. However, after oxygen levels are below the affinity of this oxidase, the absence of the cbb_3 oxidase will not allow further reduction in oxygen levels, and denitrification cannot commence.

To test the idea of oxygen concentration as the determining factor in the ability of Δ*ccoN* to denitrify, a co-culture experiment was employed. The presence of an oxygen-consuming partner should allow Δ*ccoN* to transition through aerobic to denitrifying growth. Conveniently, the *R. sphaeroides* type strain 2.4.1 has identical aerobic respiration machinery but lacks the ability to denitrify (12). We used this

strain in a co-culture with Δ*ccoN*. Co-cultures were started in either a 1:3 or 3:1 ratio of wild-type 2.4.3 or Δ*ccoN* to 2.4.1 cells. In the presence of 2.4.1, Δ*ccoN* had wild-type levels of Nir activity (Fig. 3.6). This suggests the ability of 2.4.1 to respire oxygen using the cbb_3-oxidase allows Δ*ccoN* to denitrify. Of note, these experiments were carried out under photo-denitrifying conditions. In experiments done in the dark, based on CFU/mL at the end of the experiment, 2.4.1 out-competed Δ*ccoN* by 30:1. This is consistent with the inability of Δ*ccoN* to respire after the highly aerobic growth phase. These experiments implicate oxygen as an inhibitory signal for denitrification. The inhibition seems to occur at the level of *nirK* and *nor* regulation which has in common a dependence on NnrR.

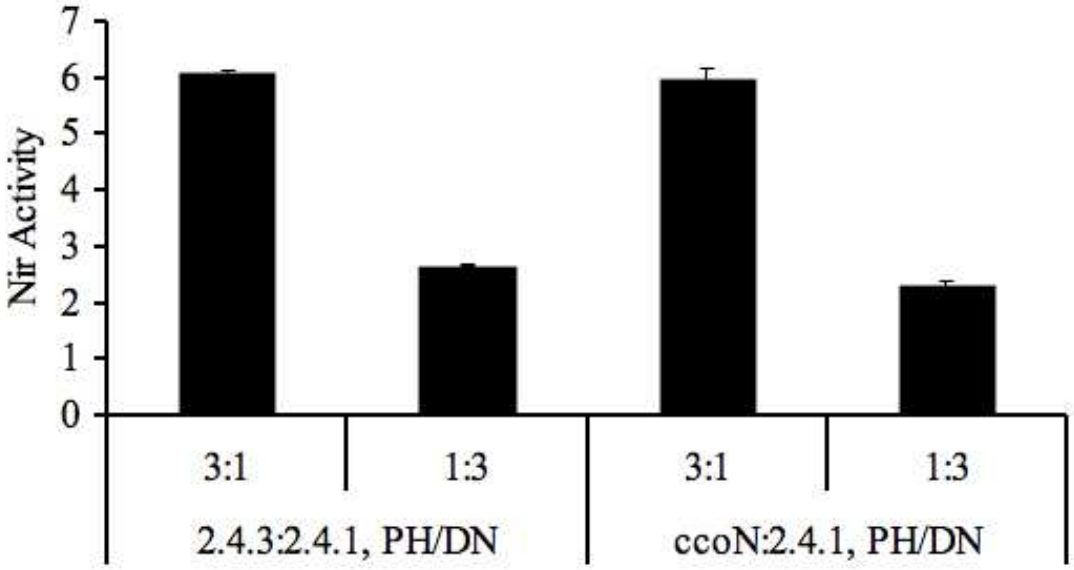

Figure 3.6: Nir activity of wild-type and Δ*ccoN* in co-culture with 2.4.1. The first data set corresponds to two different ratios of 2.4.3 to 2.4.1, and the growth condition is PH/DN (photo-denitrifying). The second data set is two different ratios of Δ*ccoN* to 2.4.1 under the same PH/DN condition.

H303A, a variant of *ccoN*. Previously, five conserved histidine residues were mutated in *ccoN* to observe the effect on catalysis and signaling to PrrB (18). One of

these histidines, residue 303, resulted in apparent retention of catalytic activity but loss of signal to PrrB when converted to alanine (18). This should allow oxygen to be efficiently respired to very low levels, while PrrA-P levels are also constitutively high. We would then predict that in Δ*ccoN* with pUI2803H303A, the plasmid carrying the variant genes coding for cbb_3, denitrification would be wild-type. In this strain, denitrification does not occur as nitrite accumulates. However, this strain is also not able to grow aerobically under low oxygen conditions in a three cycled N_2 jar, suggesting that this variant of cbb_3 may not have the same affinity for oxygen as wild-type.

NnrR mutant isolation. If NnrR is inhibited by oxygen in Δ*ccoN*, it may be possible to utilize this background for isolating mutants of NnrR with increased oxygen tolerance. This has been done for other members of the Fnr family (14). Attempts were made at both random and UV-induced mutagenesis to isolate an oxygen insensitive NnrR mutant, but we were unsuccessful. Two mutants were obtained that seemed to have an intermediate phenotype, with some low level of denitrification in Δ*ccoN*. However, sequencing *nnrR* from these strains revealed no mutations.

Conclusion

Here we have established an oxygen window where *Rhodobacter sphaeroides* 2.4.3 lacking the cbb_3 oxidase is unable to grow by aerobic respiration or denitrification. Below this oxygen window, these cells can grow in the presence of nitrate by denitrification. Importantly, cbb_3 mutant cells started aerobically are unable to respire oxygen below the threshold for Nir and Nor activity. We suggest the lack of denitrification in Δ*ccoN* is due to oxygen sensitivity of the denitrification regulator NnrR which regulates *nir* and *nor*. Although we were unsuccessful in isolating an NnrR O_2-insensitive mutant, there is precedent for this in regulators closely related to

NnrR. Studies on NNR from *Paracoccus denitrificans* show rapid inactivation of NNR upon exposure to oxygen (14). In this case, mutants of NNR were obtained that were less sensitive to oxygen and showed substantial activity in aerobic cultures. There is also indirect evidence that NNR may be a heme-based sensor. DNR, a relative of NnrR and NNR, has recently been shown to have a hydrophobic cavity that accommodates heme (7). We have the potential to learn a great deal about NnrR by analogy to the related NNR and DNR systems.

REFERENCES

1. **Baek, S., A. Hartsock, and J. Shapleigh.** 2008. *Agrobacterium tumefaciens* C58 uses ActR and FnrN to control nirK and nor expression. J. Bacteriol. **190:**78-86.

2. **Bartnikas, T., I. Tosques, W. Laratta, J. Shi, and J. Shapleigh.** 1997. Characterization of the nitric oxide reductase-encoding region in *Rhodobacter sphaeroides* 2.4.3. J. Bacteriol. **179:**3534-40.

3. **Bedmar, E. J., E. F. Robles, and M. J. Delgado.** 2005. The complete denitrification pathway of the symbiotic, nitrogen-fixing bacterium *Bradyrhizobium japonicum*. Biochem. Soc. Trans. **33:**141-4.

4. **Chung, C. T., S. L. Niemela, and R. H. Miller.** 1989. One-step preparation of competent *Escherichia coli*: transformation and storage of bacterial cells in the same solution. Proc. Natl. Acad. Sci. U. S. A. **86:**2172-2175.

5. **de Bruijn, F., S. Rossbach, C. Bruand, and J. R. Parrish.** 2006. A highly conserved *Sinorhizobium meliloti* operon is induced microaerobically via the FixLJ system and by nitric oxide (NO) via NnrR. Environ. Microbiol. **8:**1371-81.

6. **Eraso, J., J. Roh, X. Zeng, S. Callister, M. Lipton, and S. Kaplan.** 2008. Role of the global transcriptional regulator PrrA in *Rhodobacter sphaeroides* 2.4.1: combined transcriptome and proteome analysis. J. Bacteriol. **190:**4831-48.

7. **Giardina, G., S. Rinaldo, K. A. Johnson, A. Di Matteo, M. Brunori, and F. Cutruzzola.** 2008. NO sensing in *Pseudomonas aeruginosa*: structure of the transcriptional regulator DNR. Journal of Molecular Biology **378:**1002-15.

8. **Keen, N. T., S. Tamaki, D. Kobayashi, and D. Trollinger.** 1988. Improved broad-host-range plasmids for DNA cloning in gram-negative bacteria. Gene **70:**191-197.

9. **Kokotek, W. and W. Lotz.** 1989. Construction of a lacZ-kanamycin-resistance cassette, useful for site-directed mutagenesis and as a promoter probe. Gene **84:**467-471.

10. **Kovach, M. E., P. H. Elzer, D. S. Hill, G. T. Robertson, M. A. Farris, R. M. Roop 2nd, and K. M. Peterson.** 1995. Four new derivatives of the broad-host-range cloning vector pBBR1MCS, carrying different antibiotic-resistance cassettes. Gene **166:**175-176.

11. **Kwiatkowski, A. V. and J. P. Shapleigh.** 1996. Requirement of nitric oxide for induction of genes whose products are involved in nitric oxide metabolism in *Rhodobacter sphaeroides* 2.4.3. J. Biol. Chem. **271:**24382-8.

12. **Kwiatkowski, A., W. Laratta, A. Toffanin, and J. Shapleigh.** 1997. Analysis of the role of the nnrR gene product in the response of *Rhodobacter sphaeroides* 2.4.1 to exogenous nitric oxide. J. Bacteriol. **179:**5618-20.

13. **Laratta, W., P. Choi, I. Tosques, and J. Shapleigh.** 2002. Involvement of the PrrB/PrrA two-component system in nitrite respiration in *Rhodobacter sphaeroides* 2.4.3: evidence for transcriptional regulation. J. Bacteriol. **184:**3521-9.

14. **Lee, Y. Y., N. Shearer, and S. Spiro.** 2006. Transcription factor NNR from *Paracoccus denitrificans* is a sensor of both nitric oxide and oxygen: isolation of nnr* alleles encoding effector-independent proteins and evidence for a haem-based sensing mechanism. Microbiology (Reading, Engl.) **152:**1461-70.

15. **Lueking, D., R. Fraley, and S. Kaplan.** 1978. Intracytoplasmic membrane synthesis in synchronous cell populations of *Rhodopseudomonas sphaeroides*. Journal of Biological Chemistry **253:**451-457.

16. **Maniatis, T., E. F. Fritsch, and J. Sambrook.** 1982. Molecular Cloning: a laboratory manual. Cold Spring Harbor Laboratory Press, Cold Spring Harbor, NY.

17. **O'Gara, J., J. Eraso, and S. Kaplan.** 1998. A redox-responsive pathway for aerobic regulation of photosynthesis gene expression in *Rhodobacter sphaeroides* 2.4.1. J. Bacteriol. **180:**4044-50.

18. **Oh, J. I.** 2006. Effect of mutations of five conserved histidine residues in the catalytic subunit of the cbb3 cytochrome c oxidase on its function. J Microbiol **44:**284-92.

19. **Oh, J., I. Ko, and S. Kaplan.** 2004. Reconstitution of the *Rhodobacter sphaeroides* cbb3-PrrBA signal transduction pathway in vitro. Biochemistry **43:**7915-23.

20. **Pabian, L.** Ultraviolet Light Mutagenesis of *Rhodobacter sphaeroides*. murphylibrary. uwlax. edu

21. **Preisig, O., R. Zufferey, L. Thony-Meyer, C. A. Appleby, and H. Hennecke.** 1996. A high-affinity cbb3-type cytochrome oxidase terminates the symbiosis-specific respiratory chain of *Bradyrhizobium japonicum*. J. Bacteriol **178:**1532-8.

22. **Prentki, P. and H. M. Krisch.** 1984. In vitro insertional mutagenesis with a selectable DNA fragment. Gene **29:**303-13.

23. **Risgaard-Petersen, N., A. M. Langezaal, S. Ingvardsen, M. C. Schmid, M. S. Jetten, d. C. Op, J. W. Derksen, E. Pina-Ochoa, S. P. Eriksson, L. P. Nielsen, N. P. Revsbech, T. Cedhagen, and van der Zwaan,G.J.** 2006. Evidence for complete denitrification in a benthic foraminifer. Nature **443:**93-6.

24. **Simon, R., U. Priefer, and Pühler, A.** 1983. A broad host range mobilization system for in vivo genetic engineering: transposon mutagenesis in gram negative bacteria. Bio/Technology **1:**784-791.

25. **Spiro, S.** 2007. Regulators of bacterial responses to nitric oxide. FEMS Microbiol. Rev. **31:**193-211.

26. **Tosques, I., J. Shi, and J. Shapleigh.** 1996. Cloning and characterization of nnrR, whose product is required for the expression of proteins involved in nitric oxide metabolism in *Rhodobacter sphaeroides* 2.4.3. J. Bacteriol. **178:**4958-64.

27. **Tosques, I., A. Kwiatkowski, J. Shi, and J. Shapleigh.** 1997. Characterization and regulation of the gene encoding nitrite reductase in *Rhodobacter sphaeroides* 2.4.3. J. Bacteriol. **179:**1090-5.

28. **Yanisch-Perron, C., J. Vieira, and J. Messing.** 1985. Improved M13 phage cloning vectors and host strains: nucleotide sequences of the M13mp18 and pUC19 vectors. Gene **33:**103-19.

29. **Zumft, W.** 1997. Cell biology and molecular basis of denitrification. Microbiol. Mol. Biol. Rev. **61:**533-616.

Chapter Four

Expanding the NnrR/denitrification regulon of *Rhodobacter sphaeroides* 2.4.3

Summary

An analysis of the *Rhodobacter sphaeroides* 2.4.3 genome identified four new sequences similar to the previously determined NnrR binding site, and one additional gene under control of a previously identified NnrR site. Expression studies demonstrated three of the sequences are in promoters of genes in the NnrR regulon while the fourth, within the *tat* operon promoter, remains uncertain. One gene, *paz*, encodes a pseudoazurin that is an electron donor to nitrite reductase. Loss of pseudoazurin alone does not affect nitrite reductase activity, while loss of pseudoazurin and cytochrome c_2 significantly decreases nitrite reduction. Inactivation of *norEF* reduced nitrite reductase and nitric oxide reductase activity, and increased the sensitivity to nitrite as shown by a taxis assay. This may indicate increased NO production as a result of decreased nitric oxide reductase activity. Unexpectedly, *norEF* is not found in the other strains of *R. sphaeroides*, even though they all encode nitric oxide reductase. When *norEF* and *nirK* were mobilized into strain 2.4.1, the strain showed higher tolerance for nitrite than did a strain of 2.4.1 with *nirK* alone. Inactivation of the other identified genes did not reveal any detectable denitrification-related phenotype. The distribution of members of the NnrR regulon in the *R. sphaeroides* strains revealed co-selection patterns. As expected, *paz* is co-selected with *nirK*. *nnrV*, which encodes a cytoplasmic protein of unknown function, was found in all strains and may co-select with *nnrR*. Despite a lack of phenotype, the strong co-selection of these genes may indicate functional importance under real world conditions.

Introduction

Nitric oxide (NO) is a diffusible signaling molecule in both eukaryotic and bacterial organisms (6, 44). NO is also an obligatory intermediate of denitrification, the dissimilatory reduction of nitrogen oxides to nitrogen gas (51). During denitrification, NO is produced by nitrite reductase (Nir) and serves as a terminal oxidant during its reduction by nitric oxide reductase (Nor). NO is an effector of transcriptional regulators that regulate genes required for its production and consumption (39). Prokaryotes contain a diverse array of regulatory proteins whose function is modulated by NO. A number of these are members of the FNR/CRP family (44). One of these regulators, NnrR, is found most commonly in denitrifiers that utilize a copper-containing nitrite reductase, as opposed to a heme-containing nitrite reductase (23). Frequently, these bacteria are members of the α-proteobacteria and one of the best-studied NnrR proteins from a member of this group is from *Rhodobacter sphaeroides* strain 2.4.3 (46). Members of the FNR/CRP family typically bind a small molecule signal and are then activated for DNA binding (44). NnrR has not been shown to directly bind NO, however available evidence strongly suggests NO as the activating signal (12, 25). A related protein, DNR, has recently been shown to contain heme which is the likely site of NO binding (14).

R. sphaeroides 2.4.3 is a purple non-sulfur bacterium, capable of denitrification in addition to a host of metabolic attributes including aerobic respiration and anoxygenic photosynthesis. Denitrification is utilized only when oxygen is limiting and respirable nitrogen oxides, like nitrate or nitrite, are readily available (51). Oxygen controls expression of nitrate reductase (Hartsock and Shapleigh, unpublished) and has been shown to control expression of *nirK* via the global two-component response regulatory system, PrrBA (28). NnrR mediates the nitrogen oxide dependent regulation of *nirK* and *norCBQD*, the operon encoding Nor

(46). The synthesis of nitrite reductase results in the production of NO, which acts as a signal for NnrR creating a feedback loop in which enhanced NO production leads to increased expression of *nirK*. Presumably, the coordinated expression of these key denitrification enzymes is required to prevent accumulation of toxic levels of NO. In addition, NnrR activates expression of *nnrS*, a heme-copper membrane protein of unknown function (4), as well as negatively autoregulating its own expression (46). The promoters of genes under NnrR control in 2.4.3 share a common sequence (5'-TTG(C/T)GNNNNC(G/A)CAA-3') that is required for expression and is predicted to be the NnrR binding site (46). This site has a high degree of similarity to the known FNR binding site (5'-TTGATNNNNATCAA-3') supporting the assignment of the consensus sequence to NnrR (45). Mutagenesis of the predicted NnrR binding site of *nnrS* into the FNR site resulted in *nnrS* becoming a member of the FNR regulon, demonstrating the identified consensus sequence is a binding site for a member of the FNR family (4).

Genome sequencing has shown that the *R. sphaeroides* type strain, 2.4.1, is a partial denitrifier since it contains *nap*, *nor* and *nnrR* but lacks *nirK* (26). Partial denitrifiers are very common among purple photosynthetic bacteria (18). A computational analysis of the putative NnrR regulon in 2.4.1 identified NnrR binding sites upstream of *norCBQD* and *nnrS/nnrR* (39). The only other gene predicted to be part of the regulon was *hemN*. The motif in the *hemN* promoter that is similar to the FNR/NnrR consensus is made up of an upstream half-site which is a perfect FNR site, TTGAT, while the downstream half site matches the NnrR consensus. *hemN*, which is essential for photosynthesis, has been shown to be regulated in response to oxygen by FnrL (34). However, it is unknown if this gene is in the NnrR regulon.

There are currently four *R. sphaeroides* strains with sequenced genomes, the aforementioned 2.4.1 and 2.4.3 as well as 17029 and KD131 (8, 31). All four retain

nnrR and *norCBQD*. However, only 2.4.3 is capable of endogenous NO production under typical denitrification conditions, that is, high nitrate and low O_2. This is because 2.4.1 and 17029 lack *nirK* while KD131 lacks nitrate reductase. KD131 retains *nirK* but its activity requires nitrite from exogenous sources. Since a key function of NnrR is to modulate NO levels it is of interest to compare the NnrR regulons of these strains. In particular, it is of interest to determine if the NnrR regulon of 2.4.3, the only strain likely to encounter the chronic exposure to NO typical of most denitrifiers, include genes not found in the other strains. This manuscript describes experiments to identify and characterize the function of additional genes in the NnrR regulon of 2.4.3. Five new members were identified. Only one of these is present in all the other strains while one other is found only in KD131. The significance of these genes and their distribution among the various strains is discussed.

Materials and Methods

Bacterial Strains and Culture Conditions. Two strains of *Rhodobacter sphaeroides* were used in this study, the denitrifying strain 2.4.3 (ATCC 17025) and the non-denitrifying strain 2.4.1 (ATCC 17023). Mutants of these strains used in this study are listed in Table 4.1. *Escherichia coli* strain DH5-α was used for transformations, and S17-1 was used for biparental conjugations.

Rhodobacter strains were grown in Sistrom's medium (32) at 32°C, and antibiotics were added when necessary at the following concentrations: tetracycline, 1.0 μg/ml; kanamycin, 25 μg/ml; streptomycin, 50 μg/ml; and gentamicin 20 μg/ml. For denitrifying growth, nitrate (KNO_3) was added as a substrate to a final concentration of 12mM. Growth conditions have been previously described (46). All *E. coli* strains were grown in Luria-Bertani medium (33) at 32°C with aeration and, when necessary, supplemented with antibiotics at the following concentrations:

Table 4.1: Strains and plasmids used in this study.

Strains or plasmid	Genotype or Description	Reference or source
Strains		
DH5αF'	*E. coli* cloning host: F' 80 *lacZm15 redA endA1 gyrA96 thi-1hsdR17* ($r_k m_v$) *supE44 relA1 deoR* (*lacZYA–argF*)*U169*	
S17-1	For conjugal transfer of plasmids: *recA thi pro hasdRM*$^+$ *RP4:*2-Tc:*Mu:*Km:TnZ	
C58	Wild-type strain of *Agrobacterium tumefaciens*	ATCC33970
2.4.3	Wild-type strain of *Rhodobacter sphaeroides*	ATCC17025
2.4.1	Wild-type strain of *Rhodobacter sphaeroides*	Type strain
nnrR	2.4.3 derivative with ΩSm/Sp in *nnrR*; NnrR mutant	(46)
prrA	*prrA::aph*, 2.4.3 derivative, Km^R	(28)
fnrL	FnrL deficient strain of 2.4.3	(19)
nirK	*nirK*::Tn5, nitrite reductase mutant, Tp^R	(47)
cycA	*cycA*::*aph*, 2.4.3 derivative, Km^R	(27)
Δ*norEF*	2.4.3 derivative with ΩSm/Sp in *norEF*, partial deletion	this study
Δ*paz*	2.4.3 derivative with ΩSm/Sp in *paz*, partial deletion	this study
Δ*paz*/*cycA*	Double mutant, combined Δ*paz* and *cycA*	this study
Δ*nnrV*	2.4.3 derivative with ΩSm/Sp in *nnrV*, partial deletion	this study
Δ*cdg1*	2.4.3 derivative with ΩSm/Sp in *cdg1*, partial deletion	this study
Plasmids		
pUC19	Used for cloning in *E. coli* DH5-α (Ap^R)	(49)
pRK415	Broad-host-range plasmid (Tc^R)	(21)
pBBR1MCS-5	Broad-host-range plasmid (Gm^R)	(24)
pSUP202-1	Mobilizable suicide vector (Tc^R, Ap^R, Cm^R)	(43)
pKOK-6	Source of *lacZ*-Km cassette (Tc^R, Km^R, Ap^R)	(22)
pHP45Ω	Source of *aadA*$^+$-Sm^R cassette (Ap^R, Sm^R)	(38)
pAK1	pRK415 with *nirK* promoter and orf (Tc^R)	(25)
pNIR298	pRK415 with 298 bases of the *nirK* promoter fused to *lacZ*, transcriptional reporter (Tc^R, Km^R)	(28)
pIT9	pRK415 with the *nor* operon promoter fused to *lacZ*, transcriptional reporter (Tc^R, Km^R)	(46)
pYSW35	pRK415 carrying the *prrnB* ribosomal promoter (Tc^R)	(27)
pWLNIR	pRK415 with *prrnB*::*nirK* (Tc^R)	(28)

Table 4.1 (Continued)

pnirkOXP	pBBR1-MCS5 with *prrnB-nirK* fusion (Gm^R)	this study
pnorEFZ	pRK415 with *norEF-lacZ* transcriptional fusion (Tc^R, Km^R)	this study
pnorEFKO	pSUP202-1 with *norEF*:: Ω*aadA*$^+$ (Tc^R, Sm^R)	this study
pnorEF	pBBR1-MCS5 with the *norEF* operon (Gm^R)	this study
pnorE	pBBR1-MCS5 with the *norE* gene (Gm^R)	this study
ppazZ	pRK415 with *paz-lacZ* transcriptional fusion (Tc^R, Km^R)	this study
ppazKO	pSUP202-1 with *paz*:: Ω*aadA*$^+$ (Tc^R, Sm^R)	this study
ppaz	pRK415 with the *paz* gene (Tc^R)	this study
pnnrVZ	pRK415 with *nnrV-lacZ* transcriptional fusion (Tc^R, Km^R)	this study
pnnrVKO	pSUP202-1 with *nnrV*:: Ω*aadA*$^+$ (Tc^R, Sm^R)	this study
pnnrVOXP	YSW35 with *prrnB'-nnrV* fusion (Tc^R)	this study
pnnrV	pRK415 with the *nnrV* gene (Tc^R)	this study
pcdg1Z	pRK415 with *cdg1-lacZ* transcriptional fusion (Tc^R, Km^R)	this study
pcdg1KO	pSUP202-1 with *cdg1*:: Ω*aadA*$^+$ (Tc^R, Sm^R)	this study
pcdg1OXP	YSW35 with *prrnB'-cdg1* fusion (Tc^R)	this study
ptatAZ	pRK415 with *tatA-lacZ* transcriptional fusion (Tc^R, Km^R)	this study

ampicillin, 100 μg/ml; tetracycline, 10 μg/ml; streptomycin, 25 μg/ml; and kanamycin, 25 μg/ml.

Construction of Plasmids and Strains. Chromosomal DNA was isolated from strain 2.4.3 using the Puregene DNA Isolation Kit and subsequently used for PCR reactions. All oligonucleotide primers used for cloning purposes are listed in Table 4.2 and were purchased from Integrated DNA Technologies (IDT). Plasmid isolation was done by the alkaline lysis method (33). Plasmids are listed in Table 4.1. Standard methods were used for restriction digests, ligations, and biparental conjugations. Transformations into *E. coli* strains were done by the TSS method (9).

Mutant strains. *norEF* (Rsph17025_3679, 3678), *paz* (Rsph17025_2686), *nnrV* (Rsph17025_0969), and *cdgA* (Rsph17025_3576) were inactivated by deletion of a central portion of each gene, via double homologous recombination events, replacing

Table 4.2: Oligonucleotide primers used in this study.

Oligonucleotide	Sequence (5' to 3')
norE-Up	CAGGAATTCAGCACCATCGCATCGAAC
norE-lacZ	CGAGGTACCGACGATCAGGAACACCAG
norEKO1	CGGAATTCTTGCCAATGCCTCGCTGTG
norEKO4	AGACTGCAGATCGAGCGTGACACCGTTC
norF-Down	CGGGGTACCCTTGCCAATGCCTCGCTGTG
norE-R	CAGGGTACCCTCAGCTCAGCAGATAGAC
pazZ-F	GCGGAATTCAAAAGCTCGGTCATCGTGTC
pazZ-R	GCGGGATCCCCTTGTCGGTGGCCTTGAAG
pazKO1	CAGAATTCTATCCGCAGCTCGACTTC
pazKO2	CAGGATCCTCTACGGCGTCAAATGCG
pazKO3	CGGGATCCCCCTTGTTGAGCATGATG
pazKO4	CGACTGCAGTGCCGCCATACCATTCCTG
nnrVZ-F	CGACTGCAGTGGAAGGGCGCGATGGGAC
nnrVZ-R	GAGGTACCACAGGCCGCGCTTTTCC
nnrR/nnrV-F	CATCTGCAGATATCGGACCGGGGCAGCTG
nnrR/nnrV-R	GAGAATTCTGGAAGCCTGCGCCGAAT
nnrV/norC-F	CGGAATTCTGGAAGGGCGCGATGGG
nnrV/norC-R	CGACTGCAGACATAATTGTGGCTCTG
nnrVrbs+orf-F	AAGGATCCATCGGTCGGGCCTCTC
nnrVrbs+orf-R	CGGAATTCAGGGAATCGTCGAGAGCAC
cdg1Z-F	CAGCTGCAGAACTCGATCGTCACC
cdg1Z-R	CAGGAATTCGCGATCTGGAACGTCATG
cdg1KO1	AGTCTGCAGAAGTCGGACAGCCTGATGG
cdg1KO2	CAGGGATCCATCGACCGCAGCTTTGTG
cdg1KO3	CAGGATCCAGAGCGCACTGAGGAC
cdg1KO4	GAGAATTCGCGATCTGGAACGTCATG
cdg1OXP-F	CAGAATTCCTGTCCTTGCAGCTGAAG
cdg2OXP-R	CAGGTACCGGTGTGGCATCATCTAG
tatZ-F	AGACTGCAGTTGCCAACCTCGCCCATGAG
tatZ-R	GCAGAATTCTTCTCGGACATCAACGTG

it with a streptomycin resistance cassette. In each case, the suicide vector was constructed and transformed into *E. coli* S17-1. This strain was then used for conjugal transfer of the vector into *R. sphaeroides* 2.4.3 by biparental mating. For the Δ*paz*/*cycA* strain, the *paz* suicide vector was conjugated into the existing *cycA* strain. Mutant strains were verified by PCR.

The *norEF* mutant was generated by amplifying the *norEF* genomic region using the primers norEKO1 and norEKO4. The amplicon was digested with EcoRI and PstI and cloned into pUC19. The resulting clone was digested with BamHI and the streptomycin resistance cassette, *aadA*, from pHP45Ω was ligated into the vector. There are two BamHI sites in the *norEF* amplicon, resulting in deletion of 522 base pairs from the center of the operon. The resulting *norEF*::*aadA* fragment was cloned into the suicide vector pSUP202-1 via EcoRI and PstI. The *paz* mutant was generated by amplifying the ends of the gene using the primer pairs pazKO1/pazKO2 and pazKO3/pazKO4. The resulting amplicons were cloned into pUC19 by EcoRI/BamHI and BamHI/PstI, respectively. The two fragments were then joined at the BamHI site in a new pUC19 construct and *aadA* was cloned into the BamHI site. The *paz*::*aadA* fragment was then cloned into pSUP202-1 via EcoRI and PstI. The *nnrV* mutant was generated by amplifying the genomic region surrounding the gene using the primer pairs nnrR/nnrV-F, nnrR/nnrV-R and nnrV/norC-F, nnrV/norC-R. These fragments were then cloned into pUC19 by HindIII/EcoRI and EcoRI/PstI, respectively. The *aadA* cassette was cloned into the EcoRI site. The resulting *nnrV*::*aadA* construct was cloned into pSUP202-1 by HindIII and PstI. The *cdgA* mutant was generated by amplifying the genomic region surrounding the gene using the primer pairs cdgAKO1/cdgAKO2 and cdgAKO3/cdgAKO4. The resulting amplicons were cloned into pUC19 by PstI/BamHI and BamHI/EcoRI, respectively. The *aadA* cassette was then cloned into the BamHI site. The *cdgA*::*aadA* fragment was cloned into pSUP202-1 by PstI and EcoRI.

Overexpression constructs. Overexpression constructs were made using YSW35 which carries the *Rhodobacter* ribosomal RNA promoter *prrnB'*. Genes of interest, containing their native ribosome binding site and open reading frame, were cloned downstream of the *prrnB'* promoter. For overexpression of *nnrV*, primers

nnrVrbs+orf-F and nnrVrbs+orf-R were used for PCR amplification of the gene, which was subsequently cloned into YSW35 with BamHI and EcoRI. For overexpression of *cdgA*, primers cdgAOXP-F and cdgAOXP-R were used to PCR amplify the gene, which was then cloned into YSW35 by BamHI and EcoRI. For overexpression of *nirK*, an existing overexpression construct fusing *prrnB'* and *nirK* was moved into a new vector background, pBBR1-MCS5, by HindIII and EcoRI.

***lacZ* expression fusions.** Expression fusions were made by fusing the predicted promoter of the gene of interest to the *lacZ* gene. Fusions were cloned into the broad host range vector pRK415 and conjugated into relevant strains. Initially, promoters were amplified from 2.4.3 genomic DNA and cloned into pUC19. The promoter fragment was then transferred into pRK415 and the *lacZ* cassette was added using the PstI fragment of pKOK-6, which contains the *lacZ* gene in addition to a kanamycin resistance marker. The *norEF* promoter was PCR amplified using primers norE-Up and norE-lacZ and cloned via EcoRI and KpnI. We believe the annotated start site of *norE* is incorrect and we place the start 54 bases into the open reading frame. The construct contains 263 bp upstream of the predicted translation start site for *norE*. The *paz* promoter was PCR amplified using primers pazZ-F and pazZ-R and cloned via EcoRI and BamHI. The annotated start for *paz* also appears to be incorrect and we place the start 87 bases into the open reading frame. The construct contains 245 bp upstream of the predicted translation start site. The *nnrV* promoter was amplified using primers nnrVZ-F and nnrVZ-R and cloned via PstI and KpnI. The construct contains 528 bp upstream of the predicted translation start site. The *cdgA* promoter was amplified using primers cdgAZ-F and cdgAZ-R and cloned via PstI and EcoRI. The construct contains 476 bp upstream of the predicted translation start site. The *tatA* promoter was amplified using primers tatZ-F and tatZ-R and cloned via PstI and EcoRI. The construct contains 598 bp upstream of the predicted translation start site.

Complementation constructs. *norEF*, *norE*, and *paz* complementation constructs were made to confirm mutant phenotypes. In each case, the gene was PCR amplified and cloned into the broad host range vector pRK415. This construct was then conjugated into the relevant mutant background. The *norEF* complementation construct was made using primers norE-Up and norF-Down, and cloned via EcoRI and KpnI. This construct contains the entire *norEF* operon. The *norE* vector was made using primers norE-Up and norE-R, and cloned using EcoRI and KpnI. This construct truncates the *norEF* operon and only includes *norE*. The *paz* vector was made using primers pazKO1 and pazKO4, and cloned using EcoRI and PstI.

Enzymatic assays. β-galactosidase assays were used to determine relative gene expression levels and were performed as previously described (33). Activity was determined based on three independently grown cultures. Samples were taken at various time points throughout growth and the values for each relevant growth phase were averaged. Error bars represent one standard deviation.

Whole-cell Nir activity was determined according to a previously described colorimetric assay (28). Activity was determined for three independently grown cultures. Samples were taken throughout growth and the highest values were recorded. Values were averaged and error bars represent one standard deviation.

Denitrification enzyme activity was measured gas chromatographically using a GOW-MAC Series 550 thermal conductivity chromatograph with a 1m x 2mm column packed with 120/140 Carbosieve S (Supelco Inc, Bellafonte, PA). The carrier gas was helium at a flow rate of 50 mL min^{-1}. For these assays, cells were grown microaerobically with nitrate to induce denitrification. Cells were harvested at an optical density (OD_{600nm}) of 0.8-1.0, concentrated and resuspended in 5mL of Sistrom's medium containing 1mM KNO_2. The cells were sealed in 15mL vials that

were flushed with N_2 gas for 30s and then incubated with shaking at 32°C. The headspace was sampled periodically to detect production of N_2O.

Taxis assay. Taxis assays were performed as previously described (29) using nitrite plugs which contained 360mM nitrite. Experiments were done in a sealed jar under a N_2 atmosphere.

Results

Identification of potential NnrR-dependent promoters. The motif discovery program MEME was used to identify shared motifs in the *nirK*, *nor*, and *nnrS* promoters (3). As expected, one of these motifs was identical to the previously predicted NnrR binding site (46). The genome of 2.4.3 was searched for occurrences of this motif using the program FIMO (3). Motifs were eliminated that did not contain the 5'-TTGN_8CAA-3' motif conserved in members of the FNR/CRP family. MEME analysis indicated the G and C at positions 5 and 10 of the 14 base motif were conserved, so motifs without these bases were eliminated. Using these criteria, five occurrences of this motif were discovered in putative promoter regions of previously unidentified genes. No occurrences of the consensus sequence were found inside predicted protein encoding open reading frames. One of these sites, in the promoter of *nnrV*, was previously found to regulate the divergently transcribed *norCBQD* operon. The predicted motifs and adjacent genes are listed in Table 4.3. Explanations for gene names are provided below. The proximity of the binding site to the predicted start of translation for *norEF*, *paz*, *nnrV*, and *cdgA* suggest Class II type regulation by NnrR at these promoters (5). For *tatA*, the proximity of the binding site to the start of translation does not discriminate the type of NnrR regulation.

Table 4.3: Predicted members of the NnrR regulon.

Locus Tag	Gene Name	NnrR Binding Site	Position[a]
Rsph17025_3679, 3678	*norEF*	TTGCGN$_4$CGCAA	-72
Rsph17025_2686	*paz*	TTGCGN$_4$CACAA	-55
Rsph17025_0969	*nnrV*	TTGCGN$_4$CACAA	-73
Rsph17025_3576	*cdg1*	TTGCGN$_4$CGCAA	-58
Rsph17025_1983	*tatA*	TTGTGN$_4$CGCAA	-115

[a]Position is from the predicted start of translation to the NnrR binding site.

A similar search for this motif was done in the other three strains of *R. sphaeroides* whose genomes are available, 2.4.1, 2.4.9 and KD131 (8, 31). Analysis of these strains revealed NnrR consensus binding sites adjacent to *nnrR/nnrS* and *nor*. The site upstream of *nor* may also be used for expression of *nnrV*. KD131 also has an NnrR binding site upstream of a *paz* ortholog not present in 2.4.1 or 2.4.9. All three of these strains have an NnrR consensus binding site located upstream of a gene designated *bolA* (gene RSP_2952 in 2.4.1) due to its homology to the *bolA* family of morphogenes (48). While this gene is conserved in strain 2.4.3, the NnrR binding site is not present in the promoter region. Experiments using a transcriptional fusion between the promoter of *bolA* from 2.4.1 and *lacZ* showed that expression was not dependent on NnrR or nitrogen oxides (data not shown). Finally, in strain 2.4.1 there is an occurrence of the motif centered 11 bases upstream of the predicted translation start of RSP_4122. Given the unusual proximity of the motif to the start of translation, the predicted gene product being a DNA primase unlikely to be involved in nitrogen oxide respiration, and the lack of this gene in the other three strains it was not investigated further.

Expression of the identified genes in 2.4.3. To determine if the new motifs identified genes in the NnrR regulon of 2.4.3, a series of *lacZ* expression fusions were generated. Expression was monitored under oxic, microoxic and denitrifying (microoxic plus 12 mM nitrate) conditions. The expression pattern for genes under NnrR control is

denitrifying >> microoxic > oxic (46). The *norEF*, *paz*, and *nnrV* expression fusions had expression patterns consistent with their inclusion in the NnrR regulon (Fig. 4.1). To confirm this, expression was assessed in an *nnrR* mutant. As expected, expression of these genes did not increase under denitrifying conditions in the absence of NnrR. The *cdgA* fusion showed a slightly different expression pattern. As with the other NnrR regulated genes, maximal expression was observed under denitrifying conditions. However, expression only showed a modest (~20%) increase when nitrate was added to microoxic cultures. In the *nnrR* mutant, expression of *cdgA* increased under microoxic conditions, but there was no nitrate-dependent increase. The expression results suggest that a decrease in oxygen may be the predominant signal for

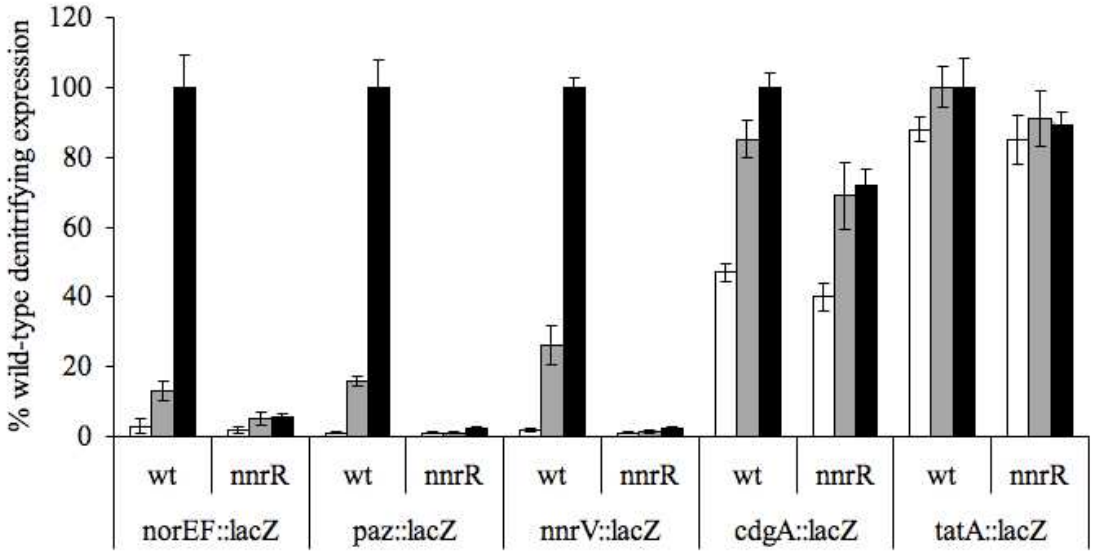

Figure 4.1: Expression of *lacZ* fusions as a percentage of wild-type denitrifying expression. For each expression fusion data for both wild-type (wt) and the *nnrR* mutant is shown. Expression was measured by β-galactosidase activity. For each condition, activity was determined in triplicate and averaged, error bars represent one standard deviation. Absolute values were converted to the percentage of wild-type denitrifying expression. White bars represent aerobic conditions, grey bars represent microaerobic conditions, and black bars represent denitrifying conditions.

increased *cdgA* expression. Two global oxygen responsive regulators in *R. sphaeroides* are PrrA and FnrL (13, 50). To test whether these regulators directly or indirectly contribute to *cdgA* expression, the fusion was mobilized into *prrA* and *fnrL* mutant backgrounds. *cdgA* expression was similar to wild type in both mutant backgrounds. In the *prrA* background expression was 139±22 Units under aerobic conditions and 215±29 Units under low oxygen conditions. In the *fnrL* background expression was 114±10 Units under aerobic conditions and 229±22 Units under low oxygen conditions. This suggests that NnrR enhances expression of *cdgA* in conjunction with some unknown oxygen-dependent regulator, but NnrR is not an absolute requirement for expression as seen for *norEF*, *paz*, and *nnrV*.

The *tatA* expression fusion showed no NnrR-dependent expression. Expression was high under all conditions and there was no significant change in the *nnrR* mutant. The *tatA* gene is part of a predicted operon, *tatABC*, that encodes the proteins required for the Tat transport system. This operon is conserved in all strains of *R. sphaeroides*, however, the putative NnrR binding site is only found in strain 2.4.3. Genes upstream of the *tat* operon are transcribed in the same orientation as *tat* indicating the putative NnrR binding site could only be involved in *tat* regulation.

norEF. The expression studies support the inclusion of *norEF*, *paz*, *nnrV*, and *cdgA* in the NnrR regulon of strain 2.4.3. These genes and their products were then further characterized. Gene 3679 was designated as *norE* due to significant similarity to other known *norE* genes in α-proteobacteria (37). Typically, *norE* is found in association with a gene designated *norF* (37). The *norF* product is not highly conserved, even among closely related bacteria, however most putative NorF proteins have two predicted transmembrane regions. Since gene 3678 encodes a small hydrophobic protein predicted to have two transmembrane regions, it was designated *norF*. There are only 3 base pairs separating *norE* and *norF* suggesting they form an operon.

NorE proteins have homology to subunit III of the cytochrome oxidase (52). This suggests NorE may associate with the Nor enzyme complex since Nor is in the cytochrome oxidase superfamily. This conclusion is supported by the observation that the *norEF* genes are commonly in close proximity to the *norCBQD* operon (37). This is not the case with 2.4.3 since *norEF* is found on chromosome II while the *nor* cluster is on chromosome I. None of the other *R. sphaeroides* strains have *norEF* despite all having the *nor* operon.

A mutant of *norEF* was made by insertional inactivation, resulting in the deletion of the last 512 nucleotides of *norE*, and the first 269 nucleotides of *norF*. The Nir activity of Δ*norEF* was about half that of wild type under microoxic conditions with and without nitrate amendment (Fig. 4.2). Reduced Nir activity was not due to a

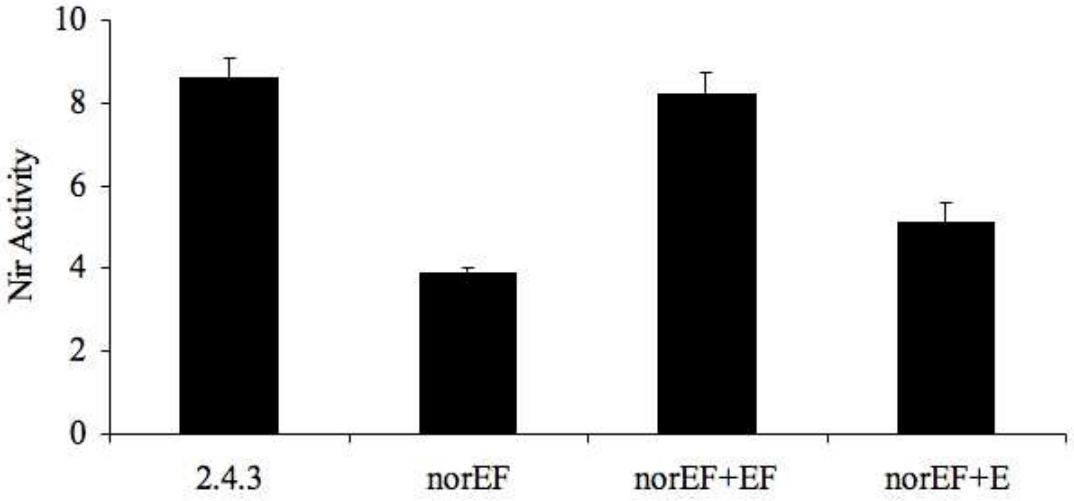

Figure 4.2: Nir activity of 2.4.3, the *norEF* mutant, complemented *norEF* (norEF+EF), and *norEF* complemented with only *norE* (norEF+E). All strains were grown under microaerobic conditions with 10mM nitrate. Values reported are the highest activity observed for each strain.

decrease in *nirK* expression since a *nirK-lacZ* fusion was expressed at wild-type levels during denitrifying growth (1442±37 Units). *nor* was also expressed at wild type levels in Δ*norEF* (868±30 Units). Wild-type Nir activity was restored in Δ*norEF* by the addition of plasmid-borne *norEF*, but not by the addition of *norE* alone (Fig. 4.2), suggesting both gene products are required for optimal denitrification in strain 2.4.3.

To gain additional insight into how the loss of *norEF* impacts denitrification, the cellular response to nitrite was assessed using a taxis assay (Fig. 4.3). Wild type 2.4.3 accumulates in a well-defined ring around a concentrated nitrite source and this behavior requires Nir activity (29). The region where cells accumulate likely corresponds to a concentration of nitrite where NO generation and consumption is

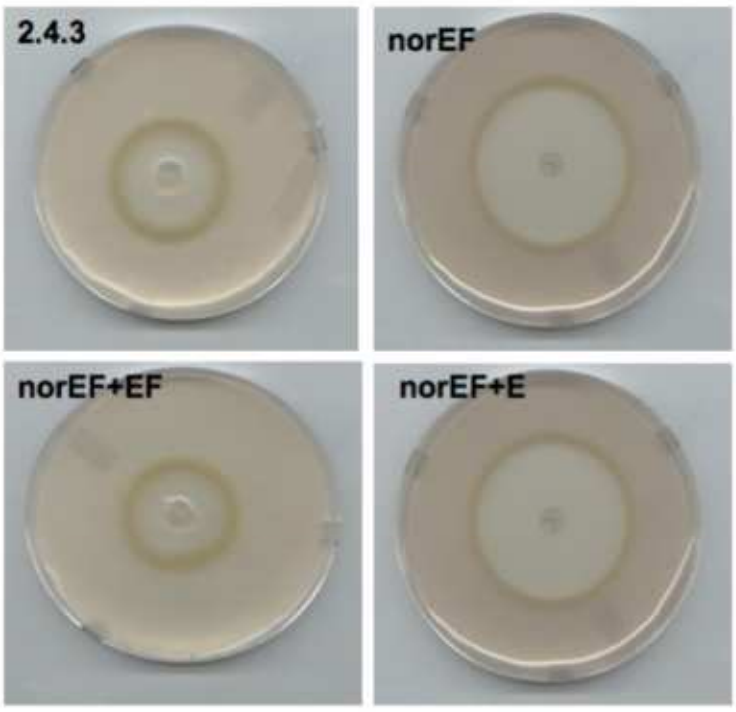

Figure 4.3: Taxis response of 2.4.3, *norEF*, and *norEF* complemented strains to nitrite. norEF+EF is the *norEF* mutant complemented with *norEF*, and norEF+E is the *norEF* mutant complemented with *norE* only. The nitrite source is an agar plug located in the middle of the plate. The ring in each plate is where cells have accumulated.

optimal. Like wild type, Δ*norEF* was found to produce a well-defined ring around the nitrite source (Fig. 4.3). However, the mutant consistently accumulated further from the source than wild type. The ring formed by wild type had a radius of 1.16±0.15cm, while the ring formed by Δ*norEF* had a radius of 2.03±0.06cm. The complementation strain containing *norEF* in trans showed a wild-type response to nitrite with a radius of 1.43±0.11cm, while cells with *norE* alone gave a radius of 2.26±0.06cm indicating both genes are needed to restore the taxis response. The taxis and Nir assays indicated that inactivation of *norEF* impacts the cell's ability to respire nitrite. This was further investigated using gas chromatography to assess the ability of the mutant to reduce nitrite to nitrous oxide (N_2O). N_2O is the major end product of denitrification in strain 2.4.3 likely due to a frame shift in gene 3318, which is a putative *nosR* ortholog (7). The wild-type strain generated N_2O rapidly over the first 10-15 minutes of incubation, after which levels did not change significantly (Fig. 4.4).

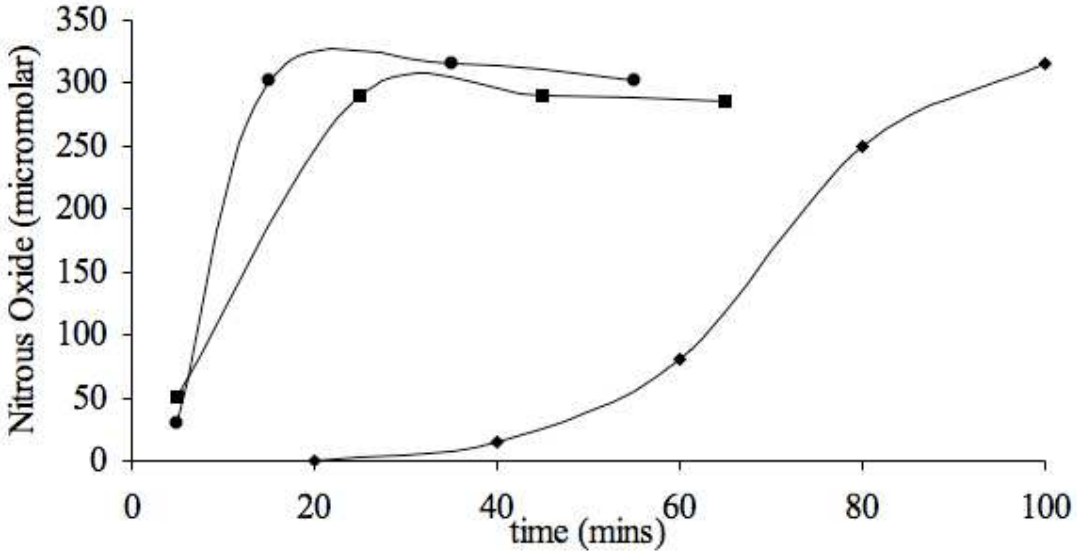

Figure 4.4: Production of nitrous oxide over time in 2.4.3 (●), Δ*norEF* (◆), and complemented Δ*norEF* (■). Cells were incubated with 1mM nitrite. The headspace was sampled over time and nitrous oxide was detected by gas chromatography.

In contrast, Δ*norEF* significantly lagged in N_2O production, taking approximately ten times longer to accumulate N_2O levels comparable to wild- type. A wild-type rate of N_2O production was restored by complementation with *norEF*.

All of the other *R. sphaeroides* strains lack *norEF*. To gain additional insight into the function of NorEF, the *norEF* genes were mobilized into strain 2.4.1 along with *nirK*. When grown under denitrifying conditions the 2.4.1/*nirK* + *norEF* strain had 2-3 fold higher Nir activity than the strain with *nirK* alone (Fig. 4.5). This is consistent with wild type 2.4.3 having a higher Nir activity than the Δ*norEF* mutant. With this similarity in behavior, it might be expected that the taxis behavior of 2.4.1/*nirK* would also be similar to Δ*norEF* and differ from that of 2.4.3 and 2.4.1/*nirK* + *norEF*. However, previous work from this lab reported that the taxis response of 2.4.1/*nirK* and 2.4.3 to nitrite were identical (29). This result was retested using a new 2.4.1/*nirK* strain generated during this work. It was found that addition of *nirK* to 2.4.1 does not, in fact, result in 2.4.3-like taxis to nitrite. Instead, 2.4.1/*nirK* showed a zone of inhibition but lacked the well-defined ring of cells at a fixed distance

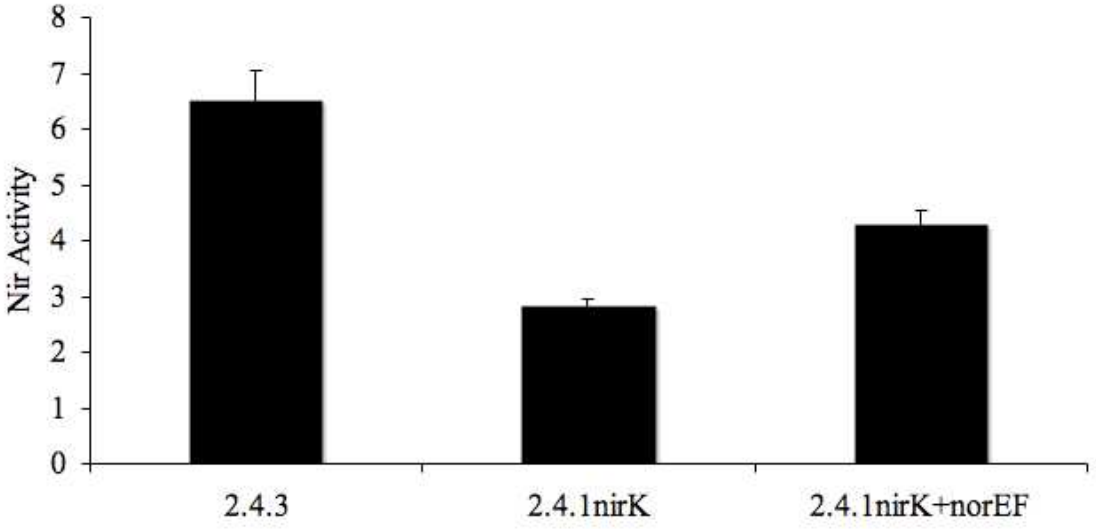

Figure 4.5: Nir activity of 2.4.1 with *nirK* and *norEF* in comparison to 2.4.3. Activity was measured under denitrifying conditions and represents maximal values.

from the nitrite source that is a hallmark of 2.4.3 taxis behavior. In addition, the distance between the center of the nitrite source and the leading edge of the zone of inhibition was 2.16±0.15cm, twice the distance measured in 2.4.3. The presence of *norEF* in 2.4.1/*nirK* reduced the distance between the source and the leading edge to 1.45±0.07cm. So, even though the taxis behavior of 2.4.1 and 2.4.3 are somewhat different the presence of *norEF* reduces the distance the cells move from the nitrite source in both strains. Reexamination of the strain used in the original 2.4.1/*nirK* taxis experiments revealed it was unable to grow on dimethylsulfoxide (DMSO) under anoxic conditions demonstrating it was derived from 2.4.3 not 2.4.1, since the latter contains a DMSO reductase while the former does not.

paz. The *paz* gene codes for the blue copper protein pseudoazurin, which in other denitrifiers is known to mediate electron transfer to nitrite reductase (36). Alignment of chromosome I of the four strains of *R. sphaeroides* revealed that *paz* in 2.4.3 is located within a region that is highly conserved in all strains. Closer examination of the genomes of 2.4.1 and 2.4.9 revealed each has a fragmented *paz* orf containing a series of deletions identical to the other and with a promoter region that does not contain an NnrR binding site (not shown). The internal deletions suggest the *paz* gene product is not functional and in 2.4.1 gene arrays, the fragment, designated as RSP_1250, is not expressed under any condition (35). In 2.4.3 and KD131, *paz* is not found in proximity to any other known denitrification genes.

In those cases where it has been examined, Nir has been found to have more than one electron donor, usually a cytochrome and a pseudoazurin (36, 51). In 2.4.3 it has been shown that cytochrome c_2 will donate electrons to Nir (27). Inactivation of the gene encoding c_2 did not result in any decrease in Nir activity, suggesting that 2.4.3 also has multiple electron donors to Nir. To determine if *paz* is involved in

electron transfer to Nir, a strain lacking *paz* as well as a strain lacking both *paz* and *cycA*, which encodes cytochrome c_2, were constructed. Δ*paz* had levels of Nir activity similar to wild type and the *cycA* mutant (Fig. 4.6). However, the strain lacking both *cycA* and *paz* had Nir activity that was greater than 10-fold lower than wild type. Nir activity was restored to near wild type levels in the double mutant if the *paz* gene was present in trans (data not shown). These results were also supported by the cell taxis response to nitrite. The double Δ*paz/cycA* mutant showed no clearing or ring formation, consistent with a lack of Nir activity (not shown) (29).

Lack of Nir activity in the Δ*paz/cycA* double mutant does not conclusively demonstrate these two proteins are the electron donors to Nir. Inactivation of *cycA* and *cycY*, which encodes cytochrome c_Y, also resulted in a >10-fold decrease in Nir

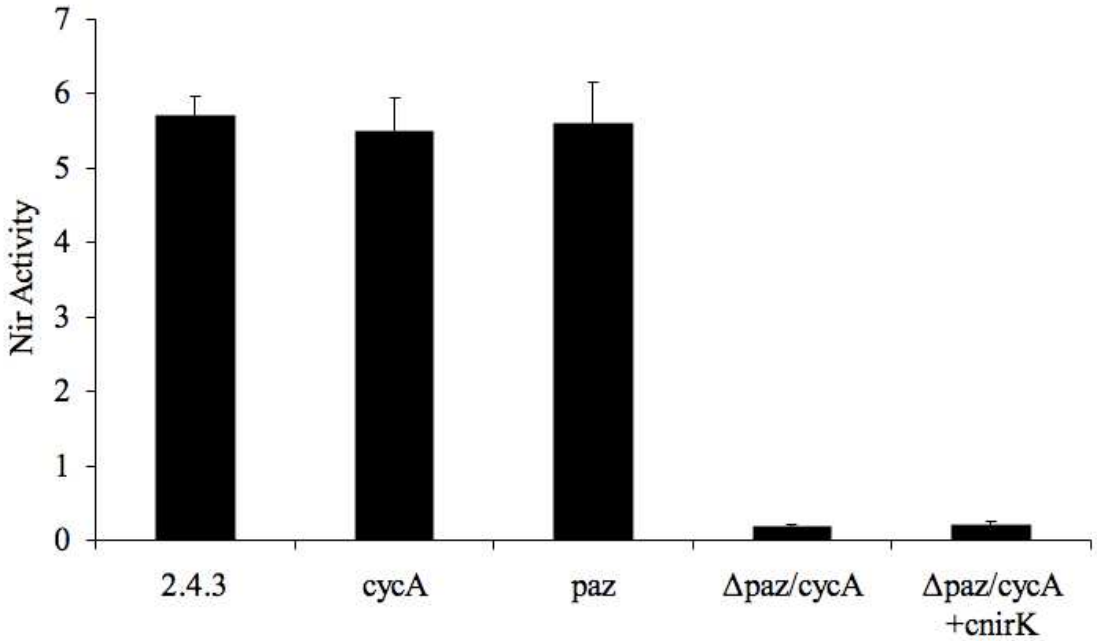

Figure 4.6: Nir activity of 2.4.3, the *cycA* mutant, the Δ*paz* mutant, the Δ*paz/cycA* double mutant, and the double mutant expressing *nirK* constitutively (+cnirK). Activity was determined for cultures grown microaerobically with 10mM nitrate.

activity (27). Expression of *nirK* from a heterologous promoter restored Nir activity in this double mutant, indicating the decrease in Nir activity was a result of a decrease in *nirK* expression not electron flow to Nir. To control for decreased *nirK* expression in the *Δpaz/cycA* strain, a construct that constitutively expresses *nirK* was mobilized into the double mutant background. Unlike the *cycA-cycY* strain, changing the regulation of *nirK* did not restore Nir activity in the *Δpaz*/*cycA* mutant, demonstrating lack of Nir activity is due to lack of suitable electron donors to Nir (Fig. 4.6).

Recent work has shown that *paz* in *A. tumefaciens* is regulated by FnrN and the ActRS two component system (2). In 2.4.3, the ortholog of the ActRS system is PrrAB and *nirK* expression has been shown to require this system (28). Expression of *paz* in 2.4.3 decreased significantly in a *prrA* mutant background to 30% of wild-type expression (Fig. 4.7). While this suggests *paz* regulation is dependent on PrrA, interpretation of this result is complicated by the fact that function of NnrR, which

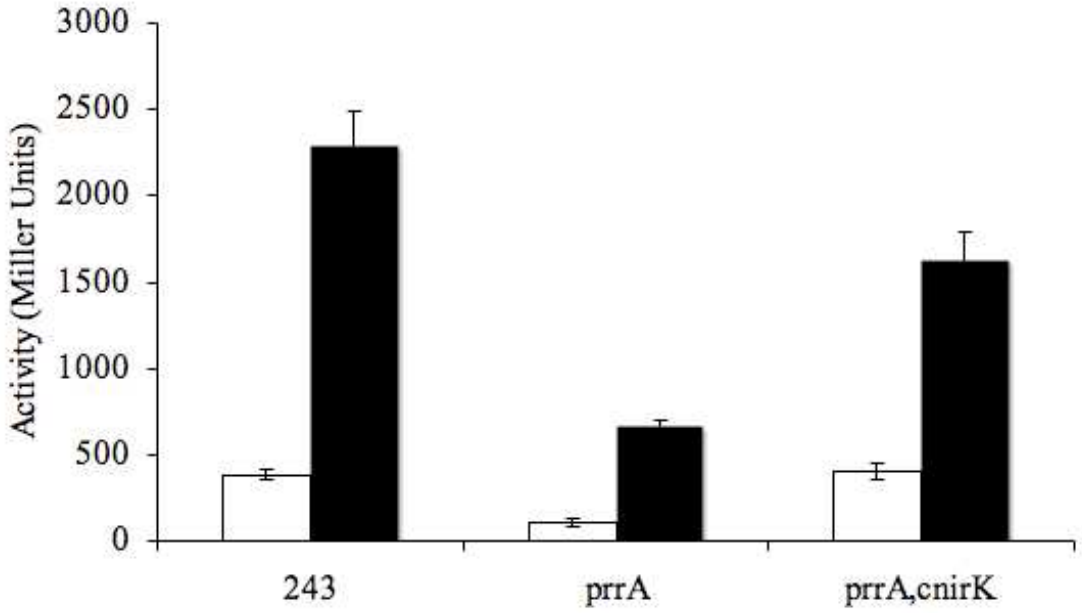

Figure 4.7: Expression of *paz* in a *prrA* mutant and *prrA* with a plasmid constitutively expressing *nirK* (cnirK). The white bars are aerobic expression and black bars are denitrifying expression.

regulates *paz*, is dependent on Nir activity. Since *nirK* expression relies on PrrA, the decrease in expression may be due to a decrease in Nir activity limiting the function of NnrR. To reduce the interdependent nature of the regulation, expression of *paz* was measured in a *prrA* mutant strain that contained constitutively expressed *nirK*. Expression of *paz* in this strain was increased to 70% of wild-type expression. These trends in expression are similar to those observed with *nor,* which is not under PrrA control in 2.4.3 (28). Therefore, it seems likely that *paz* is not under direct PrrA control.

***nnrV*.** The locus assigned in the genome sequence as 0969 does not have a known function and is not a member of a known gene family; therefore it was assigned the generic *nnr* designation since it is a member of the NnrR regulon. *nnrV* is conserved in the four sequenced strains of *R. sphaeroides* and is predicted to encode a 68 amino acid protein of unknown function. NnrV orthologs are not wide spread. Most are found in α-proteobacterial denitrifiers with a few putative orthologs in non-denitrifying clostridia. Alignment of NnrV with its putative orthologs reveals that while overall identity is low there are two cysteine residues and one methionine residue, forming a –MXCXXC- motif, that are highly conserved, indicating the potential for metal binding. Examination of the *nnrV* locus in other α-proteobacteria reveals that in almost every case *nnrV* lies within one or two genes of an FNR-type regulator and either *nirK* or *nor* genes suggesting a link with denitrification.

In order to assess the functional activity of NnrV, a deletion was made in *nnrV*. Under denitrifying conditions with nitrate as a substrate, Δ*nnrV* had wild-type nitrite reductase activity. Similarly, under denitrifying conditions with nitrite as a substrate, Δ*nnrV* had wild-type rates of N_2O production, indicating wild-type Nir and Nor activity. Consistent with the wild-type denitrifying ability, expression of the two major

denitrification reductases, *nirK* and *nor*, was identical to wild-type in the *nnrV* mutant. The *nnrV* mutant also had a wild-type taxis response to nitrite. Since there was no phenotype associated with deletion, *nnrV* was placed under control of the strong, constitutive *prrnB′* promoter to determine if overexpression might impact denitrification. However, there was no change in any of the assessed phenotypes as a consequence of changing the regulation of *nnrV*.

***cdgA*.** The gene located on Chromosome II at locus 3576 has been designated as *cdg* since it is predicted to either produce or degrade cyclic-diguanosine monophosphate (c-di-GMP) and gene A since there are multiple genes encoding proteins of this family in 2.4.3 that have yet to be characterized. *cdgA* is predicted to encode a modular protein containing four distinct domains. There are two N-terminal PAS domains, followed by a GGDEF domain and an EAL domain. The most N-terminal PAS domain is predicted to bind heme, and may confer a sensory function (15). The GGDEF domain is predicted to be functional for diguanylate cyclase activity, generating c-di-GMP (40). The EAL domain is predicted to be functional for phosphodiesterase activity, degrading c-di-GMP (41). Even though there are many proteins of this family in the *R. sphaeroides* strains there are no close orthologs of *cdgA* in the other three strains.

No growth phenotype was observed in a *cdgA* mutant strain under aerobic, denitrifying, or photosynthetic conditions (data not shown). There was also no impact on *nirK* expression or Nir activity and the taxis response to nitrite was identical to wild type. In addition, there was no detectable change in cell morphology or motility as assessed by phase contrast microscopy. It is not uncommon for inactivation of genes encoding diguanylate cyclases and phosphodiesterases to result in an undetectable phenotype. In some of these cases a phenotype was observed if the gene was overexpressed (42). However, expression of *cdgA* from the *prrnB′* promoter did not

result in a detectable phenotype and the strain had wild-type growth, morphology, and denitrification enzyme activity and gene expression. To determine if the protein encoded by *cdgA* has diguanylate cyclase or phosphodiesterase activity, an indirect means of assessing activity was employed. Previously, it has been shown that high levels of c-di-GMP promote cellulose biosynthesis in exponentially growing *Agrobacterium tumefaciens* (1). To see if *cdgA* could impact cellulose biosynthesis the *cdgA* overexpression construct was conjugated into wild-type *A. tumefaciens*, where the expression of genes from the *Rhodobacter prrnB'* promoter is constitutive (not shown). Expression of *cdgA* resulted in visible cell clumping during exponential growth under aerobic conditions. This clumping indicates increased cellulose biosynthesis likely a result of the diguanylate cyclase activity of CdgA(data not shown).

Discussion

By searching for a conserved sequence motif, five genes in strain 2.4.3 were identified and then confirmed to be within the NnrR regulon. While the function of every member of the NnrR regulon has not been determined, the function of those that have been are dedicated to denitrification and more specifically NO metabolism. This makes it likely that the size of the NnrR regulon is small. In *Neisseria meningitidis*, the NO-responsive regulator NsrR also regulates a small set of genes involved in denitrification and NO detoxification, suggesting that NO metabolism during denitrification requires only a modest sized complement of proteins (17). Members of the NnrR regulon in 2.4.3 are found on both chromosomes I and II, with most members being in single gene units or small operons. This is in contrast to many denitrifiers where denitrification genes are clustered in one area of the genome (52).

Using the MEME program, the promoter regions of all the genes identified as being in the NnrR regulon were aligned to further refine the NnrR binding motif, and to determine if there were other common motifs (3). The only inverted repeat containing motif identified in all sequences was the NnrR binding site. The conserved motif predicted using all the sequences has been extended to 20 bases in length because base 1 and base 20 are only A or T (Fig. 4.8). Since the genome of 2.4.3 is ~69% G+C, the conservation of A or T at these positions is likely to be structurally significant. The putative NnrR binding site upstream of *bolA* in strain 2.4.1 has G at these sites, perhaps explaining why it is not regulated by NnrR. By contrast, the motif identified upstream of the *tat* operon contains A at positions 1 and 20, suggesting this sequence is an NnrR binding site. The Tat transport system is important under all growth conditions, including denitrifying conditions since the Mo-pterin binding subunit of the respiratory nitrate reductase, Nir and NirV all have the twin arginine motif within their signal sequences. While expression of *tat* is essential under all conditions, it is possible the pathways regulating its expression change with changing environmental cues. This could mean that NnrR- dependent expression only occurs under unique conditions not encountered in laboratory cultures.

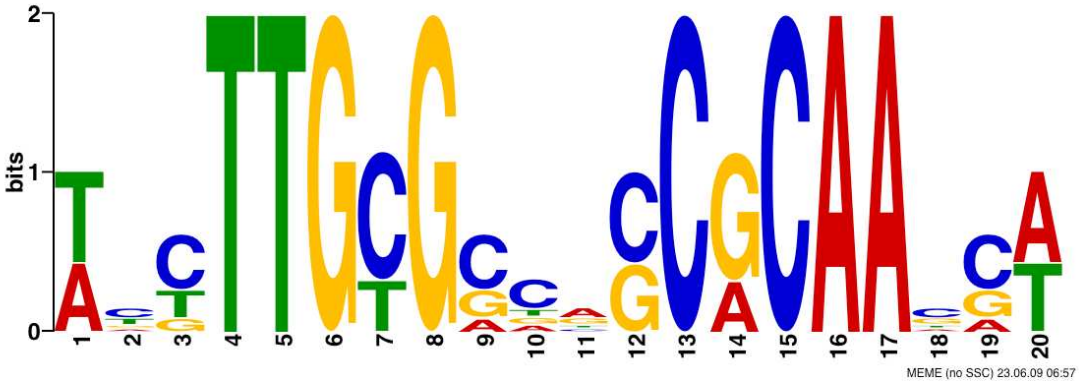

Figure 4.8: The NnrR binding site predicted by aligning the promoters of known NnrR-dependent genes. The motif was generated by the MEME program (3).

While the 20 base motif is likely the optimal NnrR binding site, other sequences may also be associated with some degree of NnrR regulation. One example of a different motif that could be recognized by NnrR is the hybrid FnrL/NnrR sites found upstream of genes such as *ppaZ* (see below) and *hemN*. Previous work has suggested *ppaZ* may be weakly activated by NnrR, but that FnrL is the more important regulator (19). FIMO analysis predicts five sites of this type located in positions that could be consistent with regulation of nearby genes.

While the size of the regulon has been extended, the function of only one of these new members has been definitively assigned. Pseudoazurin was demonstrated to be an electron donor to Nir, along with cytochrome c_2. The involvement of both a heme and copper protein in electron transfer to Nir has been observed in other denitrifiers (36). In 2.4.3, c_2 is more catholic in its function, being involved in electron transfer during both aerobic and anaerobic respiration, as well as photosynthesis (10, 16, 27). The absence of *paz* in strains with *nor*, but not *nirK*, suggests this protein is not involved in NO reduction. Similarly, the fact that strains with *nirK* retain *paz* suggests that pseudoazurin is a preferred electron donor to Nir. However, under standard non-photosynthetic, denitrifying conditions there was no evidence that Paz is a preferred donor, since there was no change in Nir activity in a Δ*paz* mutant, probably because c_2 was present. Even under photosynthetic conditions, where c_2 should be heavily used to support cyclic electron transfer, the Δ*paz* mutant had Nir activity equivalent to wild type (data not shown). As long as c_2 is present, it seems to function as well as Paz but there may be as of yet unidentified conditions where Paz is the predominant donor to Nir.

While only two strains retain *paz*, all four sequenced *R. sphaeroides* strains contain a *paz* ortholog, termed *ppaz*. Naturally occurring mutations in this gene result

in a protein that cannot bind copper and therefore cannot be used for redox purposes (19). In both 2.4.3 and KD131, *ppaz* is located adjacent to *nirK*. Analysis of the genomes of 2.4.1 and 17029 suggests that as these strains evolved *nirK* was lost via a deletion that did not affect *ppaz* (19). This loss of *nirK* may have led to the loss of *paz* since it is not required for other functions. *ppaZ* is highly expressed under microoxic conditions in both 2.4.1 and 2.4.3, suggesting the PpaZ protein is being produced (19). Evidence the protein is performing some function is provided by the high identity of the protein sequence (>90%) among the four strains. This high level of identity indicates functional constraints are limiting mutational drift.

The only other locus whose function could be linked to denitrification was *norEF*. Compared to wild type, strains lacking NorEF preferred areas of the plate with lower nitrite concentrations in the taxis assay. As shown by the absence of any taxis response in the Δ*paz/cycA* double mutant, neither nitrite nor an inactive nitrite reductase will generate a taxis response (29). This indicates the response requires the production of NO, a well-known inhibitor of respiration. In this assay, cells accumulate where respiration is optimal, which likely reflects the region of the plate where conditions allow a high rate of electron flow to the terminal oxidant, without accumulation of inhibitory compounds like NO. The preference of the Δ*norEF* mutant for regions with lower nitrite concentrations indicates higher nitrite levels lead to suboptimal respiration, possibly due to NO accumulating to inhibitory levels. One possible scenario explaining this response is that NorEF is required for optimal Nor activity. In their absence, Nor would be less active, leading to accumulation of NO and reducing the overall respiration rate. Attempts to demonstrate high levels of NO in Δ*norEF* cells using the NO sensor Cu-fluorescein were unsuccessful (data not shown) (30). However, high levels of NO produced by a Nor mutant were detectable. This does not invalidate this hypothesis however, since NO is preferentially soluble in

membranes (20), and the increase required to observe the phenotype might be small. Another scenario is that NorEF allows both Nor and the cbb_3 oxidase, both members of the heme copper oxidase family to which a protein like NorE might bind, to remain functional at the higher NO levels occurring during denitrification. This scenario would also result in decreased Nor activity, but it would also directly impact activity of the cbb_3 oxidase perhaps contributing to the taxis observations.

Another phenotypic change associated with inactivation of *norEF* was a decrease in Nir and Nor activity (Figs. 2 and 4). Previous studies of *norEF* from *Paracoccus denitrificans* also noted a decrease in denitrifying enzyme activity, specifically Nir and Nor activity, in the absence of NorEF (11). A coordinate decrease in Nir and Nor activity alone would seem unlikely to lead to the altered taxis response. In Δ*norEF* the rate of disappearance of nitrite, measured by the Nir assay, and rate of appearance of product, N_2O, measured by gas chromatography suggests an imbalance in their activities relative to the rates seen in wild type. In the Nir assay nitrite is reduced at half the wild-type rate. In contrast, N_2O is produced almost 10-fold more slowly from nitrite in the absence of *norEF*. The relative differences in the changes in Nir and Nor activity upon loss of *norEF* are consistent with a condition where NO would accumulate, accounting for the observed taxis response.

In *nirK*-containing α-proteobacteria, genomic analysis shows that *norEF* has strong genetic linkage to the *norCBQD* operon, with *norEF* being immediately upstream or downstream of *norCBQD*. For example, the five denitrifying members of the *Rhizobiaceae* all have *norEF* immediately upstream of *norCBQD*. The one exception for this linkage is in the family *Rhodobacteraceae*, where all members with *nirK* and *norCBQD*, except 2.4.3, lack *norEF*. There are several members of this family that have a heme-type Nir and *norCBQD*, such as *P. denitrificans*, and all have *norEF*. In this subgroup, *norEF* is located immediately downstream of the *norCBQD*

operon. *R. sphaeroides* shows no evidence of ever having *norEF* in the vicinity of the *norCBQD* operon. The absence of *norEF* indicates that either the last common ancestor of these strains acquired a *norCBQD* operon lacking *norEF*, or the deletion of *norEF* from the vicinity of the *nor* operon was complete. If the latter occurred, it is possible a chromosomal rearrangement resulted in the transfer of *norEF* to chromosome II, after which it was lost from the three partial denitrifiers. Unlike *nirK* and *paz*, however, there is no remnant of *norEF* in these bacteria to provide support for this hypothesis. The fact that *norEF* is located on chromosome II may support *norEF* being acquired by lateral gene transfer. Recent work suggests chromosome II is evolving more rapidly than chromosome I, and that lateral gene transfer from organisms with similar GC content is relatively frequent (8). Acquisition of *norEF* via lateral gene transfer would explain why 2.4.3 is the only member of the *Rhodobacteraceae* family with both *nirK* and *norEF*. Since *norEF* has a significant impact on the denitrification ability of 2.4.3, it would provide a selectable benefit and likely be retained. In 2.4.1 and 17029, which lack *nirK* and where Nor is likely used to mitigate the toxic effects of NO, it is possible the lack of *norEF* could actually be advantageous. The lack of *norEF* may enhance the NO stress response, ensuring that cells avoid environments with high levels of NO. The same would be true of KD131 except it would be responsive to both nitrite and NO, since it retains *nirK*.

The only gene identified here that is present in all four strains is *nnrV*. NnrV is also unique in that it is predicted to be located in the cytoplasm. This indicates it is not likely to be directly involved in reduction of nitrogen oxides. The only protein in the NnrR regulon shown to be important for denitrification and located in the cytoplasm is NnrR itself (46). Interestingly, over 90% of the time *nnrV* is found in an α-proteobacterial denitrifier it is adjacent to and convergently transcribed with a putative *nnrR* ortholog, as in *R. sphaeroides.* In a few clostridia, *nnrV* orthologs are also found

in close proximity to genes encoding Fnr-type regulators. This close association may indicate the function of NnrV is linked with NnrR in some way. However, *nnrV* is not widespread among related denitrifiers and is not strongly associated with any particular phylogenetic group. It is unclear if *nnrV* is being lost by denitrifiers with *nnrR*, or is a function required only in a few.

In the analysis of genes in the NnrR regulons of *R. sphaeroides* strains, the co-selection of certain sets of genes is noticeable. *paz* and *nirK/nirV* are co-selected, but the conditions justifying this strong co-selection remain elusive. Nevertheless, this set of genes appears to be sufficient for producing a functional Nir. *norCBQD*, *nnrS* and *nnrV* also appear to be co-selected given they are retained in strains lacking Nir, as well as their tight genetic linkage. This suggests this set of genes is required for NO reduction. However, *nnrV* may actually be co-selected with *nnrR*, as discussed above. These groupings indicate that *nirK*/*nirV*, *paz*, *nnrS*, *nnrV*, and *norCBQD*, along with *nnrR*, are the suite of genes required for *R. sphaeroides* to be physiologically competent for nitrite reduction to NO and NO reduction to N_2O. Within this set, four genes, *paz*, *nirV*, *nnrS* and *nnrV*, can be inactivated with no loss of denitrification capacity under laboratory conditions (4, 19). In the case of *paz*, the presence of a functionally redundant protein accounts for its lack of phenotype. In the case of the other three, it is unclear if there are functionally redundant genes, or if laboratory conditions mask any potential phenotypic changes. Nevertheless, the strong co-selection of these genes with the structural genes for the nitrogen oxide reductases indicates they have functional importance under real world conditions.

In conclusion, these experiments have expanded the NnrR regulon of *R. sphaeroides* 2.4.3 by five genes. There is also some evidence presented for the physiological role of three of these gene products, NorEF and pseudoazurin. The NnrR regulon in 2.4.3 seems to be synonymous with a denitrification regulon as all

characterized members contribute to denitrification physiology. The presence of conserved, and possibly co-selected, genes like *nnrV*, *nirV*, and *nnrS* suggest we still have a lot to learn about denitrification in strain 2.4.3. Discovering the physiological roles of these gene products may reveal the logic behind their conservation within denitrification regulons.

REFERENCES

1. **Ausmees, N., R. Mayer, H. Weinhouse, G. Volman, D. Amikam, M. Benziman, and M. Lindberg.** 2001. Genetic data indicate that proteins containing the GGDEF domain possess diguanylate cyclase activity. FEMS Microbiol. Lett. **204:**163-7.

2. **Baek, S., A. Hartsock, and J. Shapleigh.** 2008. *Agrobacterium tumefaciens* C58 uses ActR and FnrN to control nirK and nor expression. J. Bacteriol. **190:**78-86.

3. **Bailey, T. L. and C. Elkan.** 1994. Fitting a mixture model by expectation maximization to discover motifs in biopolymers. Proc. Int. Conf. Intell. Syst. Mol. Biol. **2:**28-36.

4. **Bartnikas, T., Y. Wang, T. Bobo, A. Veselov, C. Scholes, and J. Shapleigh.** 2002. Characterization of a member of the NnrR regulon in *Rhodobacter sphaeroides* 2.4.3 encoding a haem-copper protein. Microbiology (Reading, Engl.) **148:**825-33.

5. **Busby, S. and R. H. Ebright.** 1999. Transcription activation by catabolite activator protein (CAP). J. Mol. Biol. **293:**199-213.

6. **Cary, S., J. Winger, E. Derbyshire, and M. Marletta.** 2006. Nitric oxide signaling: no longer simply on or off. Trends Biochem. Sci. **31:**231-9.

7. **Choi, P., Z. Naal, C. Moore, E. Casado-Rivera, H. Abruna, J. Helmann, and J. Shapleigh.** 2006. Assessing the impact of denitrifier-produced nitric oxide on other bacteria. Appl. Environ. Microbiol. **72:**2200-5.

8. **Choudhary, M., X. Zanhua, Y. Fu, and S. Kaplan.** 2007. Genome analyses of three strains of *Rhodobacter sphaeroides*: evidence of rapid evolution of chromosome II. J. Bacteriol. **189:**1914-21.

9. **Chung, C. T., S. L. Niemela, and R. H. Miller.** 1989. One-step preparation of competent *Escherichia coli*: transformation and storage of bacterial cells in the same solution. Proc. Natl. Acad. Sci. U. S. A. **86:**2172-2175.

10. **Daldal, F., S. Mandaci, C. Winterstein, H. Myllykallio, K. Duyck, and D. Zannoni.** 2001. Mobile cytochrome c2 and membrane-anchored cytochrome cy are both efficient electron donors to the cbb3- and aa3-type cytochrome c oxidases during respiratory growth of *Rhodobacter sphaeroides*. J. Bacteriol. **183:**2013-24.

11. **de Boer, A., J. van der Oost, W. Reijnders, H. Westerhoff, A. Stouthamer, and R. van Spanning.** 1996. Mutational analysis of the nor gene cluster which encodes nitric-oxide reductase from *Paracoccus denitrificans*. Eur. J. Biochem. **242:**592-600.

12. **de Bruijn, F., S. Rossbach, C. Bruand, and J. R. Parrish.** 2006. A highly conserved *Sinorhizobium meliloti* operon is induced microaerobically via the FixLJ system and by nitric oxide (NO) via NnrR. Environ. Microbiol. **8:**1371-81.

13. **Eraso, J., J. Roh, X. Zeng, S. Callister, M. Lipton, and S. Kaplan.** 2008. Role of the global transcriptional regulator PrrA in *Rhodobacter sphaeroides* 2.4.1: combined transcriptome and proteome analysis. J. Bacteriol. **190:**4831-48.

14. **Giardina, G., S. Rinaldo, K. A. Johnson, A. Di Matteo, M. Brunori, and F. Cutruzzola.** 2008. NO sensing in *Pseudomonas aeruginosa*: structure of the transcriptional regulator DNR. J. Mol. Biol. **378:**1002-15.

15. **Gilles-Gonzalez, M. and G. Gonzalez.** 2004. Signal transduction by heme-containing PAS-domain proteins. J. Appl. Physiol. **96:**774-83.

16. **Herbert, R., A. Ranchou-Peyruse, R. Duran, R. Guyoneaud, and S. Schwabe.** 2005. Characterization of purple sulfur bacteria from the South Andros Black Hole cave system: highlights taxonomic problems for ecological studies among the genera *Allochromatium* and *Thiocapsa*. Environ. Microbiol. **7:**1260-8.

17. **Heurlier, K., M. Thomson, N. Aziz, and J. Moir.** 2008. The nitric oxide (NO)-sensing repressor NsrR of *Neisseria meningitidis* has a compact regulon of genes involved in NO synthesis and detoxification. J. Bacteriol. **190:**2488-95.

18. **Hunter, C. N., F. Daldal, M. C. Thurnauer, and J. T. Beatty.** 2009. The Purple Phototrophic Bacteria. Springer, Dordrecht, The Netherlands.

19. **Jain, R. and J. Shapleigh.** 2001. Characterization of nirV and a gene encoding a novel pseudoazurin in *Rhodobacter sphaeroides* 2.4.3. Microbiology (Reading, Engl.) **147:**2505-15.

20. **Joshi, M. S., T. B. Ferguson, T. H. Han, D. R. Hyduke, J. C. Liao, T. Rassaf, N. Bryan, M. Feelisch, and J. R. Lancaster.** 2002. Nitric oxide is consumed, rather than conserved, by reaction with oxyhemoglobin under physiological conditions. Proc. Natl. Acad. Sci. USA **99:**10341-6.

21. **Keen, N. T., S. Tamaki, D. Kobayashi, and D. Trollinger.** 1988. Improved broad-host-range plasmids for DNA cloning in gram-negative bacteria. Gene **70:**191-197.

22. **Kokotek, W. and W. Lotz.** 1989. Construction of a lacZ-kanamycin-resistance cassette, useful for site-directed mutagenesis and as a promoter probe. Gene **84:**467-471.

23. **Korner, H., H. Sofia, and W. Zumft.** 2003. Phylogeny of the bacterial superfamily of Crp-Fnr transcription regulators: exploiting the metabolic spectrum by controlling alternative gene programs. FEMS Microbiol. Rev. **27:**559-92.

24. **Kovach, M. E., P. H. Elzer, D. S. Hill, G. T. Robertson, M. A. Farris, R. M. Roop 2nd, and K. M. Peterson.** 1995. Four new derivatives of the broad-host-range cloning vector pBBR1MCS, carrying different antibiotic-resistance cassettes. Gene **166:**175-176.

25. **Kwiatkowski, A. and J. Shapleigh.** 1996. Requirement of nitric oxide for induction of genes whose products are involved in nitric oxide metabolism in *Rhodobacter sphaeroides* 2.4.3. J. Biol. Chem. **271:**24382-8.

26. **Kwiatkowski, A., W. Laratta, A. Toffanin, and J. Shapleigh.** 1997. Analysis of the role of the nnrR gene product in the response of *Rhodobacter sphaeroides* 2.4.1 to exogenous nitric oxide. J. Bacteriol. **179:**5618-20.

27. **Laratta, W., M. Nanaszko, and J. Shapleigh.** 2006. Electron transfer to nitrite reductase of *Rhodobacter sphaeroides* 2.4.3: examination of cytochromes c2 and cY. Microbiology (Reading, Engl.) **152:**1479-88.

28. **Laratta, W., P. Choi, I. Tosques, and J. Shapleigh.** 2002. Involvement of the PrrB/PrrA two-component system in nitrite respiration in *Rhodobacter sphaeroides* 2.4.3: evidence for transcriptional regulation. J. Bacteriol. **184:**3521-9.

29. **Lee, D., A. Ramos, L. Macomber, and J. Shapleigh.** 2002. Taxis response of various denitrifying bacteria to nitrate and nitrite. Appl. Environ. Microbiol. **68:**2140-7.

30. **Lim, M. H., D. Xu, and S. J. Lippard.** 2006. Visualization of nitric oxide in living cells by a copper-based fluorescent probe. Nat. Chem. Biol. **2:**375-80.

31. **Lim, S. K., S. J. Kim, S. H. Cha, Y. K. Oh, H. J. Rhee, M. S. Kim, and J. K. Lee.** 2009. Complete genome sequence of *Rhodobacter sphaeroides* KD131. Journal of Bacteriology **191:**1118-9.

32. **Lueking, D. R., R. T. Fraley, and S. Kaplan.** 1978. Intracytoplasmic membrane synthesis in synchronous cell populations of *Rhodopseudomonas sphaeroides*. J. Biol. Chem. **253:**451-457.

33. **Maniatis, T., E. F. Fritsch, and J. Sambrook.** 1982. Molecular Cloning: a laboratory manual. Cold Spring Harbor Laboratory Press, Cold Spring Harbor, NY.

34. **Oh, J. I., J. M. Eraso, and S. Kaplan.** 2000. Interacting regulatory circuits involved in orderly control of photosynthesis gene expression in *Rhodobacter sphaeroides* 2.4.1. J. Bacteriol. **182:**3081-7.

35. **Pappas, C., J. Sram, O. Moskvin, P. Ivanov, R. Mackenzie, M. Choudhary, M. Land, F. Larimer, S. Kaplan, and M. Gomelsky.** 2004. Construction and validation of the *Rhodobacter sphaeroides* 2.4.1 DNA microarray: transcriptome flexibility at diverse growth modes. J. Bacteriol. **186:**4748-58.

36. **Pearson, I., M. Page, R. van Spanning, and S. Ferguson.** 2003. A mutant of *Paracoccus denitrificans* with disrupted genes coding for cytochrome c550 and pseudoazurin establishes these two proteins as the in vivo electron donors to cytochrome cd1 nitrite reductase. J. Bacteriol. **185:**6308-15.

37. **Philippot, L.** 2002. Denitrifying genes in bacterial and Archaeal genomes. Biochim. Biophys. Acta **1577:**355-76.

38. **Prentki, P. and H. M. Krisch.** 1984. In vitro insertional mutagenesis with a selectable DNA fragment. Gene **29:**303-13.

39. **Rodionov, D., I. Dubchak, A. Arkin, E. Alm, and M. Gelfand.** 2005. Dissimilatory metabolism of nitrogen oxides in bacteria: comparative reconstruction of transcriptional networks. PLoS Comput Biol **1:**e55.

40. **Ryjenkov, D., M. Tarutina, O. Moskvin, and M. Gomelsky.** 2005. Cyclic diguanylate is a ubiquitous signaling molecule in bacteria: insights into biochemistry of the GGDEF protein domain. J. Bacteriol. **187:**1792-8.

41. **Schmidt, A., D. Ryjenkov, and M. Gomelsky.** 2005. The ubiquitous protein domain EAL is a cyclic diguanylate-specific phosphodiesterase: enzymatically active and inactive EAL domains. J. Bacteriol. **187:**4774-81.

42. **Simm, R., A. Lusch, A. Kader, M. Andersson, and U. Romling.** 2007. Role of EAL-containing proteins in multicellular behavior of *Salmonella enterica* serovar Typhimurium. J. Bacteriol. **189:**3613-23.

43. **Simon, R., U. Priefer, and Pühler, A.** 1983. A broad host range mobilization system for in vivo genetic engineering: transposon mutagenesis in gram negative bacteria. Bio/Technology **1:**784-791.

44. **Spiro, S.** 2007. Regulators of bacterial responses to nitric oxide. FEMS Microbiol. Rev. **31:**193-211.

45. **Spiro, S.** 1994. The FNR family of transcriptional regulators. Antonie Van Leeuwenhoek **66:**23-36.

46. **Tosques, I., J. Shi, and J. Shapleigh.** 1996. Cloning and characterization of nnrR, whose product is required for the expression of proteins involved in nitric oxide metabolism in *Rhodobacter sphaeroides* 2.4.3. J. Bacteriol. **178:**4958-64.

47. **Tosques, I., A. Kwiatkowski, J. Shi, and J. Shapleigh.** 1997. Characterization and regulation of the gene encoding nitrite reductase in *Rhodobacter sphaeroides* 2.4.3. J. Bacteriol. **179:**1090-5.

48. **Vieira, H., P. Freire, and C. Arraiano.** 2004. Effect of *Escherichia coli* morphogene bolA on biofilms. Appl. Environ. Microbiol. **70:**5682-4.

49. **Yanisch-Perron, C., J. Vieira, and J. Messing.** 1985. Improved M13 phage cloning vectors and host strains: nucleotide sequences of the M13mp18 and pUC19 vectors. Gene **33:**103-19.

50. **Zeilstra-Ryalls, J. and S. Kaplan.** 1995. Aerobic and anaerobic regulation in *Rhodobacter sphaeroides* 2.4.1: the role of the fnrL gene. J. Bacteriol. **177:**6422-31.

51. **Zumft, W.** 1997. Cell biology and molecular basis of denitrification. Microbiol. Mol. Biol. Rev. **61:**533-616.

52. **Zumft, W. and H. Korner.** 1997. Enzyme diversity and mosaic gene organization in denitrification. Antonie Van Leeuwenhoek **71:**43-58.

Chapter 5

Regulation and function of the *Sphaeroides* Heme Protein (SHP) in *Rhodobacter sphaeroides* 2.4.1

Summary

The *Sphaeroides* Heme Protein (SHP) is a novel member of the cytochrome *c* family. Purified SHP has been shown to bind both NO and O_2 with high affinity, and SHP was recently shown to have nitric oxide dioxygenase activity. Here we studied the regulation and function of SHP in *Rhodobacter sphaeroides* strain 2.4.1, the organism from which it was first discovered and characterized. The expression of *shp* is undetectable under most laboratory culture conditions. However, during stationary phase growth under anaerobic photoheterotrophic conditions, *shp* is highly expressed. This pattern of expression does not correlate with the predicted function of SHP as the substrates NO and O_2 are not predicted to be present. We also studied a mutant of *shp*. In general, the mutant has wild-type growth phenotypes. In a series of co-culture experiments under aerobic and photosynthetic conditions, *shp* competed effectively with wild-type. However, under anaerobic/DMSO conditions wild-type did out compete *shp* by 5:1. We also consider the SHP family and the potential association between SHP and a two-component signaling system.

Introduction

Rhodobacter sphaeroides is a metabolically versatile α-proteobacterium capable of anoxygenic photosynthesis, aerobic and anaerobic respiration, carbon fixation, and nitrogen fixation (12). *R. sphaeroides* encodes five soluble *c*-type cytochromes (1, 14). One of these is the *Sphaeroides* Heme Protein (SHP), an O_2-

binding *c*-type cytochrome with a single high spin heme (6). The structure of *R. sphaeroides* SHP has been solved for both the oxidized and reduced forms, and it is structurally similar to class I *c*-type cytochromes (9). In the oxidized (SHP^{+3}) form of the protein the heme iron is six-coordinate with the sixth ligand being the side-chain amide oxygen of an asparagine residue. Upon reduction, the heme-asparagine bond is broken leaving the heme open to ligand binding. SHP has been shown to bind diatomic species including oxygen, nitric oxide, and cyanide (6). SHP binds oxygen with a K_d of 20μM, similar to the oxygen-sensory proteins FixL, Dos, and PDEA1 (4). The K_d of SHP for NO binding is even lower and is sub-micromolar (4).

Currently, there is no known physiological role for SHP. However, *shp* is typically found in an operon with genes encoding a diheme cytochrome *c* (DHC) and a membrane-bound cytochrome b_{561}. These three proteins together could constitute an electron transfer pathway. In fact, SHP and DHC have been shown to interact, and DHC is capable of rapidly transferring electrons to SHP (4). DHC has two distinct domains, one that is similar to class I *c*-type cytochromes and one that is unique in the cytochrome family (4). The domains are bridged by a tyrosine residue that facilitates rapid electron transfer (4). The reduction potentials of SHP and DHC also make it plausible for these proteins to act as a functioning electron transport pathway in vivo. The DHC hemes have reduction potentials of -310 and -240mV, and SHP has a reduction potential of -105mV (4). The interaction between DHC and SHP becomes weak at high salt concentrations suggesting important electrostatic interactions (4). Consistent with this, SHP has positively charged residues localized in one region of the protein and negatively charged residues localized in another region on the surface of the protein (9). For a functioning electron transfer pathway the membrane-bound cytochrome *b* could transfer electrons to DHC, which in turn could reduce SHP.

Recent biochemical studies of purified SHP from *R. sphaeroides* 2.4.1 have demonstrated nitric oxide dioxygenase activity (10). Because SHP binds both oxygen and NO, these ligands were investigated as potential substrates for the enzyme. When purified SHP binds oxygen, it can react with NO to form nitrate. Also, when SHP binds NO it can react with superoxide to also form nitrate. The physiological relevance of this activity is not clear, but it could be a mechanism for mitigating NO toxicity. Further research in a diverse set of organisms is required for an understanding of the physiological role of SHP. Here we investigated expression of the *shp* operon in *R. sphaeroides* and found expression to be dependent on anoxic photosynthetic conditions. We also constructed an *shp* mutant and assessed the phenotype and fitness of this strain relative to wild-type. While there is no defect in growth, wild-type modestly out-competes the mutant under anoxic conditions during growth on DMSO.

Materials and Methods

Bacterial Strains and growth conditions. *Rhodobacter sphaeroides* strain 2.4.1 is the type strain and is a partial denitrifier (8). *Rhodobacter sphaeroides* strain 2.4.3 (ATCC 17025) is a denitrifier and was used as a comparison to strain 2.4.1 (18). For expression studies in strain 2.4.3, a *nirK* mutant was used (19). *E. coli* strains DH5α and JM109(λ*pir*) were used as cloning backgrounds, and S17-1 and S17-1λ*pir* were used for conjugations.

Rhodobacter strains were grown in Sistrom's medium (11) at 32°C. When necessary, antibiotics were added at the following concentrations: kanamycin 25μg/mL, streptomycin 50μg/mL, and gentamicin 20μg/mL. For some cultures, nitrate was added to 10mM (KNO_3). For photosynthetic growth, cells were grown in 15mL sealed vials filled with media. Vials were incubated at room temperature with shaking, close to an incandescent light source. For DMSO (dimethyl sulfoxide)

growth, cells were grown in 15mL sealed vials filled with Sistrom's containing 10% Luria-Bertani medium and 0.3% DMSO. Vials were wrapped in foil and incubated at room temperature with shaking. Flask culture conditions have been previously described (18). *E. coli* strains were grown in Luria-Bertani medium (13) at 32°C with shaking.

Rhodobacter genomic DNA used for PCR and cloning purposes was isolated using the Puregene Genomic DNA Isolation Kit. All oligonucleotides were purchased from Integrated DNA Technologies (IDT), and most were designed with restriction sites at the 5' end to facilitate cloning. In oligonucleotide sequences that follow restriction sites are underlined. All restriction digests, plasmid preparations, and ligations were done according to standard methods. Transformations were by the TSS-method (3). Conjugations were biparental matings between *E. coli* S17-1 and *Rhodobacter*.

Construction of the *shp* mutant. *shp* was disrupted in strain 2.4.1 by double homologous recombination using a suicide plasmid carrying a streptomycin resistance cassette (2). Two noncontiguous regions of the *shp* operon were amplified using primer pairs SHPKO5'UP (5'-GGGGTACCTTCTGGTCGTTCGAGGCC-3') and SHPKO3'UP (5'-GGGGATCCTAGCCTGCGATGAGCTGC-3'), and SHPKO5'DOWN (5'-GGGGATCCCTTCCTGTCGACCCAGAC-3') and SHPKO3'2DOWN (5'-AACTGCAGTCAGTCGTCGTCGAACAG-3'). The first region (SHPKO-UP) was cloned into pUC19 via KpnI and BamHI. The second region (SHPKO-DOWN) was then cloned into this construct via BamHI and PstI. The BamHI fragment of pHP45Ω, which contains the streptomycin cassette, was cloned between the two SHP fragments (16). The entire construct was then moved into the suicide vector pSUP202-1 via KpnI and PstI (17). The final construct was transformed into *E. coli* S17-1 and conjugated into *R. sphaeroides* 2.4.1 to generate the mutant.

The mutant was selected by streptomycin resistance, and the double recombination event was screened for by tetracycline sensitivity.

Construction of the *shp-lacZ* transcriptional fusion. The promoter of RSP_2022 was amplified by PCR using primers 5'-GGGAATTCACAGAGGCGGATCGGTGC-3' and 5'-GGGGATCCATCAGGGCCAGCACCATC-3'. The amplicon was cloned into pRK415 via EcoRI and BamHI (5). The PstI fragment of pKOK-6 carrying the *lacZ* cassette was ligated into the BamHI site to create the transcriptional fusion (7). The final construct was transformed into *E. coli* S17-1 and conjugated into strain 2.4.1 (2). The 2.4.1shp-lacZ strain was used for expression studies (2). Expression was measured by β-galactosidase activity (13). Activity was measured for at least three independent cultures. Relevant values were averaged, and error bars represent one standard deviation. The expression construct was conjugated into 2.4.1*nirK*, strain 2.4.3, and the *nirK* mutant of strain 2.4.3.

2.4.1 strain containing *nirK*. The plasmid pBBRNIRB carries the *nirK* gene encoding nitrite reductase from strain 2.4.3 (19). pBBRNIRB is the vector backbone pBBR1MCS-5 containing 7kb of the *nirK* region of strain 2.4.3. This plasmid was conjugated into strain 2.4.1, generating the 2.4.1*nirK* strain (2).

Competition assays. 2.4.1 and *shp* were grown in co-culture to determine the relative fitness of *shp* in different growth conditions. For aerobic growth, 2.4.1 and *shp* were inoculated into 50mL Sistrom's flasks and grown overnight in the dark with vigorous shaking. Photosynthetic and DMSO culture conditions were as described above. In all cases, the cultures used for inoculation were normalized by optical density at 600nm, and then equal amounts of 2.4.1 and *shp* were used. After growth, cultures were serially diluted and plated on Sistrom's and Sistrom's with streptomycin to select only for viable *shp*. The CFU/mL for Sistrom's versus Sistrom's with streptomycin were compared to determine relative fitness.

Results

Rhodobacter sphaeroides strains 2.4.1, 2.4.9, and KD131 all encode the *shp* operon on Chromosome I. In 2.4.1, the operon consists of three genes from 2020-2022. Here, these genes will be referred to as *shpA*, encoding the membrane-bound *b*-type cytochrome, *shpB*, encoding SHP, and *shpC*, encoding the DHC. Although the physiological roles of these proteins are uncertain, their occurrence in an operon suggests their function may be related. As this is the organism from which SHP was first studied and crystallized, we began characterizing the regulation and function of SHP in this background.

Expression of *shp*. The predicted promoter region upstream of *shpA* was fused to *lacZ* to generate a transcriptional fusion. Expression was monitored under a variety of growth conditions. Under aerobic and microaerobic growth conditions, there was no detectable expression of *shp*. However, under anoxic photoheterotrophic conditions, *shp* expression increased 100 fold (Fig. 5.1, panel A). The increased expression occurred at high cell density and at high pH (Fig. 5.1, panel B, and C). The increase in expression is not specific to high cell density as dense aerobic cultures did not display increased expression. Increased expression is also not solely dependent on elevated pH, as cultures grown in the dark with the pH adjusted to 7.5, 8.0, 8.5, and 9.0 did not show induction of *shpABC*. This suggests induction may be dependent on anoxia or on some feature of photoanoxic growth. *R. sphaeroides* 2.4.1 can grow anaerobically via DMSO reduction. When cells were grown in this condition, there was modest 5-fold induction of *shpABC* (Fig. 5.2). However, levels did not approach the induction seen during photosynthetic conditions suggesting factors specific to anoxic photosynthetic growth may be playing a role in expression.

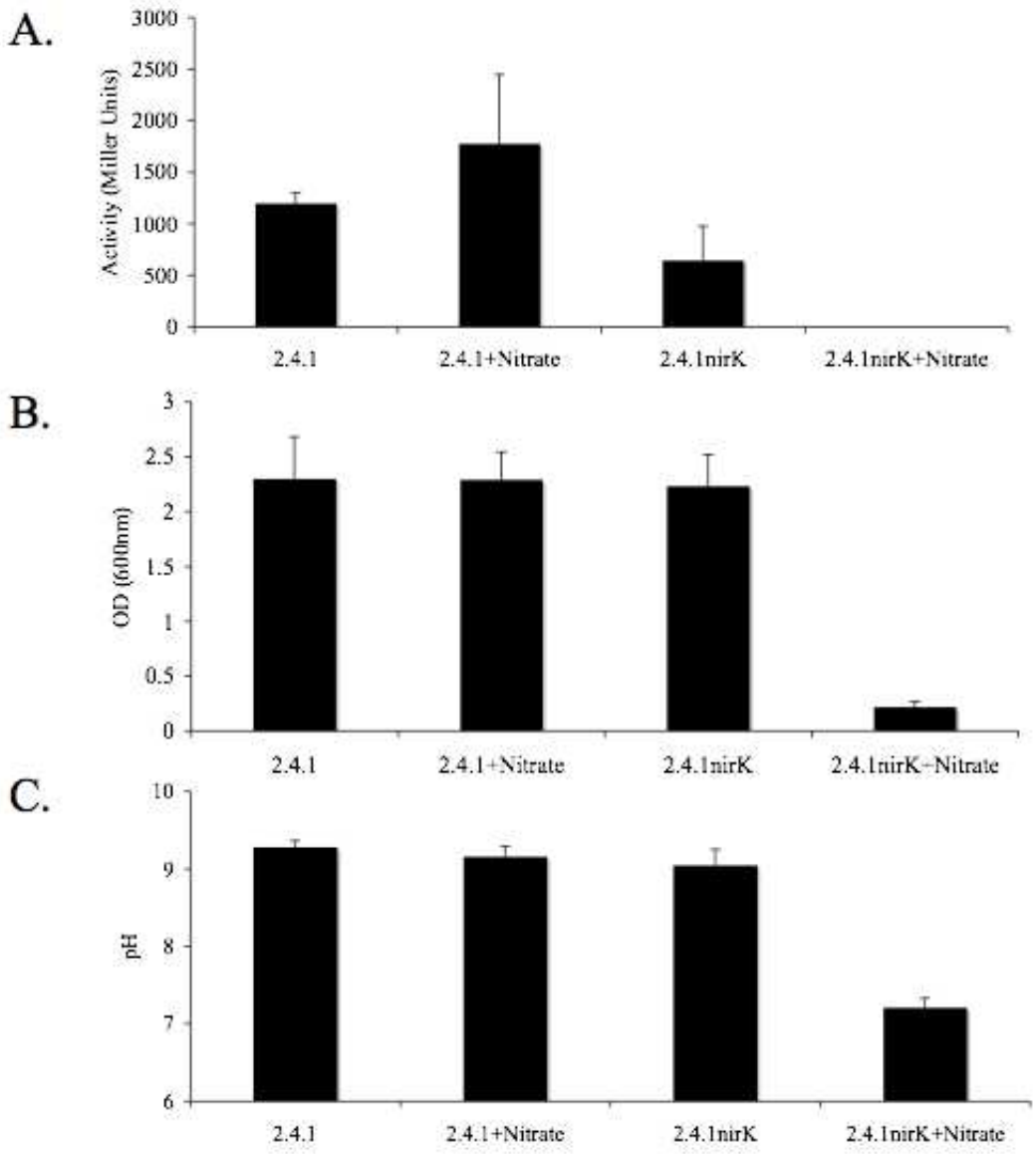

Figure 5.1: Expression of *shp* in 2.4.1 and 2.4.1*nirK* under anaerobic photosynthetic conditions. Panel A is the expression measured by β-galactosidase activity. Panel B is the optical density at the time of the assay. Panel C is the pH at the time of the assay.

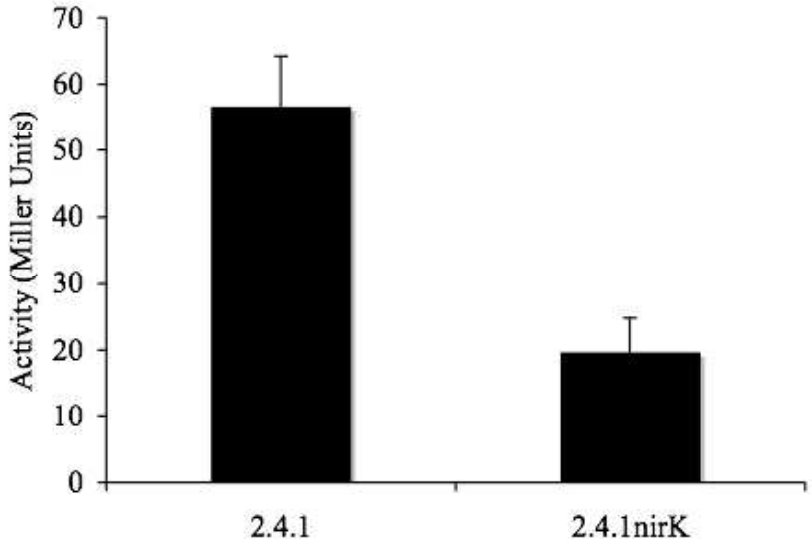

Figure 5.2: Expression of *shp* in 2.4.1 and 2.4.1*nirK* under anaerobic DMSO conditions. Expression was measured by β-galactosidase activity.

Based on the proposed function of SHP and the ability to bind NO, we also investigated expression in a strain of 2.4.1 capable of endogenously producing NO. *R. sphaeroides* strain 2.4.3 is a denitrifier and has a copper-containing nitrite reductase (Nir) (18). A plasmid carrying the *nirK* gene, which encodes Nir, was conjugated into strain 2.4.1. This will allow strain 2.4.1 to reduce nitrite, producing NO. The NO that is produced can be further reduced as 2.4.1 encodes a nitric oxide reductase (Nor) (8). However, the presence of Nir should allow for some low level of NO to be endogenously produced. In the 2.4.1*nirK* strain, *shp* expression is reduced in comparison to wild-type 2.4.1 (Fig. 5.1). Induction still occurs under photoanoxic conditions; however, maximal levels are 50% of wild-type. This is also true during growth on DMSO (Fig. 5.2). It is unclear why the 2.4.1*nirK* strain grew poorly under photosynthetic conditions with nitrate; however, this strain grew normally under dark conditions with nitrate.

To determine if the capacity for denitrification is the factor responsible for decreasing *shp* expression in 2.4.1*nirK*, the *shp-lacZ* construct was conjugated into strain 2.4.3. Strain 2.4.3 is a denitrifier and lacks the *shp* operon. In this background there was no detectable expression under aerobic, photosynthetic, and denitrifying conditions (not shown). Strain 2.4.3 cannot grow on DMSO, so this condition was not tested. It is not clear if the lack of expression in strain 2.4.3 is due to denitrification potential, or to lack of a regulation mechanism that is required for *shp* expression. To test this, we conjugated the *shp-lacZ* construct into a *nirK* mutant background of 2.4.3. This makes the denitrification capacity of 2.4.3 practically identical to that of wild-type 2.4.1. In the *nirK* background, there was no detectable expression under aerobic, photosynthetic, and denitrifying conditions (not shown). This suggests the regulatory mechanism is not conserved across strains 2.4.1 and 2.4.3.

If SHP is playing a role in protection against toxic oxygen and nitrogen species, some of these toxins may induce expression. Expression was monitored under photosynthetic and aerobic conditions in the presence of sodium nitroprusside (SNP), an NO generator, and methyl viologen and methylene blue, compounds that produce reactive oxygen species. In all cases, expression was not induced by the presence of these compounds, even at unrealistically high concentrations (not shown).

Mutant phenotype of *shp*. The gene encoding SHP, *shpB*, was inactivated by deletion. This mutant had no obvious growth defects under standard culture conditions, including aerobic growth and photosynthetic growth. If SHP plays a role in protecting the cell from toxic oxygen and nitrogen species, *shp* may be at a competitive disadvantage against wild-type 2.4.1 when grown in co-culture. A series of competition experiments were done under aerobic, photoanoxygenic, and anoxic DMSO conditions. After co-culture, cells were plated on non-selective media for total CFU/mL and on *shp*-selective media for CFU/mL for *shp* to obtain a ratio of

2.4.1:*shp*. Under aerobic conditions and photoanoxic conditions, *shp* competes effectively with wild-type, and cell numbers remain approximately equal in the co-culture (1:1). In DMSO conditions, wild-type was able to out compete *shp* by 5:1.

Co-cultures were also done under the same growth conditions in the presence of 1mM nitrite added at the start of incubation. Nitrite is itself considered toxic and can chemically convert to NO. If SHP is conferring some resistance to toxic nitrogen species, the mutant may be impaired. Nitrite did not significantly impact the ability of *shp* to compete with wild-type under aerobic and photosynthetic conditions. Under DMSO conditions with nitrite wild-type out competed *shp* by 3:1. This is comparable to the ratios seen in the absence of nitrite during growth on DMSO.

Phylogeny of the SHP family. The predicted function of SHP, involving oxygen species, and the anoxic expression pattern do not correlate. This led us to consider how the SHP system of *Rhodobacter* compares to that of other sequenced organisms. The protein sequence of SHP was used to search for putative orthologs in other organisms. SHP is found in a diverse set of proteobacteria (Fig. 5.3). The majority of organisms are from the β-group, a few are from the ε and α-groups, and the *Shewanella* represent the γ-group. For each organism where SHP was found, the genetic locus was examined to detect other genes associated with *shp*. As expected, almost all organisms had three genes encoding SHP, DHC, and a *b*-type cytochrome. The majority of organisms also had, in addition to *shpABC*, two genes encoding a two-component regulatory system that were either in the same operon or divergent from the *shp* operon (Fig. 5.3). In some cases, the operon includes additional genes, such as in the *Shewanella*, where the operons are six or seven genes long and include a pro-peptidase gene. Based on the phylogeny of SHP, the association between the regulatory system and SHP is conserved.

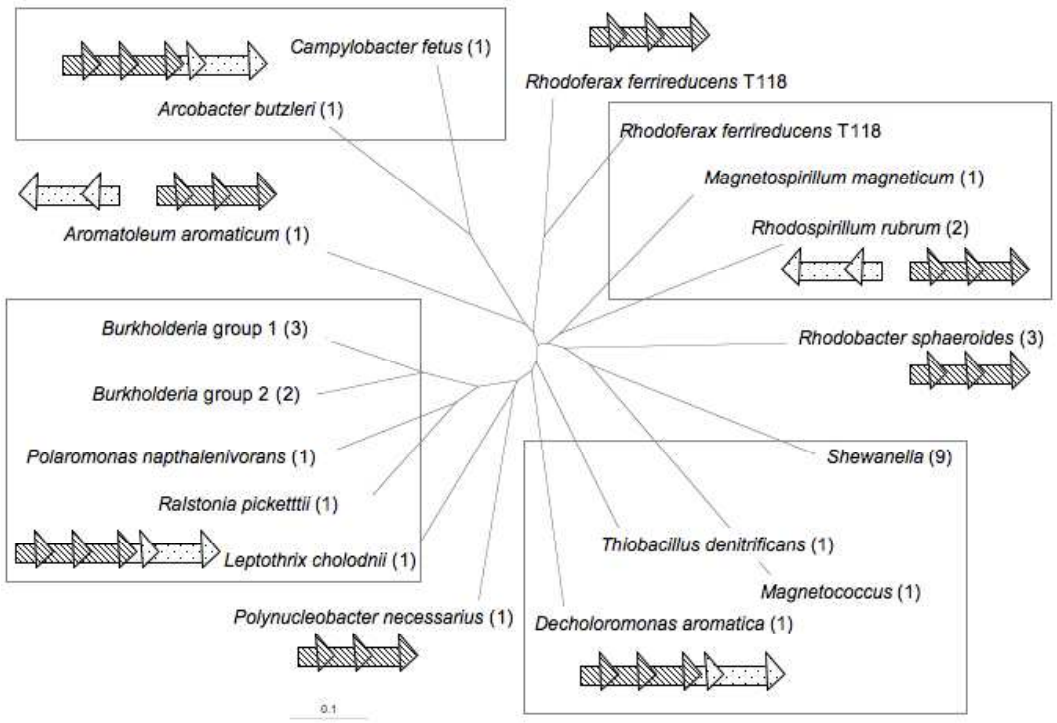

Figure 5.3: SHP tree showing the various operon structures. The three gene striped operon represents *shpABC*, and the two gene stippled operon represents the two-component regulatory system. Organism names are followed by parenthetical numbers indicating the number of species or strains having that operon structure. There are two *Burkholderia* groups because group 2 has a disrupted *shp* operon. *R. ferrireducens* T118 is represented twice because there are two separate loci encoding a SHP-like protein. This is a neighbor-joining tree generated using the Phylip program and a ClustalX alignment of selected SHP sequences.

Discussion

These experiments have demonstrated a culture condition in which the *shp* operon is highly expressed. Under photosynthetic conditions, at high cell densities and high pH, expression increases approximately 100 fold. However, SHP does not seem to confer a selective advantage when *shp* mutant cells are cultured with wild-type. This could suggest that SHP activity is infrequent and may be associated with some transient signal or substrate.

There is microarray data available for strain 2.4.1 under a variety of growth conditions (15). The microarray data shows no correlation between any mode of growth (aerobic, microaerobic, photosynthetic, and DMSO) and expression of *shp*. In most cases, *shpA* is considered absent, *shpB* is considered present, and *shpC* is variable. This supports our observations of very low expression under most growth conditions. Expression under our photosynthetic conditions may not be directly comparable to the microarray data for photosynthetic growth. In our experiments, cells were grown to very high densities in intense light. It is possible that some feature of our photosynthetic growth condition represents a case where *shp* is induced. Consistent with this, in *Rhodobacter* protein expression profiles SHP cannot be detected in aerobic cells, but small amounts are detected under photosynthetic conditions (1).

It is interesting to note that the expression pattern we observed does not correlate with the functional prediction for SHP. If SHP is acting as a nitric oxide dioxygenase, we would expect SHP to be expressed under conditions where oxygen and nitric oxide may be present together. The most likely condition would seem to be during high or low oxygen growth, where oxygen is present as a substrate. It is possible that SHP exists to quickly transform any contaminating NO or O_2 into harmless nitrate during photoanoxic growth. This may also explain why, based on protein expression profiles, it is present at very low levels (1). A small amount of enzyme may be sufficient for mitigating NO and O_2 toxicity. However, it is also possible that the in vitro nitric oxide dioxygenase activity and the physiological function are not the same. Besides NO and O_2, SHP has been shown to bind hydroxylamine (9).

The association between the *shp* operon and a two-component system is also intriguing. While *R. sphaeroides* 2.4.1 lacks the two-component system linked to the

shp operon, it could serve as a useful comparison to those organisms that do. There are two possible scenarios for how this system could be linked to SHP. One, the two component system could sense a signal and then induce expression of itself and *shp*. Two, the two component system could be expressed along with *shp* and then receive a signal from SHP activity that then modulates expression of other genes. It will be informative to study *shp* expression and function in an organism that has this type of operon composition. A good candidate would be one of the *Shewanella* species as all 9 species/strains having *shp* also have the two-component system.

REFERENCES

1. **Bartsch, R. G., R. P. Ambler, T. E. Meyer, and M. A. Cusanovich.** 1989. Effect of aerobic growth conditions on the soluble cytochrome content of the purple phototrophic bacterium *Rhodobacter sphaeroides*: induction of cytochrome c554. Arch. Biochem. Biophys. **271:**433-40.

2. **Choi, P.** 2004. Dissertation/Thesis. Cornell University, Ithaca.,

3. **Chung, C. T., S. L. Niemela, and R. H. Miller.** 1989. One-step preparation of competent *Escherichia coli*: transformation and storage of bacterial cells in the same solution. Proc. Natl. Acad. Sci. U. S. A. **86:**2172-2175.

4. **Gibson, H., C. Mowat, C. Miles, B. Li, D. Leys, G. Reid, and S. Chapman.** 2006. Structural and functional studies on DHC, the diheme cytochrome c from *Rhodobacter sphaeroides*, and its interaction with SHP, the sphaeroides heme protein. Biochemistry **45:**6363-71.

5. **Keen, N. T., S. Tamaki, D. Kobayashi, and D. Trollinger.** 1988. Improved broad-host-range plasmids for DNA cloning in gram-negative bacteria. Gene **70:**191-197.

6. **Klarskov, K., G. Van Driessche, K. Backers, C. Dumortier, T. Meyer, G. Tollin, M. Cusanovich, and J. Van Beeumen.** 1998. Ligand binding and covalent structure of an oxygen-binding heme protein from *Rhodobacter sphaeroides*, a representative of a new structural family of c-type cytochromes. Biochemistry **37:**5995-6002.

7. **Kokotek, W. and W. Lotz.** 1989. Construction of a lacZ-kanamycin-resistance cassette, useful for site-directed mutagenesis and as a promoter probe. Gene **84:**467-471.

8. **Kwiatkowski, A., W. Laratta, A. Toffanin, and J. Shapleigh.** 1997. Analysis of the role of the nnrR gene product in the response of *Rhodobacter sphaeroides* 2.4.1 to exogenous nitric oxide. J. Bacteriol. **179:**5618-20.

9. **Leys, D., K. Backers, T. Meyer, W. Hagen, M. Cusanovich, and J. Van Beeumen.** 2000. Crystal structures of an oxygen-binding cytochrome c from *Rhodobacter sphaeroides*. J. Biol. Chem. **275:**16050-6.

10. **Li, B. R., J. L. Anderson, C. G. Mowat, C. S. Miles, G. A. Reid, and S. K. Chapman.** 2008. *Rhodobacter sphaeroides* haem protein: a novel cytochrome with nitric oxide dioxygenase activity. Biochem. Soc. Trans. **36:**992-5.

11. **Lueking, D. R., R. T. Fraley, and S. Kaplan.** 1978. Intracytoplasmic membrane synthesis in synchronous cell populations of *Rhodopseudomonas sphaeroides*. J. Biol Chem **253:**451-457.

12. **Mackenzie, C., J. M. Eraso, M. Choudhary, J. H. Roh, X. Zeng, P. Bruscella, A. Puskas, and S. Kaplan.** 2006. Postgenomic Adventures with *Rhodobacter sphaeroides*. Annu. Rev. Microbiol. **61:**283-307.

13. **Maniatis, T., E. F. Fritsch, and J. Sambrook.** 1982. Molecular Cloning: a laboratory manual. Cold Spring Harbor Laboratory Press, Cold Spring Harbor, NY.

14. **Meyer, T. E. and M. A. Cusanovich.** 1985. Soluble cytochrome composition of the purple phototrophic bacterium, *Rhodopseudomonas sphaeroides* ATCC 17023. Biochim. Biophys. Acta **807:**308-19.

15. **Pappas, C.T., J. Sram, O.V. Moskvin, P.S. Ivanov, R.C. Mackenzie, M. Choudhary, M.L. Land, F.W. Larimer, S. Kaplan, and M. Gomelsky.** 2004. Construction and validation of the *Rhodobacter sphaeroides* 2.4.1 DNA microarray: Transcriptome flexibility at diverse growth modes. J. Bacteriol. **186:**4748-58.

16. **Prentki, P. and H. M. Krisch.** 1984. In vitro insertional mutagenesis with a selectable DNA fragment. Gene **29:**303-13.

17. **Simon, R., U. Priefer, and Pühler, A.** 1983. A broad host range mobilization system for in vivo genetic engineering: transposon mutagenesis in gram negative bacteria. Bio/Technology **1:**784-791.

18. **Tosques, I., J. Shi, and J. Shapleigh.** 1996. Cloning and characterization of nnrR, whose product is required for the expression of proteins involved in nitric oxide metabolism in *Rhodobacter sphaeroides* 2.4.3. J. Bacteriol. **178:**4958-64.

19. **Tosques, I., A. Kwiatkowski, J. Shi, and J. Shapleigh.** 1997. Characterization and regulation of the gene encoding nitrite reductase in *Rhodobacter sphaeroides* 2.4.3. J. Bacteriol. **179:**1090-5.

Chapter Six

A link between nitric oxide and c-di-GMP signaling

Summary

In the last decade, the second messenger cyclic diguanosine monophosphate (c-di-GMP) has emerged as an important signaling molecule in bacterial cells. c-di-GMP has been linked to many cell surface associated phenotypes, such as motility and biofilm formation, as well as to changes in global gene expression. *Rhodobacter sphaeroides* strain 2.4.3 encodes 16 putative diguanylate cyclases and phosphodiesterases, the enzymes involved in the synthesis and breakdown of c-di-GMP, respectively. Here we attempted to study the signaling pathway of a two gene operon encoding a diguanylate cyclase and a nitric oxide binding protein. The products of this two gene operon are predicted to interact and may play a role in nitric oxide signaling These experiments were largely unsuccessful due to what seems to be toxicity of these two proteins when overexpressed in *E. coli* cells. Also, in the native background there was no detectable phenotype for knockouts of these genes.

Introduction

Cyclic diguanosine monophosphate (c-di-GMP) is a small molecule involved in second messenger signaling in bacteria (6, 31). This signal molecule has been linked to cellular processes including biofilm formation (15, 23), motility (25), cellulose synthesis (3, 8), gene expression (22, 39), and cell differentiation (1). c-di-GMP is synthesized from 2 molecules of GTP via diguanylate cyclase (DGC) activity, and is degraded to pGpG by phosphodiesterase (PDE) activity (Fig. 6.1). The DGC activity is localized to GGDEF domains, which indicates the amino acid residues

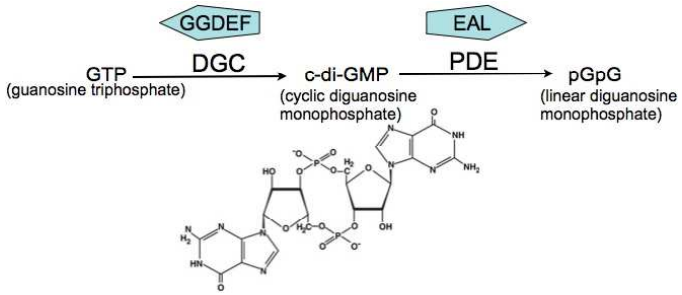

Figure 6.1: The production and breakdown of c-di-GMP. DGC is diguanylate cyclase, and GGDEF is the protein domain having DGC activity. PDE is phosphodiesterase, and EAL is the protein domain having PDE activity.

(glycine, glycine, aspartic acid, glutamic acid, phenylalanine) involved in the active site (34). The PDE activity is localized to the EAL domain, again where the letters indicate the amino acid residues (glutamic acid, alanine, leucine) involved in the active site (35). These domains are widespread in the Bacteria, but have not been found in the Eukarya or Archaea. The DGC domain does, however, have similarity to the adenylyl cyclase domain of Eukarya (9). Many bacterial species contain upwards of ten putative DGC or PDE proteins, typically in a modular format. Most commonly, the N terminal region of these proteins contains sensory domains, for instance GAF or PAS domains, and the C terminal region contains the DGC or PDE domain, or both domains arranged in tandem (31). The widespread presence of DGC and PDE domains, and their modular arrangement with diverse sensory input domains, supports the potential for global c-di-GMP signaling to control a wide variety of cellular processes.

The second messenger c-di-GMP was first researched in the cellulose synthesizing bacterium, *Gluconacetobacter xylinum* (previously *Acetobacter xylinum*) (32). In *G. xylinum*, c-di-GMP acts as an allosteric activator of the cellulose synthase (32). Three operons were identified in *G. xylinum*, which code for putative DGCs or PDEs, that when disrupted result in reduced cellulose production, supporting the role of c-di-GMP signaling in cellulose synthesis (37). Following these discoveries, c-di-

GMP signaling has been linked to a growing number of cellular processes. *Vibrio cholerae* encodes 53 proteins having GGDEF or EAL domains potentially involved in c-di-GMP signaling (19). So far, c-di-GMP signaling has been linked to polysaccharide synthesis (19), virulence factor production (19, 39), swarming motility (13), and biofilm formation (40). In enterobacteria, the PilZ domain has been identified as a receptor for c-di-GMP (33). The PilZ domain is part of the protein YcgR, which controls motility (33). The PilZ domain is also found in the cellulose synthase enzyme of *G. xylinum* supporting its role as a c-di-GMP binding domain. However, the PilZ domain is not present in all bacterial genomes, and the presence of PilZ domains does not correlate with the presence of DGCs or PDEs, suggesting multiple, as of yet unidentified, receptors or sensors of c-di-GMP (2). In *Pseudomonas aeruginosa*, BifA, a c-di-GMP PDE, and SadC, a DGC, have been shown to regulate biofilm formation and swarming motility (15, 23). In the phytopathogen *Xanthomonas axonopodis* pv citri, a direct link has been established between the Rpf quorum sensing pathway and c-di-GMP levels in the cell (4). The many phenotypes resulting from altered c-di-GMP levels could be partly explained by altered gene expression. In *E. coli*, the transcriptional profile in response to high levels of c-di-GMP was determined. High c-di-GMP resulted in altered expression of many genes, including those encoding surface structures, motility proteins, and membrane bound proteins, as well as altered expression of a number of transcriptional regulators (22). The most well studied DGC is PleD of *Caulobacter crescentus*. Enzymatic and structural studies of PleD have revealed that phosphorylation promotes dimer formation, which is essential for catalytic activity (27, 41). In addition, the active site was resolved to show the orientation of the two bound GTP molecules, which is reminiscent of the mammalian adenylate cyclase active site (41). The array of c-di-GMP associated phenotypes emphasizes a global role for this signaling molecule in bacterial cells. The

research also highlights the infancy of this field, as many DGC and PDE proteins have been discovered, but the mechanism of sensing and responding to c-di-GMP has not been determined for many of these phenotypes.

Our laboratory studies the purple non-sulfur bacterium, *Rhodobacter sphaeroides*. These bacteria are among the most metabolically versatile organisms known. *Rhodobacter* is capable of energy generation via anoxygenic photosynthesis, lithotrophy, and aerobic and anaerobic respiration (20). In our lab, we study strain 2.4.3 (ATCC17025), which in addition to the previously mentioned metabolic attributes, is capable of denitrification. Our primary research focus is on generating a model for denitrification in strain 2.4.3, including denitrification gene regulation by the transcriptional regulator NnrR, and denitrification enzyme activity. Recently, the genome sequence of strain 2.4.3 was released allowing a genome wide analysis for genes involved in mitigating toxic effects of the denitrification intermediate nitric oxide (NO). A putative two gene operon was identified which is predicted to encode an NO-binding heme protein (H-NOX) and a diguanylate cyclase. This operon is located on Chromosome I at locus Rsph17025_2333 and Rsph17025_2334. The NO-binding heme has been designated *hnox* and the diguanylate cyclase has been designated *cdg2*. These genes are present in all four sequenced strains of *R. sphaeroides*. Here these proteins were studied as a possible link between NO signaling and c-di-GMP signaling.

The H-NOX (heme nitric oxide and oxygen binding) protein domain was first characterized as a subunit of the mammalian soluble guanylyl cyclase (sGC) (9). In mammals, nitric oxide (NO) acts as a neurotransmitter that is sensed by the H-NOX domain of sGC, activating the enzyme for production of cGMP from GTP. The cGMP signal then elicits downstream responses that control a variety of cellular processes, including apoptosis and vasodilation (9). Eukaryotic and bacterial genome sequencing

has shown the H-NOX domain to be widely distributed in animals and bacteria and conserved across the two kingdoms. Based on sequence diversity and evolutionary analysis, a bacterial origin of the H-NOX sensory domain has been suggested (9). However, while H-NOX is associated with guanylyl cyclase activity in animals, in bacteria the H-NOX domain is found as part of methyl-accepting chemotaxis proteins, or present as a stand-alone protein that is associated in an operon with genes encoding signal transduction proteins including, histidine kinases, methyl-accepting chemotaxis proteins, and diguanylate cyclases and phosphodiesterases. Thus, while the association with cGMP signaling is not conserved, the general signaling role of the H-NOX domain is conserved.

Rhodobacter sphaeroides 2.4.3 encodes sixteen putative DGC or PDE domain containing proteins. Of these sixteen, eleven are conserved across the three strains of *R. sphaeroides*. Previously, one of these conserved DGC/PDE proteins involved in light sensing was characterized in strain 2.4.1 (38). Photosynthetic organisms are known to encode phytochrome proteins, used for sensing and responding to red/far red light using biliverdin. Typically, phytochromes have a light sensory domain linked to a histidine kinase output domain. However, in *Rhodobacter* the phytochromes are light sensory domains linked to GGDEF/EAL domains. The function of the phytochrome protein was studied by protein purification and *in vitro* assays. Both the GGDEF and EAL domains were functional and the EAL domain was found to exist as a cleaved species from the rest of the protein (38). This is the first bifunctional GGDEF/EAL protein identified and is the first research on c-di-GMP signaling in *Rhodobacter*. Here we attempt to expand on c-di-GMP signaling in *Rhodobacter* by studying the association between H-NOX and a diguanylate cyclase.

Materials and Methods

Bacterial Strains and Culture Conditions. *Rhodobacter sphaeroides* strain 2.4.3 (ATCC 17025) was used in this study. Mutants of this strain are listed in Table 6.1. *Rhodobacter* was cultured in Sistrom's medium at 32°C. When necessary antibiotics were added at the following concentrations: kanamycin 25μg/mL, tetracycline 1μg/mL, and streptomycin 50μg/mL. *Escherichia coli* strains DH5-α and JM109 were used as cloning backgrounds, while strains S17-1 and S17-1λ*pir* were used for conjugations with *Rhodobacter*. For protein overexpression and purification the *E. coli* host BL21 pLysS was used.

Construction of Plasmids and Strains. Plasmids used in this study are listed in Table 6.1. *Rhodobacter* genomic DNA was isolated using the Puregene DNA Isolation Kit. Oligonucleotides for PCR were purchased from Integrated DNA Technologies (IDT) and most have restriction sites added at the 5' end to facilitate cloning, these sites are underlined in primer sequences that follow. Plasmid isolation was done by the alkaline lysis method (21). Standard methods were used for restriction digests, ligations, and biparental conjugations. Transformation was by the TSS method (7).

***lacZ* fusion.** *hnox* and *cdg2* are in a predicted operon as the stop codon of *hnox* and the start codon of *cdg2* overlap. Upstream of *hnox/cdg2* there are two open reading frames in the same direction, it is unclear if these genes are part of a larger operon. For our purposes we designed a promoter-*lacZ* fusion that assumed only a two gene *hnox/cdg2* operon. Primers 5'-ACACTGCAGTGCGAGACGAGATAGGTCCC-3' (hnoxlacZ F) and 5'-CAGAATTCGTCGAGATTGCCAACCTG-3' (hnoxlacZ R) were used to amplify the promoter region including 470 bases upstream of the start of *hnox*. This amplicon was cloned into pUC19 via EcoRI and PstI and verified by

Table 6.1: Strains and plasmids used in this study

Strains or plasmid	Genotype or Description	Reference or source
Strains		
DH5αF'	*E. coli* cloning host: F' 80 *lacZm15 redA endA1 gyrA96 thi-1hsdR17* ($r_k m_v$) *supE44 relA1 deoR* (*lacZYA–argF*)*U169*	
JM109	*E. coli* cloning host: λ*pir* strain supports the pJP5603 suicide vector.	
S17-1	For conjugation: *recA thi pro hasdRM*$^+$ *RP4:*2-Tc:*Mu:*Km:TnZ	
S17-1λ*pir*	S17-1 with λ*pir* to support pJP5603.	
BL21pLysS	*E. coli* expression host: F$^-$ *ompT hsdS*$_B$*(*$r_B^- m_B^-$*) gal dcm (DE3)* pLysS	
2.4.3	Wild-type strain of *Rhodobacter sphaeroides*	ATCC17025
Δ*hnox/cdg2*	2.4.3 with a deletion in the *hnox/cdg2* operon	This study
Plasmids		
pUC19	Used for cloning in *E. coli* DH5-α (Ap^R)	(43)
pRK415	Broad-host-range plasmid (Tc^R)	(12)
pJP5603	Mobilizable suicide vector (Km^R)	(28)
pSUP202-1	Mobilizable suicide vector (Tc^R, Ap^R, Cm^R)	(36)
pKOK-6	Source of *lacZ*-Km cassette (Tc^R, Km^R, Ap^R)	(14)
pHP45Ω	Source of *aadA*$^+$-Sm^R cassette (Ap^R, Sm^R)	(29)
YS35	pRK415 with the *prrnB'* promoter (Tc^R)	(16)
hnox-lacZ	pRK415 with *hnox* promoter fused to *lacZ*, transcriptional fusion (Tc^R, Km^R)	This study
hnoxKO	pSUP202-1 with *hnox*::*aadA* for deletion of *hnox/cdg2*	This study
hnoxOXP	pET28b(+) with the *hnox* orf having a C-terminal 6x histidine tag (Km^R)	This study
hnox/cdgOXP	pET28b(+) with the *hnox/cdg2* orfs and *cdg2* having a C-terminal 6x histidine tag (Km^R)	This study
prrnBhnox	pRK415 with *prrnB'* fused to *hnox* having a C-terminal 6x histidine tag (Tc^R)	This study
prrnBhnox/cdg	pRK415 with *prrnB'* fused to *hnox/cdg2* with *cdg2* having a C-terminal 6x histidine tag (Tc^R)	This study
pJPhnox	pJP5603 with *prrnB'* fused to *nirK* RBS fused to 5' end of *hnox* encoding a C-terminal 6x histidine tag (Km^R)	This study

sequencing. The promoter was cloned into the broad host range plasmid pRK415. The *lacZ* cassette of pKOK-6 was cloned downstream of the promoter by PstI. The final construct was transformed into S17-1 and subsequently conjugated into *Rhodobacter* strains.

Mutant strain. Double homologous recombination was used to delete a large portion of the *hnox/cdg2* operon, replacing it with a streptomycin resistance cassette. Two fragments were amplified that include the outside edges of the operon. The first fragment used primers 5'-CGGAATTCCAAGGCGGTCTGTTTCAC-3' (hnoxKO1) and 5'-GTTCATGATGATCTTCCCCGG-3' (hnoxKO2). The second fragment used primers 5'-CAGGATCCGATGCGAGACGAGATAGG-3' (hnoxKO3) and 5'-GCCGATCTTGATCCCTACAC-3' (hnoxKO4). The fragments were cloned into pUC19 via EcoRI/BamHI and BamHI/PstI and verified by sequencing. They were then joined into one construct and the streptomycin resistance cassette (*aadA*$^{+}$) BamHI fragment of pHP45 was added between the fragments. The entire construct was then moved into pSUP202-1 via PstI, transformed into *E. coli* S17-1, and conjugated into *Rhodobacter*. The double recombination event was confirmed by PCR. This results in deletion of 910 bases out of 1020 for *cdg2* and 360 bases out of 588 for *hnox*.

Overexpression constructs. There are several overexpression constructs that were made for *hnox* or both *hnox* and *cdg2*. Figure 6.2 shows a schematic of three constructs described below that may be useful for future experiments. An overexpression construct for *hnox* was made by cloning the open reading frame into pET28b(+) to generate a C-terminal 6x histidine tag (Fig. 6.2). Primers used were 5'-CGGAATTCCATGGGACATGGCTTGGTGAAC-3' (hnoxCHIS-F(Eco/Nco)), which has both an EcoRI site and a NcoI site, and 5'-CGAAAGCTTGCCCAGACGCTCCGCCAG-3' (hnoxCHIS-R), which has a HindIII site. Originally, the amplicon was sub-cloned into pUC19 via EcoRI and

HindIII. The insert was then cloned into pET28b(+) via NcoI and HindIII. This construct was sequenced and found to have a mutation in the *hnox* open reading frame that changes a glycine codon to a serine codon. To generate a wild-type construct the pUC19 sub-cloning step was skipped. Instead the original PCR amplicon was cloned directly into pET28b(+) via NcoI and HindIII. This construct was verified by sequencing and found to have no mutations. Both the mutant and wild-type constructs were transformed into the expression host *E. coli* BL21 pLysS.

An overexpression construct for *cdg2* was made by cloning the open reading frame into pET28b(+) to generate a C-terminal 6x histidine tag. Primers used were 5'-CAGAATTCCATGGGGGCCGCGGCGACCGGGATC-3' (cdg2CHIS-F), which

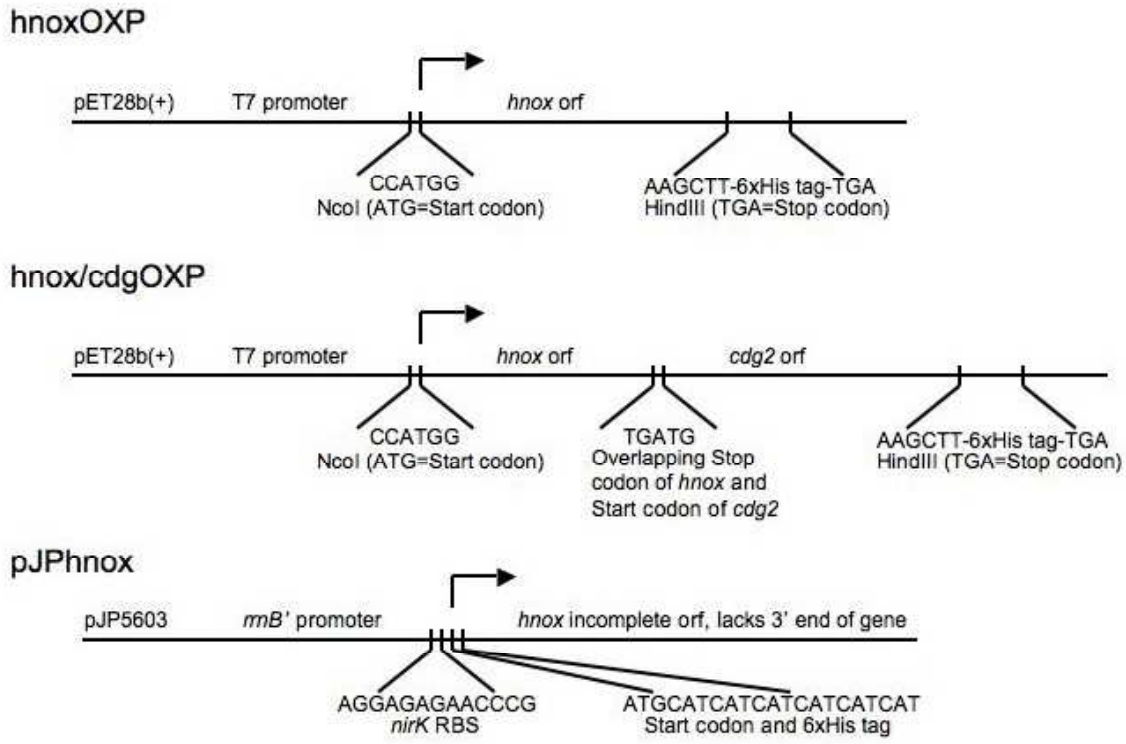

Figure 6.2: Schematic of overexpression constructs for *hnox* and *cdg2*.

has both an EcoRI site and a NcoI site, and 5'-CGAAGCTTGGGGCCCGGCTGCGCGC-3' (cdg2CHIS-R), which has a HindIII site. The amplicon was first sub-cloned into pUC19 via EcoRI and HindIII and verified by sequencing. The confirmed insert was then cloned into pET28b(+) via NcoI and HindIII and the final construct was verified by sequencing. The construct was then transformed into the overexpression host *E. coli* BL21 pLysS.

An overexpression construct was made that contained both the *hnox* and *cdg2* open reading frames with *cdg2* having the C-terminal 6x histidine tag (Fig. 6.2). This takes advantage of the fact that the stop codon of *hnox* and the start codon of *cdg2* overlap. Primers used were 5'- CGGAATTCCATGGGACATGGCTTGGTGAAC-3' (hnoxCHIS-F (Eco/Nco)) and 5'- CGAAGCTTGGGGCCCGGCTGCGCGC-3' (cdg2CHIS-R). The amplicon was cloned directly into pET28b(+) via NcoI and HindIII. The construct was verified by sequencing and transformed into the expression host *E. coli* BL21 pLysS.

To facilitate overexpression of *hnox* in the native *Rhodobacter* background the *hnox* open reading frame was cloned downstream of the *prrnB'* promoter and the *nirK* ribosome binding site (RBS). The *nirK* RBS was used because *hnox* does not have a canonical RBS upstream of the orf. Primers used were 5'-ACAGGATCCAGGAGAGAACCCGATGGGACATGGC-3' (prrnBhnox-F) and 5'-AGTGAATTCCCTTTCGGGCTTTGTTAG-3' (prrnBhnox-R). The amplicon was generated from the pET28b(+)*hnox* construct so that the open reading frame will include the 6x histidine tag. The amplicon was cloned into pUC19 via BamHI and EcoRI. This construct was verified by sequencing. The insert was then moved into pRK415 carrying the *prrnB*' promoter via BamHI and EcoRI. This final construct was then transformed into *E. coli* S17-1 and then conjugated into *R. sphaeroides* 2.4.3.

A construct for overexpression of both *hnox* and *cdg2* in *Rhodobacter* was made using the *prrnB'* promoter and the *nirK* RBS. Primers used were 5'-CTAGGTACCAGGAGAGAACCCGATGGGACATGGC-3' (prrnBhnox-Fnew) and 5'-AGTGAATTCCCTTTCGGGCTTTGTTAG-3' (prrnBhnox-R). The amplicon was generated from the pET28b(+)*hnox-cdg2* construct so that it will include both the *hnox* and *cdg2* open reading frames with the C-terminal 6x histidine tag on *cdg2*. The amplicon was cloned into pRK415 with the *prrnB'* promoter via KpnI and EcoRI. The final construct was transformed into *E. coli* S17-1 and then conjugated into *R. sphaeroides*.

Due to issues with sub-cloning *hnox* and *cdg2* in *E. coli*, a construct was made for a chromosomal cross-in of the *prrnB'* promoter and *nirK* RBS in front of the *hnox-cdg2* operon (Fig. 6.2). To facilitate protein purification the construct was designed to have a N-terminal 6x histidine tag on *hnox*. Primers used were 5'ACAGGATCCAGGAGAGAACCCGATGCATCATCATCATCATCATCATGGC TTGGTGAACAG-3' (rBhnoxNH-F), which has an EcoRI site, the *nirK* RBS, and the N-terminal 6x histidine tag, and 5'-CAAGAATTCAATCGGCAAAGGTCACGC-3' (rBhnoxNH-R). The amplicon was first cloned into pUC19 via BamHI and EcoRI and verified by sequencing. The confirmed insert was then cloned into pRK415 carrying the *prrnB'* promoter, via BamHI and EcoRI, to fuse the promoter to the RBS and 5' end of *hnox*. The fusion was then cloned into the suicide vector pJP5603 in the *E. coli* JM109 background. The final construct was then moved into *E. coli* S17-1λ*pir* and conjugated into *R. sphaeroides* 2.4.3 to generate the cross-in.

Enzyme assays. Gene expression levels were measured as a function of β-galactosidase activity (21). Activity was determined based on three independent cultures. Nir activity was determined using a colorimetric Nir assay (16). Activity was determined for three independent cultures.

Taxis assays. Taxis assays were carried out as previously described (18). Of note, the nitrite stimulus contained 360mM nitrite.

Protein purification. Overexpression in *E. coli* was induced by IPTG, for H-NOX purification aminolevulinic acid was added at ~20mg per 1L of cells. Cells were harvested by centrifugation, washed with 50mM phosphate buffer (pH7.0) and pellets frozen. Thawed pellets were resuspended in 30mL buffer with added DNAse. Cells were lysed by French press at 1280psi for 3 cycles. Cell debris was separated from supernatant by centrifugation. The buffer used was 50mM Tris-HCl, 300mM NaCl and 10% (v/v) glycerol. Standard methods were used for Ni-NTA column chromatography. Column equilibration and supernatant loading were done in 10mM imidazole. Column washing was done with either 20mM imidazole or 50mM imidazole. Column elution was done with 200mM imidazole. Fractions (1mL) were collected and protein elution was monitored by absorbance at 280nm. For H-NOX purification heme scans of fractions were also done. SDS-PAGE was run to observe sample purity and size.

Results and Discussion

Rhodobacter sphaeroides encodes many putative diguanylate cyclase/phosphodiesterase (DGC/PDE) proteins. Expression data and regulation mechanisms for these genes are necessary to predict which proteins are important under different environmental or physiological conditions. In some organisms, inactivation of DGC/PDE encoding genes resulted in no detectable phenotype under laboratory conditions (10, 31, 42). Expression, used as an indicator for presence and functionality of the encoded protein, can give clues to conditions under which a phenotype may be apparent. In addition, knowing the transcriptional regulators of the genes can indicate signals necessary for gene expression. For the *hnox/cdg2* operon

there is no recognizable regulatory motif in the putative promoter region, however, a profile of expression under a variety of environmental conditions could elucidate signals or physiological states, which influence expression.

Expression of *hnox/cdg2.* The *hnox/cdg2* operon is conserved in the three strains of *Rhodobacter sphaeroides*. This allowed us to use the available microarray data from the type strain 2.4.1 to look at expression of *cdg2* (at the time of the microarray experiments the *hnox* gene had not been annotated). There is data for oxic growth (30% oxygen), micro-oxic growth (3% oxygen), photo-anoxic growth, and dark-anoxic growth. Based on these data sets, the expression of *cdg2* is not dynamic and is not highly expressed (in most cases considered absent) under the growth conditions tested (26). This is in contrast to many of the other putative DGC/PDE proteins, which are expressed at significant levels in all the conditions tested. It may be that there is a suite of DGC/PDE genes which are necessary for normal physiology and are constitutively expressed, while a sub-set are specialized and are only expressed under unique environmental conditions. Because H-NOX is predicted to be responsive to NO signals, which are presumably transient and infrequent, the expression of *hnox/cdg2* may be specific to the conditions in which it would be functional, which were not tested in the microarray studies.

A fusion between the putative promoter of the *hnox/cdg2* operon and *lacZ* was used to monitor expression in strain 2.4.3. The stop codon of *hnox* and the start codon of *cdg2* overlap, supporting the inclusion of these genes in an operon. There is an additional gene (Rsph17025_2335) upstream of *hnox*, which is transcribed in the same direction, with a spacing of 60 bases between the stop codon of this gene and the start of *hnox*. This short distance could suggest a longer operon that would include this gene. However, the microarray data does not show a correlation between the expression of gene 2335 and *cdg2* (26). Furthermore, in many other α-proteobacterial

species the *hnox/cdg* operon structure is conserved, with variability in the gene order and content upstream of *hnox*, supporting our predicted operon structure. For these reasons, the expression fusion included the putative promoter region immediately upstream of *hnox*. Expression was monitored by β-galactosidase activity under a variety of environmental conditions, including variable oxygen and nitrate concentrations, and physiological conditions, such as aerobic and microaerobic respiration, denitrification, and photosynthesis. The ability of strain 2.4.3 to denitrify gives us a system that produces NO endogenously. Therefore, if NO is acting as some signal or requirement for expression of these genes, expression could increase under denitrifying conditions. Expression studies revealed almost undetectable levels of expression under all conditions tested (data not shown). This could suggest that we do not have the appropriate promoter region. However, these results do agree with the microarray results for strain 2.4.1. It is possible that these genes are never highly expressed, or that there is an unidentified signal required for high expression. Because the predicted protein products are involved in signaling, it is possible that low levels of expression are sufficient as small amounts of protein can mediate a significant signaling response.

Mutant phenotype of *hnox/cdg2*. The *hnox/cdg2* operon arrangement is present in many members of the α-proteobacteria, including all strains of *R. sphaeroides*. In other bacteria, *hnox* is commonly in a predicted operon with a histidine kinase or a methyl-accepting chemotaxis protein (MCP). This suggests the operon structure is not accidental but reflects the potential for H-NOX to act as an NO (first messenger) signal sensor and transducer to various output domains, in this case a DGC. The *hnox* and *cdg2* genes were knocked out using a suicide vector resulting in double homologous recombination events. This deleted the central portion of the operon, replacing it with a streptomycin resistance cassette. The phenotype of the *hnox/cdg2*

knockout (Δ*hnox/cdg2*) was assessed with a focus on conditions where NO is present. In *Shewanella oneidensis*, where H-NOX is associated with a histidine kinase, it has been shown that the presence of NO, as an intermediate of denitrification, is sensed by H-NOX and the signal is transduced to the histidine kinase, regulating its autophosphorylation activity (30). The authors speculate that the activity of the kinase can then regulate downstream transcriptional events leading to adaptation to a low-oxygen, nitrate or nitrite rich environment. In other organisms, primarily obligate anaerobes, H-NOX is associated with MCPs (5). For these organisms, it has been suggested that NO is sensed as a toxic signal which results in taxis away from the signal. These studies have suggested two potential roles for H-NOX: that of sensing endogenous NO production as a sign of denitrification, and sensing environmental NO as a toxic molecule to be avoided (5). Among the α-proteobacteria, not all species/strains that have the *hnox* gene associated with a DGC gene are capable of denitrification, suggesting that the response to NO may not be specific for physiological adaptation to denitrification, but may be a response to NO toxicity.

Δ*hnox/cdg2* had wild-type denitrifying ability with normal levels of Nir activity and a wild-type taxis response to nitrite. The taxis response of *Rhodobacter* to nitrite is informative as it is predicted to be an indicator of NO tolerance (18). The cells swim to a concentration of nitrite where they can balance the production and consumption of NO, preventing NO toxicity. These results suggest that H-NOX is not involved in the previously characterized taxis response to NO during denitrification (18). Aside from denitrifying related phenotypes, Δ*hnox/cdg2* had wild-type growth rates in the presence and absence of the artificial NO donor sodium nitroprusside (SNP). In addition the cell viability was the same for wild-type and Δ*hnox/cdg2* cells grown in the presence and absence of SNP. The mutant cells were also normal in basic

cell morphology and motility as determined by phase contrast microscopy. If the mutant has a phenotype it appears to be subtle or specific to conditions not tested here.

Overexpression phenotype of *hnox/cdg2*. In the absence of a mutant phenotype, the *hnox/cdg2* operon was overexpressed to determine if altered expression resulted in a detectable phenotype. An overexpression construct was made by fusing the ribosome binding site and open reading frames of *hnox* and *cdg2* to a ribosomal RNA promoter (*prrnB*). We have successfully used this approach for overexpression in 2.4.3 and the promoter is constitutively active at high levels (17). Overexpression of *hnox/cdg2* did not result in any detectable phenotype. However, as will be discussed later, this construct may have acquired mutations that inactivated *hnox* and *cdg2*. We have found these genes are unstable in the *E. coli* cloning background and frequently the only clones obtained have frameshifts. We did not get this entire construct sequenced as we switched to a different strategy for overexpression (discussed below).

Purification of H-NOX and Cdg2. In the absence of detectable cellular phenotypes, we attempted to purify both H-NOX and Cdg2 to characterize these proteins and their predicted functional interaction. In c-di-GMP signaling, there is predicted to be a first messenger, which is an environmental or physiological signal that is sensed by domains associated with the DGC or PDE domains. The recognition of the first messenger elicits changes in the protein structure that influence the activity of the DGC or PDE domain, controlling the production or depletion of the second messenger c-di-GMP in the cell. In the H-NOX/Cdg2 pair, the H-NOX is predicted to be a first messenger sensor of gaseous ligands, specifically NO.

Several recent biochemical studies have established the functionality of the bacterial equivalent of the mammalian H-NOX. The H-NOX protein from *Shewanella* interacts with a histidine kinase and, upon binding NO, inhibits the autophosphorylation of the kinase (30). The H-NOX proteins from facultative aerobes,

like those from mammals, form 5-coordinate NO complexes and exclude O_2 as a ligand (5). However, those from obligate anaerobes are able to bind both NO and O_2, forming 6-coordinate NO complexes (5). This perhaps reflects the differences in lifestyle of these microbes, where anaerobes may require responses to both NO and O_2 as both would be transient toxic signal molecules. This trend is supported by biochemical studies on the H-NOX from *Vibrio cholerae* and *Thermoanaerobacter tengcongensis*. The H-NOX protein from the facultative aerobe, *V. cholerae*, was found to discriminately bind NO, while H-NOX from the anaerobe, *T. tengcongensis*, was found to bind both NO and O_2 (11). The H-NOX bacterial family has been found to be highly sensitive to relevant physiological concentrations of NO. In *Clostridium botulinum*, a member of the H-NOX family was found to bind NO with femtomolar sensitivity (24). This suggests the ancient H-NOX nitric oxide sensory system is functional and physiologically important in bacterial systems.

In *R. sphaeroides* 2.4.3, the DGC encoded downstream of *hnox* contains, in addition to the GGDEF domain, an HNOBA domain. The HNOBA domain is predicted to interact with H-NOX (9), supporting the potential for these two proteins to functionally interact. The secondary structure of the H-NOX domain is primarily α-helical, with a conserved histidine residue that covalently binds heme (9). In cases, which include the *Rhodobacter* H-NOX, where the histidine residue is not conserved, it has been suggested that heme binding is non-covalent. However, in 2.4.3 H-NOX there is a histidine off-set by five residues from the established heme binding residue. This histidine is conserved among the purple bacteria, and is predicted to be located in the α-helix that borders the heme pocket. This histidine may therefore act as the heme ligand.

Attempts were made to purify H-NOX and Cdg2 by adding a histidine tag to the C terminus for Ni^{2+} affinity chromatography. It is important to note that we had

significant difficulty cloning *hnox* and *cdg2*. Anytime these genes were present on plasmids in *E. coli* they acquired inactivating mutations. In addition, cloning efficiency was very low. This required direct cloning into a pET vector. The pET vector construct may be stable in the *E. coli* cloning background because it requires the T7 RNA polymerase for transcription, which is absent in this background. We did successfully make a pET28b(+)*hnox*-C6xHis construct as well as a pET28b(+)*hnox/cdg2*-C6xHis construct. However, neither of these constructs resulted in robust protein production in the *E. coli* expression host.

Mutants obtained through *E. coli* sub-cloning. Initial attempts to sub-clone the complete *hnox* open reading frame resulted in isolation of two pUC19 constructs containing *hnox*, but carrying different mutations. One was a frameshift while the second was a point mutation that changed a glycine codon to a serine codon (Fig. 6.3). This construct is perhaps interesting as it may have inactivated H-NOX by a single residue change. If eventually the expression and purification of H-NOX is optimized this may be a useful H-NOX variant that gives clues to important functional residues.

Because cloning the complete *hnox* and *cdg2* genes was problematic, and expression in *E. coli* was unsuccessful, we attempted several strategies for expression and purification from the native *Rhodobacter* background.

Native expression and purification of *hnox/cdg2*. Initially, we attempted to make a construct fusing a ribosomal RNA promoter (*prrnB'*) and the *nirK* RBS to *hnox* and *cdg2*. However, all of these cloning strategies required using complete open reading frames in the *E. coli* background that we believe to be problematic. So although we did obtain some constructs they were untrustworthy due to the potential for inactivating mutations. This included both an *hnox* alone and an *hnox-cdg2* dual construct. These constructs were moved into *Rhodobacter* but no protein was able to

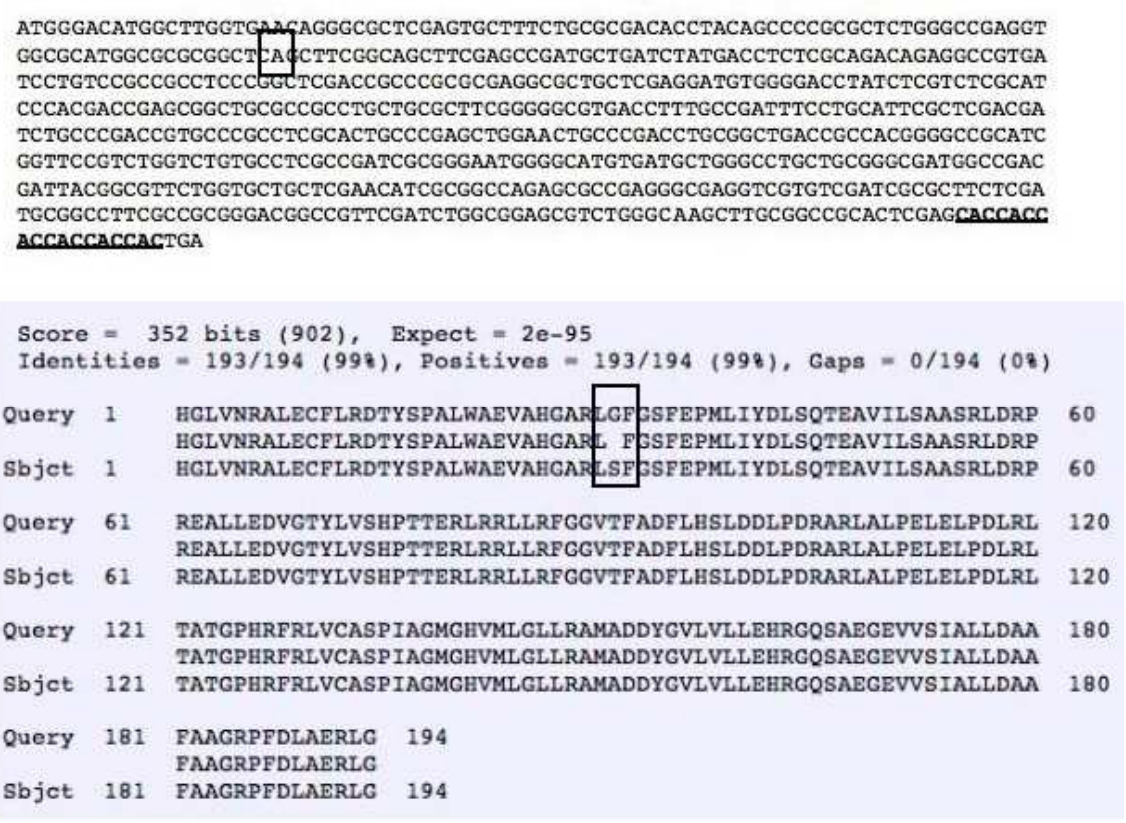

Figure 6.3: Sequence of *hnox* variant with the mutated base boxed (above). Alignment of wild-type and variant H-NOX sequences, the mutated residue (glycine to serine) is boxed (below).

be isolated. To avoid the cloning problem, we attempted a chromosomal cross-in of *prrnB'* and the *nirK* RBS directly in front of *hnox*. This construct did not require cloning all of *hnox* as it only required the 5' end of the gene including the start region where a 6x histidine tag was added. This would cross-in to the chromosome by homologous recombination into *hnox*. Currently, we have made the cross-in construct but have been unable to obtain a cross-in of the construct into the *Rhodobacter* chromosome. It is possible that, as in *E. coli*, the *hnox* and *cdg2* products are toxic in *Rhodobacter* when their native expression pattern and physiological context is altered.

REFERENCES

1. **Aldridge, P., R. Paul, P. Goymer, P. Rainey, and U. Jenal.** 2003. Role of the GGDEF regulator PleD in polar development of *Caulobacter crescentus*. Mol. Microbiol. **47:**1695-708.

2. **Amikam, D., M. Galperin, and O. Journals.** 2006. PilZ domain is part of the bacterial c-di-GMP binding protein. Bioinformatics. **22:**3-6.

3. **Amikam, D., Y. Shilo, G. Volman, P. Ohana, and M. Benziman.** 1997. c-di-GMP-binding protein, a new factor regulating cellulose synthesis in *Acetobacter xylinum*. FEBS Lett. **416:**207-11.

4. **Andrade, M., M. Alegria, C. Guzzo, C. Docena, M. Rosa, C. Ramos, and C. Farah.** 2006. The HD-GYP domain of RpfG mediates a direct linkage between the Rpf quorum-sensing pathway and a subset of diguanylate cyclase proteins in the phytopathogen *Xanthomonas axonopodis* pv citri. Mol. Microbiol. **62:**537-51.

5. **Boon, E. and M. Marletta.** 2005. Ligand discrimination in soluble guanylate cyclase and the H-NOX family of heme sensor proteins. Curr. Opin. Chem. Biol. **9:**441-6.

6. **Camilli, A. and B. Bassler.** 2006. Bacterial small-molecule signaling pathways. Science **311:**1113-6.

7. **Chung, C. T., S. L. Niemela, and R. H. Miller.** 1989. One-step preparation of competent *Escherichia coli*: transformation and storage of bacterial cells in the same solution. Proc. Natl. Acad. Sci. U. S. A. **86:**2172-2175.

8. **Garcia, B., C. Latasa, C. Solano, F. Garcia-del Portillo, C. Gamazo, and I. Lasa.** 2004. Role of the GGDEF protein family in *Salmonella* cellulose biosynthesis and biofilm formation. Mol. Microbiol. **54:**264-77.

9. **Iyer, L., V. Anantharaman, and L. Aravind.** 2003. Ancient conserved domains shared by animal soluble guanylyl cyclases and bacterial signaling proteins. BMC Genomics **4:**5.

10. **Jenal, U. and J. Malone.** 2006. Mechanisms of cyclic-di-GMP signaling in bacteria. Annu. Rev. Genet. **40:**385-407.

11. **Karow, D., D. Pan, R. Tran, P. Pellicena, A. Presley, R. Mathies, and M. Marletta.** 2004. Spectroscopic characterization of the soluble guanylate cyclase-like heme domains from *Vibrio cholerae* and *Thermoanaerobacter tengcongensis*. Biochemistry **43:**10203-11.

12. **Keen, N. T., S. Tamaki, D. Kobayashi, and D. Trollinger.** 1988. Improved broad-host-range plasmids for DNA cloning in gram-negative bacteria. Gene **70:**191-197.

13. **Kim, Y. and L. McCarter.** 2007. ScrG, a GGDEF-EAL protein, participates in regulating swarming and sticking in *Vibrio parahaemolyticus*. J. Bacteriol. **189:**4094-107.

14. **Kokotek, W. and W. Lotz.** 1989. Construction of a lacZ-kanamycin-resistance cassette, useful for site-directed mutagenesis and as a promoter probe. Gene **84:**467-471.

15. **Kuchma, S., K. Brothers, J. Merritt, N. Liberati, F. Ausubel, and G. O'Toole.** 2007. BifA, a Cyclic-Di-GMP Phosphodiesterase, Inversely Regulates Biofilm Formation and Swarming Motility by *Pseudomonas aeruginosa* PA14. J. Bacteriol. **189:**8165-78.

16. **Laratta, W., M. Nanaszko, and J. Shapleigh.** 2006. Electron transfer to nitrite reductase of *Rhodobacter sphaeroides* 2.4.3: examination of cytochromes c2 and cY. Microbiology (Reading, Engl.) **152:**1479-88.

17. **Laratta, W., P. Choi, I. Tosques, and J. Shapleigh.** 2002. Involvement of the PrrB/PrrA two-component system in nitrite respiration in *Rhodobacter sphaeroides* 2.4.3: evidence for transcriptional regulation. J. Bacteriol. **184:**3521-9.

18. **Lee, D., A. Ramos, L. Macomber, and J. Shapleigh.** 2002. Taxis response of various denitrifying bacteria to nitrate and nitrite. Appl. Environ. Microbiol. **68:**2140-7.

19. **Lim, B., S. Beyhan, and F. Yildiz.** 2007. Regulation of *Vibrio* polysaccharide synthesis and virulence factor production by CdgC, a GGDEF-EAL domain protein, in *Vibrio cholerae*. J. Bacteriol. **189:**717-29.

20. **Mackenzie, C., J. Eraso, M. Choudhary, J. Roh, and X. Zeng.** 2007. Postgenomic Adventures with *Rhodobacter sphaeroides*. Annu. Rev. Microbiol. **61:**283-307.

21. **Maniatis, T., E. F. Fritsch, and J. Sambrook.** 1982. Molecular Cloning: a laboratory manual. Cold Spring Harbor Laboratory Press, Cold Spring Harbor, NY.

22. **Mendez-Ortiz, M., M. Hyodo, Y. Hayakawa, and J. Membrillo-Hernandez.** 2006. Genome-wide transcriptional profile of *Escherichia coli* in response to high levels of the second messenger 3',5'-cyclic diguanylic acid. J. Biol. Chem. **281:**8090-9.

23. **Merritt, J., K. Brothers, S. Kuchma, and G. O'Toole.** 2007. SadC Reciprocally Influences Biofilm Formation and Swarming Motility via Modulation of Exopolysaccharide Production and Flagellar Function. J. Bacteriol. **189:**8154-64.

24. **Nioche, P., V. Berka, J. Vipond, N. Minton, A. Tsai, and C. Raman.** 2004. Femtomolar sensitivity of a NO sensor from *Clostridium botulinum*. Science **306:**1550-3.

25. **O'Shea, T., A. Klein, K. Geszvain, A. Wolfe, and K. Visick.** 2006. Diguanylate cyclases control magnesium-dependent motility of *Vibrio fischeri*. J. Bacteriol. **188:**8196-205.

26. **Pappas, C., J. Sram, O. Moskvin, P. Ivanov, R. Mackenzie, M. Choudhary, M. Land, F. Larimer, S. Kaplan, and M. Gomelsky.** 2004. Construction and validation of the *Rhodobacter sphaeroides* 2.4.1 DNA microarray: transcriptome flexibility at diverse growth modes. J. Bacteriol. **186:**4748-58.

27. **Paul, R., S. Abel, P. Wassmann, A. Beck, H. Heerklotz, and U. Jenal.** 2007. Activation of the diguanylate cyclase PleD by phosphorylation-mediated dimerization. J. Biol. Chem. **282:**29170-7.

28. **Penfold, R. J. and J. M. Pemberton.** 1992. An improved suicide vector for construction of chromosomal insertion mutations in bacteria. Gene **118:**145-6.

29. **Prentki, P. and H. M. Krisch.** 1984. In vitro insertional mutagenesis with a selectable DNA fragment. Gene **29:**303-13.

30. **Price, M., L. Chao, and M. Marletta.** 2007. *Shewanella oneidensis* MR-1 H-NOX Regulation of a Histidine Kinase by Nitric Oxide. Biochemistry **46:**13677-13683.

31. **Roemling, U., M. Gomelsky, and M. Galperin.** 2005. C-di-GMP: the dawning of a novel bacterial signalling system. Mol. Microbiol. **57:**629-39.

32. **Ross, P., R. Mayer, and M. Benziman.** 1991. Cellulose biosynthesis and function in bacteria. Microbiol. Rev. **55:**35-58.

33. **Ryjenkov, D., R. Simm, U. Roemling, and M. Gomelsky.** 2006. The PilZ domain is a receptor for the second messenger c-di-GMP: the PilZ domain protein YcgR controls motility in enterobacteria. J. Biol. Chem. **281:**30310-4.

34. **Ryjenkov, D., M. Tarutina, O. Moskvin, and M. Gomelsky.** 2005. Cyclic diguanylate is a ubiquitous signaling molecule in bacteria: insights into biochemistry of the GGDEF protein domain. J. Bacteriol. **187:**1792-8.

35. **Schmidt, A., D. Ryjenkov, and M. Gomelsky.** 2005. The ubiquitous protein domain EAL is a cyclic diguanylate-specific phosphodiesterase: enzymatically active and inactive EAL domains. J. Bacteriol. **187:**4774-81.

36. **Simon, R., U. Priefer, and Pühler, A.** 1983. A broad host range mobilization system for in vivo genetic engineering: transposon mutagenesis in gram negative bacteria. Bio/Technology **1:**784-791.

37. **Tal, R., H. Wong, R. Calhoon, D. Gelfand, A. Fear, G. Volman, R. Mayer, P. Ross, D. Amikam, H. Weinhouse, A. Cohen, S. Sapir, P. Ohana, and M. Benziman.** 1998. Three cdg operons control cellular turnover of cyclic di-GMP in *Acetobacter xylinum*: genetic organization and occurrence of conserved domains in isoenzymes. J. Bacteriol. **180:**4416-25.

38. **Tarutina, M., D. Ryjenkov, and M. Gomelsky.** 2006. An unorthodox bacteriophytochrome from *Rhodobacter sphaeroides* involved in turnover of the second messenger c-di-GMP. J. Biol. Chem. **281:**34751-8.

39. **Tischler, A. and A. Camilli.** 2005. Cyclic diguanylate regulates *Vibrio cholerae* virulence gene expression. Infect. Immun. **73:**5873-82.

40. **Tischler, A. and A. Camilli.** 2004. Cyclic diguanylate(c-di-GMP) regulates *Vibrio cholerae* biofilm formation. Mol. Microbiol. **53:**857-69.

41. **Wassmann, P., C. Chan, R. Paul, A. Beck, H. Heerklotz, U. Jenal, and T. Schirmer.** 2007. Structure of BeF3- -modified response regulator PleD: implications for diguanylate cyclase activation, catalysis, and feedback inhibition. Structure **15:**915-27.

42. **Wolfe, A. and K. Visick.** 2007. Get the message out: cyclic-di-GMP regulates multiple levels of flagellar-based motility. J. Bacteriol. **190:**463-75.

43. **Yanisch-Perron, C., J. Vieira, and J. Messing.** 1985. Improved M13 phage cloning vectors and host strains: nucleotide sequences of the M13mp18 and pUC19 vectors. Gene **33:**103-19.

Chapter 7

Conclusion

A model system for denitrification

The overarching goal of my research was to refine and expand a model for denitrification in *Rhodobacter sphaeroides* strain 2.4.3. *Rhodobacter*, along with its close relatives, is one of the most metabolically versatile organisms known (7). *R. sphaeroides* already serves as an important model system for aerobic respiration and anoxygenic photosynthesis, providing ample background on electron transfer pathways and redox-dependent metabolic regulation in this system (7). By adding a model for denitrification, we complement existing models and demonstrate how yet another metabolic pathway for energy conservation can be dovetailed into an already complex physiology.

Overall, we have defined the distinct physiological contributions of two nitrate reductases, expanded the denitrification regulon, provided circumstantial evidence for an additional layer of oxygen control on denitrification via NnrR, and explored the potential for denitrification-independent cellular responses to NO. In Chapter 2 we showed that the two periplasmic nitrate reductases in strain 2.4.3 serve two very distinct physiological purposes. oNap seems to be involved in redox homeostasis. In an organism like *Rhodobacter*, this could be a very important and frequently required role for nitrate reduction. Being primarily a phototroph, but being capable of respiration, *Rhodobacter* certainly transitions diurnally from one mode of growth to the other. In addition, *R. sphaeroides* can grow both as a heterotroph and an autotroph, depending on the availability of growth substrate. During transitions between growth modes, or between carbon sources, redox balancing could play an important role. The second nitrate reductase, rNap, seems to be devoted to denitrification based on the

regulation and mutant studies. In Chapter 3, we consider the regulation of denitrification by the transcriptional regulators PrrA and NnrR. A complexity concerning the interplay between the activity of the cbb_3-oxidase and induction of denitrification genes was resolved. The phenotype seems to be disconnected from PrrA, the regulator directly influenced by cbb_3, and instead seems to relate to the activity of NnrR, the denitrification regulator. In fact, NnrR seems to be sensitive to residual oxygen that cannot be respired by cells lacking the high affinity cbb_3. This adds an additional layer to denitrification regulation that may fine tune induction to specific oxygen levels, more so than the PrrBA system. In Chapter 4, we expanded the NnrR denitrification regulon. Important members include pseudoazurin, one of two electron donors to Nir, and NorEF, two putative additional subunits of the Nor enzyme complex that contribute to faster denitrification rates and balanced NO production/consumption. The results of these chapters have contributed significantly to our understanding of denitrification in strain 2.4.3.

Denitrification in the environment

The development of model systems not only serves as a basic understanding of cell physiology, but also as comparison to outside systems and to the real world environment. There have been numerous environmental surveys for the denitrification genes *nirK*, *nirS*, and *nosZ* (3-5, 11). *nirK* encodes the copper-type Nir, *nirS* encodes a subunit of the cd_1-Nir, and *nosZ* encodes a subunit of the nitrous oxide reductase. These genes are considered signatures of bacterial denitrifiers. In freshwater estuaries, which contribute significantly to global denitrification, α-proteobacterial denitrifiers coding *nirK* are found in high abundance (3). Specifically, clones with significant similarity to *Rhodobacter* and close rhizobia relatives are found. The freshwater, sediment rich environment is consistent with *Rhodobacter* ecology, and the prevalence

of plants could contribute to rhizobia abundance. Soil samples with distinct physicochemical traits and from widespread geographic regions also have denitrifiers of the α-proteobacterial *nirK*-type well represented (4, 5). Studies of denitrification genes in terrestrial and freshwater ecosystems, suggests that the α-proteobacteria are important members of the denitrification community. Thus, an understanding of the regulation and physiology of denitrification in *R. sphaeroides* may be broadly applicable to environments where related denitrifiers are found. Furthermore, there are several rhizobia species where denitrification has been studied in detail (2). Comparing and integrating common features of model denitrifiers may provide a context for relating certain environmental parameters, like oxygen and nitrate concentration, to denitrification capacity in a given environment.

Denitrification potential in the α-proteobacteria

Perhaps more important than the mere presence of related denitrifiers in the environment, is the potential to predict features of denitrification in other organisms based on our model. It seems that there are different "styles" of denitrification that may be niche specific. And, these styles could be shaped in part by the presence of accessory proteins, like NorE, to the major reductases involved in denitrification.

The suites of denitrification genes present in sequenced α-proteobacterial genomes were analyzed for patterns in gene distribution. Genomes were searched for denitrification genes. A binary matrix was generated where genes that were present in any given genome were assigned the value of "1" and genes not present were assigned a value of "0". Using the StatistiXL data analysis software package, suites were clustered hierarchically using Euclidean distance and the group average algorithm. The dendrogram representing the hierarchical group clustering is shown in Figure 7.1.

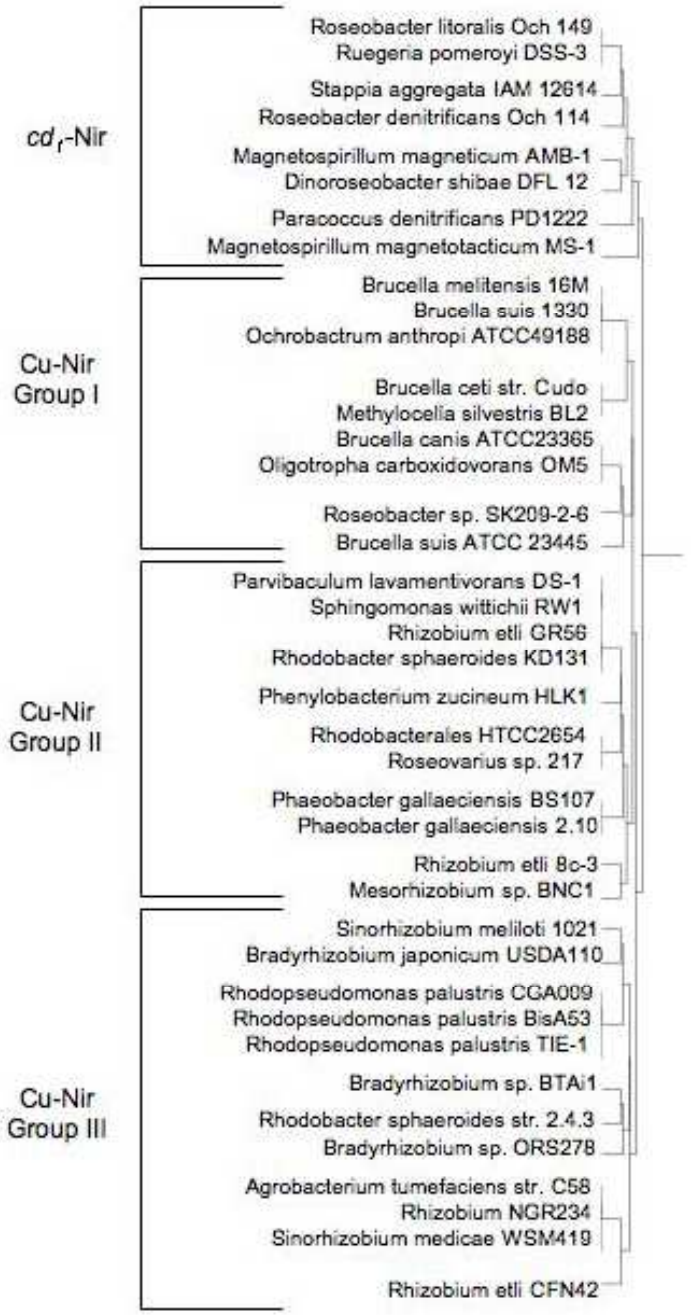

Figure 7.1: Dendrogram depicting hierarchical clustering of α-proteobacteria based on the suite of denitrification genes encoded in each genome. There are four major groups: the cd_1-Nir encoding group, the Cu-Nir Group I that utilizes Nar, the Cu-Nir Group II where most members lack nitrate reduction ability, and the Cu-Nir group III that has the Nor enzyme with the NorE subunit and mostly Nap-type nitrate reductases.

In general, there were four major group clusters. The first was the organisms that utilize the cd_1-Nir. Within this group, every organism has a Nos and all but one have a Nor that includes NorE. There is every type of nitrate reductase represented, and some organisms even have a pseudoazurin. While pseudoazurin is not required for Nir activity in this group, it could be used as an electron donor to Nor (14). The second major group cluster is the Cu-Nir Group I. Within this group, every organism uses a membrane-bound nitrate reductase (Nar) and a Cu-Nir. However, there is no pattern for NorE or pseudoazurin. Those organisms that don't have pseudoazurin must have other electron donors for Cu-Nir. Within the Cu-Nir Group II cluster, most organisms have sparse denitrification systems. Interestingly, none of these organisms have NorE, perhaps consistent with decreased denitrification potential. All but one lack nitrate reductase, and the same is true for Nos. Most have only Cu-Nir, Nor, and pseudoazurin. This group includes *R. sphaeroides* strain KD131. Significant levels of denitrification in this group would require nitrite, which is not commonly found at high levels in the environment. However, it is conceivable that these organisms could respire nitrite in the neighborhood of nitrate reducers where nitrite could be plentiful. In the last group, the Cu-Nir Group III, most organisms use Nap and all have Cu-Nir and Nor with NorE. Pseudoazurin is present in about half of species in Group III. This is the group where *R. sphaeroides* 2.4.3 fits in, along with many of the rhizobia denitrifiers.

While the organisms were clustered based on denitrification genes, the groups also somewhat correlate with the predicted ecology of the organisms and the phylogenetic relatedness. The cd_1-Nir group includes the majority of the members of the marine Roseobacter clade. The Cu-Nir Group I includes all of the *Brucella* pathogens, and the opportunistic pathogen *Ochrobactrum anthropi*, considered the sister group to *Brucella*. The Cu-Nir Group II is more scattered, with no obvious

patterns. Finally, the Cu-Nir Group III includes most of the soil-dwelling rhizobia and the freshwater/sediment phototrophs *R. sphaeroides* 2.4.3 and *Rhodopseudomonas palustris* strains.

The organisms used for cluster analysis were only those α-proteobacteria that have nitrite reductase ability. In addition to these organisms, there are organisms that lack nitrite reductase but carry other parts of the denitrification system. Table 7.1 shows these organisms and their denitrification genes. It is interesting that different strains of the same species can have very different denitrification capacity. For example, within the species *R. sphaeroides* and *Rhodopseudomonas palustris* there is the entire spectrum of capacity, from full denitrifiers down to only Nor or Nos. It is likely that different strains of the same species are experiencing different selective pressures on the denitrification system.

From the model system to the real world

There are certainly many driving forces in the evolution of denitrification systems. These driving forces could include horizontal gene transfer, evolution of enzyme variants as seen in both Nir and Nor, and lineage sorting (8). In addition, some organisms have multiple copies of denitrification genes. For example, *Magnetospirillum magnetotacticum* has three copies of *nirK* scattered on the chromosome (8). The presence of multiple copies can allow for greater flexibility in evolving distinct variants of these enzymes. In addition, the contribution of denitrification to an organism's lifestyle may also influence the capacity for, and diversity in, denitrification. In organisms where anoxia is infrequently encountered, there may be more opportunity for non-synonymous mutations in denitrification genes, as the gene products are not contributing significantly to the life cycle of the

Table 7.1: Nitrate respirers and partial denitrifiers of the α-proteobacteria

Organism	Denitrification Genes
Rhizobium leguminosarum bv. *Trifolii* WSM2304 *Rhizobium etli* CIAT 894 *Rhizobium leguminosarum* bv. *Trifolii* WSM1325	*onap*
Rhodobacter sphaeroides 2.4.1	*onap, nor*
Rhodopseudomonas palustris BisB18 *Methylobacterium* sp. 4-46	*onap, nos*
Rhodospirillum centenum SW	*onap, nor, nos*
Azorhizobium caulinodans ORS 571 *Caulobacter* sp. K31 *Methylobacterium* sp. 4-46 *Methylobacterium nodulans* ORS 2060 *Hyphomonas neptunium* ATCC 15444 *Acidiphilium cryptum* JF-5 *Nitrobacter hamburgensis* X14	*nar*
Maricaulis maris MCS10 *Methylobacterium radiotolerans* JCM 2831 *Brucella melitensis* ATCC 23457 *Roseobacter* sp. MED193	*nar, paz*
Brucella abortus bv. 1 str. 9-941	*nar, nor, norE, paz*
Rhodobacter sphaeroides 2.4.9 *Xanthobacter autotrophicus* Py2	*nor*
Roseovarius sp. TM1035 *Rhodopseudomonas palustris* HaA2	*nos*
Brucella melitensis biovar *Abortus* 2308	*norE, paz*
Brucella abortus S19	*norE*

organism (8). This could result in closely related organisms that inhabit distinct habitats evolving different variants of denitrification genes over time. This could be the case in *Rhodobacter sphaeroides* where every sequenced strain has a different denitrification capacity. By developing model systems for denitrification, we can add valuable information to predictions for denitrification activity in the environment as well as to predictions for the different selective pressures that could influence evolution of these genes.

Denitrification is particularly important in the rhizosphere of plants (6). The rhizosphere is a hotbed of microbial activity as root exudates provide a readily metabolized source of simple sugars and carbon compounds. In recent work, mock maize root exudates were applied to soil microcosms. The mock-exudates were shown to stimulate denitrification activity, with the composition of the exudates influencing the extent of denitrification in terms of the end product N_2O versus N_2 (6). In addition, an analysis of *nirK* and *nirS* transcripts in the rhizosphere of grain legumes showed a lack of *nirS* transcripts and a predominance of *nirK* transcripts (13). Sequenced *nirK* transcripts grouped with *nirK* from rhizobia species of the α-proteobacteria, however the sequences found were unique. Further evidence of the importance of denitrification in the rhizosphere is the duplication of *nirK* in *Azospirillum brasilense* (9). *A. brasilense* is known to promote wheat plant growth and association with the plant induces expression of denitrification genes (10). It is speculated that NO-produced by the Nir activity of *A. brasilense* promotes plant root formation and growth. While in a strict sense denitrification would be predicted to be detrimental to plant growth, as it depletes available nitrate in the rhizosphere, studies suggest that plant growth may actually be enhanced by denitrifiers. Studies on the regulation and physiology of denitrifiers will certainly contribute to optimizing agricultural plant growth via modulating the rhizosphere bacterial community.

Besides agriculture, denitrification is also important in sewage waste treatment and bioremediation (12). Denitrification is an efficient method of removing nitrate contamination from drinking water and efforts are ongoing to optimize this process. In addition, denitrification may play a significant role in the anaerobic degradation of environmental contaminants. There are well-studied cases of aerobic degradation of heterocyclic amine compounds, however, recently 30 organisms were isolated that couple denitrification and heterocyclic amine degradation (1). These organisms

grouped with the α and β-proteobacteria. Denitrifiers, which are capable of coupling pollutant degradation to both aerobic respiration and denitrification, can function in a wider range of conditions for remediation of contaminated sites. Understanding denitrification in these organisms would allow optimization of remediation efforts.

Final remarks

It is my hope that I have conveyed the importance of denitrification in the global N-cycle, as well as in agriculture, sewage treatment, and bioremediation (12). Especially as modern agricultural practices expand into the developing world and continue to intensify in the developed world, nitrate levels in soil and drinking waters will only increase. Likewise, industrialization and waste and pollutant accumulation will bring remediation of contaminated sites to the forefront. By developing model organisms, like *Rhodobacter*, we can add to a greater understanding of the role of denitrification in all of these processes.

REFERENCES

1. **Bae, H. S., W. T. Im, Y. Suwa, J. M. Lee, S. T. Lee, and Y. K. Chang.** 2009. Characterization of diverse heterocyclic amine-degrading denitrifying bacteria from various environments. Arch. Microbiol. **191:**329-40.

2. **Bedmar, E. J., E. F. Robles, and M. J. Delgado.** 2005. The complete denitrification pathway of the symbiotic, nitrogen-fixing bacterium *Bradyrhizobium japonicum*. Biochem. Soc. Trans. **33:**141-4.

3. **Fortunato, C. S., D. B. Carlini, E. Ewers, and K. Bushaw-Newton.** 2009. Nitrifier and denitrifier molecular operational taxonomic unit compositions from sites of a freshwater estuary of Chesapeake Bay. Can. J. Microbiol. **55:**333-46.

4. **Henry, S., D. Bru, B. Stres, S. Hallet, and L. Philippot.** 2006. Quantitative detection of the nosZ gene, encoding nitrous oxide reductase, and comparison of the abundances of 16S rRNA, narG, nirK, and nosZ genes in soils. Appl. Environ. Microbiol **72:**5181-9.

5. **Henry, S., E. Baudoin, J. C. Lopez-Gutierrez, F. Martin-Laurent, A. Brauman, and L. Philippot.** 2004. Quantification of denitrifying bacteria in soils by nirK gene targeted real-time PCR. Journal of Microbiological Methods **59:**327-35.

6. **Henry, S., S. Texier, S. Hallet, D. Bru, C. Dambreville, D. Cheneby, F. Bizouard, J. C. Germon, and L. Philippot.** 2008. Disentangling the rhizosphere effect on nitrate reducers and denitrifiers: insight into the role of root exudates. Environ. Microbiol. **10:**3082-92.

7. **Hunter, C. N., F. Daldal, M. C. Thurnauer, and J. T. Beatty.** 2009. The Purple Phototrophic Bacteria. Springer, Dordrecht, The Netherlands.

8. **Jones, C. M., B. Stres, M. Rosenquist, and S. Hallin.** 2008. Phylogenetic analysis of nitrite, nitric oxide, and nitrous oxide respiratory enzymes reveal a complex evolutionary history for denitrification. Molecular Biology and Evolution **25:**1955-66.

9. **Pothier, J. F., C. Prigent-Combaret, J. Haurat, Y. Moenne-Loccoz, and F. Wisniewski-Dye.** 2008. Duplication of plasmid-borne nitrite reductase gene nirK in the wheat-associated plant growth-promoting rhizobacterium *Azospirillum brasilense* Sp245. Mol. Plant Microbe Interact. **21:**831-42.

10. **Pothier, J. F., F. Wisniewski-Dye, M. Weiss-Gayet, Y. Moenne-Loccoz, and C. Prigent-Combaret.** 2007. Promoter-trap identification of wheat seed extract-induced genes in the plant-growth-promoting rhizobacterium *Azospirillum brasilense* Sp245. Microbiology (Reading, Engl.) **153:**3608-22.

11. **Prieme, A., G. Braker, and J. M. Tiedje.** 2002. Diversity of nitrite reductase (nirK and nirS) gene fragments in forested upland and wetland soils. Appl. Environ. Microbiol **68:**1893-900.

12. **Seitzinger, S., J. A. Harrison, J. Bohlke, A. F. Bouwman, R. Lowrance, B. Peterson, C. Tobias, and G. Van Drecht.** 2006. Denitrification across landscapes and waterscapes: a synthesis. Ecological applications : a publication of the Ecological Society of America **16:**2064-90.

13. **Sharma, S., M. K. Aneja, J. Mayer, J. C. Munch, and M. Schloter.** 2005. Diversity of transcripts of nitrite reductase genes (nirK and nirS) in rhizospheres of grain legumes. Appl. Environ. Microbiol. **71:**2001-7.

14. **Zumft, W.** 1997. Cell biology and molecular basis of denitrification. Microbiol. Mol. Biol. Rev. **61:**533-616.

APPENDIX

Brucella neotomae utilizes quinol oxidases for respiration but retains a functional cytochrome *c* maturation system

Summary

Brucella species are the causative agent of the zoonotic disease Brucellosis. *Brucella neotomae* is an oxidase negative member of the genus that selectively infects rodents. Here we investigated the free-living respiratory physiology of *B. neotomae* by investigating expression of the four terminal oxidases, type of heme present in aerobic cells, as well as functionality of the cytochrome *c* maturation system. The two quinol oxidases were most highly expressed, with the low-affinity *bo*-quinol oxidase being the predominant oxidase. The two cytochrome oxidases were expressed at lower levels, however, the high-affinity cbb_3-oxidase showed some oxygen-dependent regulation. In aerobic cells *b* type heme predominates, with no evidence of *c* type heme. In addition, we report the ability of the cells to produce a heterologous *c*-type cytochrome, establishing a functional cytochrome *c* maturation system in this organism.

Introduction

Brucella species are the causative agent of the endemic disease Brucellosis (11). Brucellosis is one of the most common zoonotic diseases and while modern agricultural and public health practices have mitigated it, in developing countries the disease is still prevalent and economically significant (11). *Brucella* causes a chronic infection in mammals that is characterized by abortion in ruminants and an undulant fever in humans (11). The *Brucella* are gram negative coccobacilli that invade host

macrophages and establish replicative niches allowing long term intracellular survival (11).

There are currently six recognized species of *Brucella*, including biovars of several of these species, and in addition two recently proposed species isolated from marine mammals (26). In general, *Brucella* species have narrow host ranges with each species having a preferred host (11). However, four of these species are capable of infecting humans (11). One species, *B. neotomae*, is found in rodents (desert wood rat) and has never been shown to cause human infection. This species is also one of the few oxidase negative species of the genus, and is the focus of the present research.

In order to survive in host macrophages, *Brucella* must be equipped to handle several stresses including low pH, nutrient limitation, and low oxygen tension (24). An important feature of successful *Brucella abortus* infection is dependence on the aerobic *bd*-quinol oxidase, perhaps aiding in survival of low oxygen tension as well as reactive oxygen species (10). Absence of the *bd*-quinol oxidase resulted in severe attenuation in the mouse model of infection. In addition, this mutant was more sensitive to reactive oxygen species, low pH, and respiratory inhibitors (10). Other research in *B. abortus* demonstrates no dependence on the bc_1-dependent branch of the electron transport chain, consistent with the cytochrome *c* oxidases not playing a role in pathogenesis (16). The link between the *bd*-quinol oxidase and resistance to stress and reactive oxygen species is not unique to *Brucella*. In *Escherichia coli*, *Azotobacter vinelandii*, *Moorella thermoacetica,* and a number of other organisms the *bd*-quinol oxidase plays a role in adaptations to stress under low oxygen tension (7, 9, 20). Importantly, the oxidase trends seen in *B. abortus* are not in agreement with those seen in *B. suis*. In *B. suis* the cbb_3-cytochrome oxidase was required for persistent infection, while lack of the *bd*-quinol oxidase resulted in a hyper-virulent state (14). This

suggests the aerobic respiratory capacity may be tailored to specific hosts and specific environments.

The majority of *Brucella* isolates are oxidase positive. However, two species of *Brucella*, *neotomae* and *ovis*, are oxidase negative. Based on the genome sequences of five *Brucella* species (*melitensis, suis, abortus, canis*, *ovis*) there are four potential oxidases (8, 13, 21). There are two cytochrome oxidases, an aa_3-type and a cbb_3-type. The aa_3 is predicted to be a low-affinity oxidase, while the cbb_3 is predicted to be a high-affinity oxidase. In addition, there are two quinol oxidases, a *bo*-type and a *bd*-type. Continuing the trend, the *bo*-type is predicted to be low-affinity, while the *bd*-type is predicted to be high oxygen affinity. The oxidase negative phenotype of *B. neotomae* indicates this species uses the quinol oxidases for free-living aerobic growth.

The majority of *Brucella* studies focus on pathogenesis with a lack of focus on the free-living, or non-host influenced, physiology. We sought to contribute to an overall understanding of respiration in an intracellular bacterial pathogen by studying the respiratory physiology of free-living *B. neotomae*. Here we investigated the expression of the aerobic oxidases in *B. neotomae*. In addition we did a pyridine-hemochrome analysis of cellular hemes as an indication of type of heme, and thus oxidase, present. And finally, we investigated the functionality of the cytochrome *c* maturation (ccm) system and its involvement in the oxidase phenotype of *B. neotomae*.

Materials and Methods

Bacterial strains and culture conditions: *Brucella neotomae* strain 5K33 was used in this study (Table A.1). This strain was lyophilized in 1965 and rehydrated for a 2004 study (1, 5). Sequencing showed the 16S rRNA of strain 5K33 to be identical to

that of the ATCC 23459 strain, which was also derived from the original 5K33 isolate (1). *Escherichia coli* strain DH5-α was used as a cloning background and for transformations, and S17-1 was used for biparental conjugations (Table A.1).

Table A.1: Strains and Plasmids used in this study.

Strains and plasmids	Genotype or Description	Reference or source
Strains		
DH5αF'	*E. coli* cloning host: F' 80 *lacZm15 redA endA1 gyrA96 thi-1hsdR17* ($r_k m_v$) *supE44 relA1 deoR* (*lacZYA–argF*)*U169*	
S17-1	For conjugal transfer of plasmids: *recA thi pro hasdRM*$^+$ *RP4:*2-Tc:*Mu:*Km:TnZ	
5K33	Wild-type strain of *Brucella neotomae*	(5)
Plasmids		
pUC19	Used for cloning in *E. coli* DH5-α (Ap^R)	(27)
pRK415	Broad-host-range plasmid (Tc^R)	(15)
pKOK-6	Source of *lacZ*-Km cassette (Tc^R, Km^R, Ap^R)	(17)
pcycA	pWL200, pRK415 with *prrnB'* fused to *cycA*	(18)
pcyoZ	pRK415 with the *cyo* promoter fused to *lacZ*. (Tc^R, Km^R)	this study
pcydZ	pRK415 with the *cyd* promoter fused to *lacZ*. (Tc^R, Km^R)	this study
pcoxZ	pRK415 with the *cox* promoter fused to *lacZ*. (Tc^R, Km^R)	this study
pccoZ	pRK415 with the *cco* promoter fused to *lacZ*. (Tc^R, Km^R)	this study

B. neotomae was grown on Brucella Broth (BD-Becton, Dickinson, and Company) at 30°C. For flask culture, cells were grown in 100mL of media. For microaerobic culture, flasks were stoppered so as cells grew and respired, oxygen levels naturally decreased. When necessary, antibiotics were added at the following concentrations: nalidixic acid 4μg/mL, polymyxin B 0.5U/mL, kanamycin 25μg/mL, tetracycline 3μg/mL, streptomycin 25μg/mL. *E. coli* was grown in Luria-Bertani (LB)

media (19) at 37°C. When necessary, antibiotics were added at the following concentrations: kanamycin 25μg/mL, tetracycline 10μg/mL.

Construction of Plasmids and Strains: Chromosomal DNA was isolated from *B. neotomae* using the Puregene DNA Isolation Kit and subsequently used for PCR reactions. All oligonucleotide primers were purchased from Integrated DNA Technologies (IDT) and are designed with a restriction enzyme site at the 5' end to facilitate cloning. These primers were designed based on the *B. abortus* biovar 1 strain 9-941 genome sequence (13). Plasmid isolation was done by the alkaline lysis method (19). Plasmids are listed in Table A.1. Standard methods were used for restriction digests, ligations, and biparental conjugations. Transformations into *E. coli* strains were done by the TSS method (3).

***lacZ* expression fusions:** Expression of target genes was determined using transcriptional fusions between the predicted promoters and the *lacZ* gene. Initially, promoters were PCR amplified from *B. neotomae* genomic DNA and cloned into pUC19. These clones were verified by sequencing. The promoter was then cloned into the broad host range vector pRK415. The *lacZ* cassette was added using the PstI fragment of pKOK-6, which contains the *lacZ* gene in addition to a kanamycin resistance marker. The final construct was conjugated into *B. neotomae*. Four expression fusions were made corresponding to the four oxidase operons. Primer pairs had EcoRI and PstI sites (underlined below) added to facilitate cloning. The *cyo* promoter was amplified using primers cyoZ-UP (5'-CGGAATTCCCATCTGGCGAAGCAAAG-3') and cyoZ-DOWN (5'-CTACTGCAGATCTTGGTCGAGTGATGC-3'). The *cyd* promoter was amplified using primers cydZ-UP (5'-CGGAATTCGCTTCTCACGCAAAGGAC-3') and cydZ-DOWN (5'-GCGCTGCAGAACTGAAATTCCATCACG-3'). The *cox* promoter was amplified using primers pcoxB-F (5'-GCGAATTCGAAAACCATGAAATCTC-3')

and pcoxB-R (5'-CGCCTGCAGGACCGAATCGAAGCTTAC-3'). The *cco* promoter was amplified using primers pccoN-F (5'-CAGAATTCACACCGGATCTCTTATATG-3') and pccoN-R (5'-CGACTGCAGGCACGACATAGAAGGACG-3').

Enzyme assays. β-galactosidase assays were used to determine relative gene expression levels and were performed as previously described (19). Activity was determined based on three independently grown cultures. Samples were taken at various time points throughout growth. Data was averaged and error bars represent one standard deviation.

Pyridine hemochrome assay. This assay is adapted from Peterson (22). Briefly, 500mL cultures were grown overnight and harvested by centrifugation. Pellets were washed with 50mM Phosphate Buffer (pH7.4) and frozen. Thawed whole cells were precipitated with 70% ethanol and the extract discarded. The pellet was dried at 120°C to a constant weight. Three volumes of acetone were added to 200mg of dry cells, centrifuged and the extract discarded. The pellet was resuspended in 5mL chloroform:methanol (2:1) using a hand homogenizer, centrifuged, and the extract discarded. The pellet was resuspended in 5mL acetone, centrifuged and the extract discarded. The pellet was resuspended in a fresh preparation of 3mL 1% HCl in acetone, centrifuged, and the extract was retained. The previous step was repeated and the next extract and pellet retained. The extracts were pooled, concentrated almost to dryness with a Zymark-TurboVap LV evaporator and resuspended in 5mL 0.1N KOH, 20% pyridine. The pellet was resuspended in 1-2mL of 0.1N KOH, 20% pyridine. Pellets and extracts were scanned immediately after adding pyridine. Dithionite-reduced minus air-oxidized absorbance spectra were obtained using a Beckman DU 640 spectrophotometer. Pellets were scanned for the presence of *c*-type heme, while extracts were scanned for the presence of *b*-type heme.

Results and Discussion

Expression of the aerobic oxidases. Expression of the four oxidases was investigated in *B. neotomae* by a series of *lacZ* transcriptional fusions. Despite not having the genome sequence for *B. neotomae*, the overall sequence conservation (>90%) among *Brucella* species allowed us to use the sequence of *B. abortus* for primer design (13). We were successful in amplifying the promoter region for all four of the predicted oxidases from *B. neotomae*. Expression was monitored via β-galactosidase activity under free-living conditions in flask culture under varying oxygen conditions. The *bo*-quinol oxidase, encoded by the *cyo* operon, was most highly expressed and was the predominant oxidase under aerobic growth conditions (Fig. A.1). Under low oxygen and early stationary phase, expression of the *bo*-quinol oxidase decreased. Expression of the *bd*-quinol oxidase, encoded by the *cyd* operon, did not increase under low oxygen as we might expect based on its high oxygen affinity. However, it is expressed

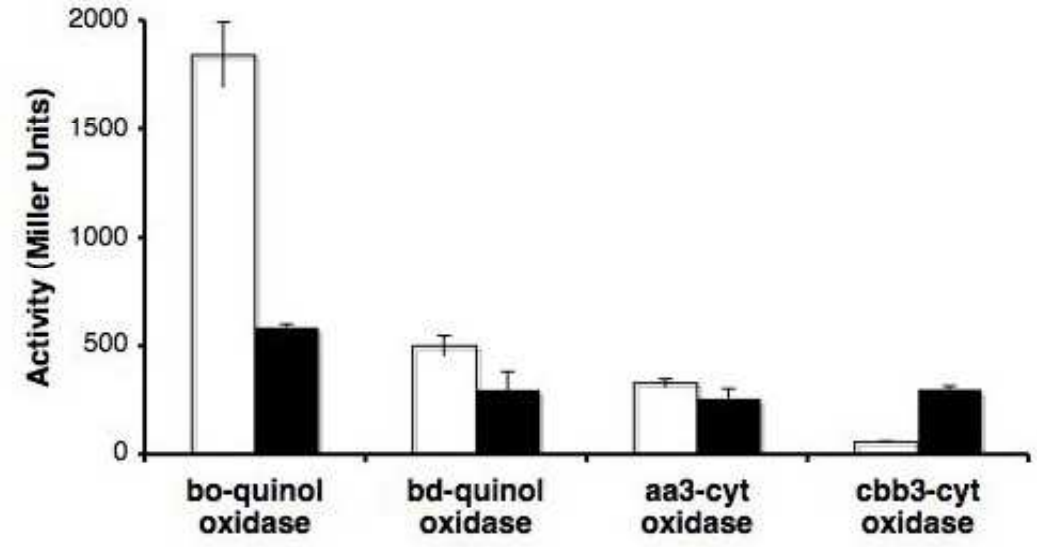

Figure A.1: Expression data for the four oxidases in *B. neotomae*. The *cyo* promoter corresponds to the *bo*-quinol oxidase, the *cyd* promoter to the *bd*-quinol oxidase, the *cox* promoter to the aa_3 oxidase, and the *cco* promoter to the cbb_3 oxidase.

at moderate levels. The non-dynamic expression of the *bd*-quinol oxidase may suggest that low-oxygen is not a signal for increased expression but that host factors, or perhaps stationary phase growth factors, play a role (23). This would be consistent with the importance of the *bd*-quinol oxidase in pathogenesis. The aa_3-cytochrome oxidase, encoded by the *cox* operon, was expressed at relatively moderate levels under high and low oxygen (Fig. A.1). Expression of the high affinity cbb_3 oxidase was nearly undetectable aerobically and increased 5-fold in response to decreasing oxygen. This is consistent with regulation of this oxidase in related bacteria, where typically an Fnr-type regulator activates expression of the oxidase in response to redox status or low oxygen (6). Consistent with this, the predicted promoter of the *ccoNOQP* operon, encoding the cbb_3 oxidase, contains two perfect Fnr-type binding sites. These sites are conserved and present in all sequenced *Brucella*, including *B. neotomae*. In agreement with these results, in *B. suis* expression of the cbb_3 oxidase increases under low oxygen in vitro, and is dependent on an Fnr-type regulator. In contrast, expression of the *bd*-quinol oxidase does not increase in vitro, but does increase in a host cell (14).

Pyridine hemochrome analysis of aerobic cells. The expression pattern of the four oxidases suggests that the quinol oxidases are the primary means of aerobic respiration in *B. neotomae*, consistent with the oxidase negative phenotype. However, we sought to further characterize the aerobic respiratory chain by doing a pyridine-hemochrome analysis, or a heme profile, on aerobically grown cells. The absorption spectra for isolated *b*-type hemes showed the characteristic soret peak at 423nm and the signature 560nm peak (Fig. A.2). In contrast, no *c*-type heme was isolated (Fig. A.3). The observed heme profile is consistent with the *b*-type hemes present in quinol oxidases, and the absence of *c*-type heme that would be present in cytochrome oxidases. This correlates with the oxidase negative phenotype of *B. neotomae*. We then further investigated the oxidase negative phenotype. Based on promoter analysis, the major

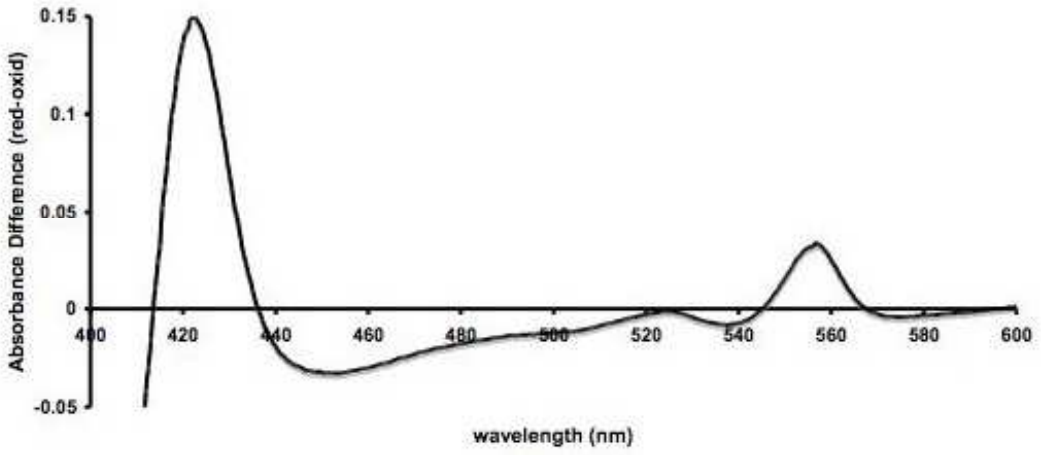

Figure A.2: Reduced minus oxidized scan for the presence of cytochrome *b* in extracts of wild-type *B. neotomae* cells.

operons encoding the four oxidases are present, so in the simplest cases, two things could explain the oxidase negative phenotype. One, the operons encoding the cytochrome *c* oxidases or auxiliary proteins involved in the cytochrome *c* dependent pathway have inactivating mutations. This is what we see in oxidase negative *B. ovis*, which has a frameshift in the *ccoO* gene encoding a subunit of the cbb_3 oxidase, and in *coxB* encoding a subunit of the aa_3 oxidase. Testing this possibility will require sequencing of the *B. neotomae* genome. Or, the second possibility is that the cytochrome *c* maturation (ccm) system is non-functional; this would result in the inability to make the two terminal cytochrome *c* oxidases as well as any intermediate cytochrome *c*-containing electron carriers. The functionality of the ccm system was tested using a heterologous cytochrome *c* from *Rhodobacter sphaeroides* 2.4.3.

Functionality of the ccm system. *R. sphaeroides* 2.4.3 is a non-sulfur purple bacterium that is an α-proteobacterial relative of *Brucella*. *R. sphaeroides* encodes a number of cytochrome *c* proteins, including the gene *cycA*, which encodes cytochrome c_2 (18). This gene was cloned downstream of the *Rhodobacter* ribosomal RNA promoter, *prrnB'*, in a broad host range plasmid. The functionality of the *prrnB* promoter was tested in *B. neotomae* by using a *prrnB::lacZ* fusion plasmid. β-

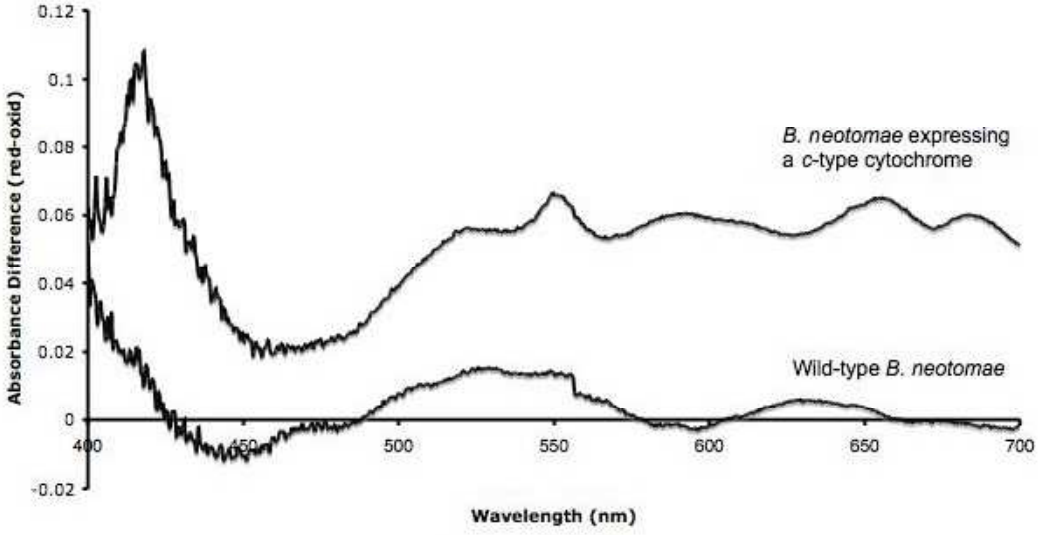

Figure A.3: Reduced minus oxidized scans for cytochrome *c* from extracts of wild-type *B. neotomae* and *B. neotomae* expressing a heterologous *c*-type cytochrome.

galactosidase activity indicated that the promoter was active and constitutive during aerobic growth in vitro (data not shown). The *prrnB::cycA* construct was conjugated into *B. neotomae* and pyridine hemochrome analysis was used to detect *c*-type heme. The presence of the heterologous, constitutively expressed *cycA* resulted in production of detectable *c*-type heme (Fig. A.3) as shown by the soret peak at 417nm and the signature peak at 550nm. This experiment demonstrates a functional ccm system in *B. neotomae*. The presence of a cytochrome *c* electron carrier did not confer an oxidase positive phenotype, suggesting additional components of the cytochrome *c*-dependent respiration pathway are lacking.

It is perhaps significant that the respiratory capacity of some *Brucella* isolates differs. Those species that are oxidase negative also have the most restricted host range. While species like *B.* suis can infect multiple mammals, including humans, *B. ovis* and *B. neotomae* have only been found to cause infection in a single host. *Brucella*, being an intracellular pathogen, is in the process of genome reduction shaped by host selective pressures (25). It is possible that the cytochrome oxidases are

not necessary for the intracellular lifestyle of *B. neotomae* and so have been lost. However, it is possible there is some selective pressure for retention of the ccm system. Research in other pathogens suggests the ccm system may play a role in iron scavenging and siderophore production (4). *Brucella* species are known to produce siderophores and there is a clear link between successful iron acquisition and survival in the intracellular state (2, 12). Or, cytochrome *c* may be required for an unidentified virulence factor not related to respiration. In the other oxidase negative species, *B. ovis*, the cytochrome oxidases are inactivated by mutations, however, the ccm system appears to be intact. Future research will determine if the ccm system is playing a role in pathogenesis by functioning outside of its traditional role.

Conclusions

Here we have shown the trend in oxidase expression for free-living *B. neotomae*. The quinol oxidases are the primary oxidases, with the *bo* quinol oxidase being highly expressed during aerobic growth. Even though *B. neotomae* does not seem to utilize a bc_1-dependent aerobic electron transport chain, it has retained a functional ccm system. This was evidenced by the production of a heterologous cytochrome *c*. After the completion of this study a draft genome of *B. neotomae* was released. In agreement with our study, the cytochrome oxidases are disrupted by frameshift mutations in *ccoN* and *coxB*. Meanwhile, the two *ccm* operons are intact.

REFERENCES

1. **Baek, S., G. Rajashekara, G. Splitter, and J. Shapleigh.** 2004. Denitrification genes regulate *Brucella* virulence in mice. J. Bacteriol. **186:**6025-31.

2. **Bellaire, B., P. Elzer, C. Baldwin, and R. Roop.** 2003. Production of the siderophore 2,3-dihydroxybenzoic acid is required for wild-type growth of *Brucella abortus* in the presence of erythritol under low-iron conditions in vitro. Infect. Immun. **71:**2927-832.

3. **Chung, C. T., S. L. Niemela, and R. H. Miller.** 1989. One-step preparation of competent *Escherichia coli*: transformation and storage of bacterial cells in the same solution. Proc. Natl. Acad. Sci. U. S. A. **86:**2172-2175.

4. **Cianciotto, N., P. Cornelis, and C. Baysse.** 2005. Impact of the bacterial type I cytochrome c maturation system on different biological processes. Mol. Microbiol. **56:**1408-15.

5. **Corbel, M. J.** 1977. Isolation and partial characterization of a phage receptor from "*Brucella neotomae*" 5K33. Ann. Sclavo. **19:**131-42.

6. **Cosseau, C. and J. Batut.** 2004. Genomics of the ccoNOQP-encoded cbb3 oxidase complex in bacteria. Arch. Microbiol. **181:**89-96.

7. **Das, A., R. Silaghi-Dumitrescu, L. G. Ljungdahl, and D. M. Kurtz.** 2005. Cytochrome bd Oxidase, Oxidative Stress, and Dioxygen Tolerance of the Strictly Anaerobic Bacterium *Moorella thermoacetica*. J. Bacteriol. **187:**2020-9.

8. **DelVecchio, V., V. Kapatral, R. Redkar, G. Patra, C. Mujer, T. Los, N. Ivanova, I. Anderson, A. Bhattacharyya, A. Lykidis, G. Reznik, L. Jablonski, N. Larsen, M. D'Souza, A. Bernal, M. Mazur, E. Goltsman, E. Selkov, P. Elzer, S. Hagius, D. O'Callaghan, J. Letesson, R. Haselkorn, N. Kyrpides, and R.**

Overbeek. 2002. The genome sequence of the facultative intracellular pathogen *Brucella melitensis*. Proc. Natl. Acad. Sci. USA **99:**443-8.

9. **Edwards, S. E., C. S. Loder, G. Wu, H. Corker, B. W. Bainbridge, S. Hill, and R. K. Poole.** 2000. Mutation of cytochrome bd quinol oxidase results in reduced stationary phase survival, iron deprivation, metal toxicity and oxidative stress in *Azotobacter vinelandii*. FEMS Microbiol. Lett. **185:**71-7.

10. **Endley, S., D. McMurray, and T. A. Ficht.** 2001. Interruption of the cydB Locus in *Brucella abortus* attenuates intracellular survival and virulence in the mouse model of infection. J. Bacteriol. **183:**2454-62.

11. **Glynn, M. K. and T. V. Lynn.** 2008. Brucellosis. J. Am. Vet. Med. Assoc. **233:**900-8.

12. **Gonzalez Carrero, M., F. Sangari, J. Aguero, and J. Garcia Lobo.** 2002. *Brucella abortus* strain 2308 produces brucebactin, a highly efficient catecholic siderophore. Microbiology (Reading, Engl.) **148:**353-60.

13. **Halling, S., B. Peterson-Burch, B. Bricker, R. Zuerner, Z. Qing, L. Li, V. Kapur, D. Alt, and S. Olsen.** 2005. Completion of the genome sequence of Brucella abortus and comparison to the highly similar genomes of *Brucella melitensis* and *Brucella suis*. J. Bacteriol. **187:**2715-26.

14. **Jimenez de Bagues, M., S. Loisel-Meyer, J. Liautard, and V. Jubier-Maurin.** 2006. Different roles of the two high-oxygen-affinity terminal oxidases of *Brucella suis*: Cytochrome c oxidase, but not ubiquinol oxidase, is required for persistence in mice. Infect. Immun. **75:**531-5.

15. **Keen, N. T., S. Tamaki, D. Kobayashi, and D. Trollinger.** 1988. Improved broad-host-range plasmids for DNA cloning in gram-negative bacteria. Gene **70:**191-197.

16. **Ko, J. and G. A. Splitter.** 2000. Residual virulence of *Brucella abortus* in the absence of the cytochrome bc(1)complex in a murine model in vitro and in vivo. Microb. Pathog. **29:**191-200.

17. **Kokotek, W. and W. Lotz.** 1989. Construction of a lacZ-kanamycin-resistance cassette, useful for site-directed mutagenesis and as a promoter probe. Gene **84:**467-471.

18. **Laratta, W., M. Nanaszko, and J. Shapleigh.** 2006. Electron transfer to nitrite reductase of *Rhodobacter sphaeroides* 2.4.3: examination of cytochromes c2 and cY. Microbiology (Reading, Engl.) **152:**1479-88.

19. **Maniatis, T., E. F. Fritsch, and J. Sambrook.** 1982. Molecular Cloning: a laboratory manual. Cold Spring Harbor Laboratory Press, Cold Spring Harbor, NY.

20. **Mason, M. G., M. Shepherd, P. Nicholls, P. S. Dobbin, K. S. Dodsworth, R. K. Poole, and C. E. Cooper.** 2009. Cytochrome bd confers nitric oxide resistance to *Escherichia coli*. Nat. Chem. Biol. **5:**94-6.

21. **Paulsen, I. T., R. Seshadri, K. E. Nelson, J. A. Eisen, J. F. Heidelberg, T. D. Read, R. J. Dodson, L. Umayam, L. M. Brinkac, M. J. Beanan, S. C. Daugherty, R. T. Deboy, A. S. Durkin, J. F. Kolonay, R. Madupu, W. C. Nelson, B. Ayodeji, M. Kraul, J. Shetty, J. Malek, S. Van Aken, S. Riedmuller, H. Tettelin, S. R. Gill, O. White, S. L. Salzberg, D. L. Hoover, L. E. Lindler, S. M. Halling, S. M. Boyle, and C. M. Fraser.** 2002. The *Brucella suis* genome reveals fundamental similarities between animal and plant pathogens and symbionts. Proc. Natl. Acad. Sci. USA **99:**13148-53.

22. **Peterson, J. A.** 1970. Cytochrome content of two pseudomonads containing mixed-function oxidase systems. J. Bacteriol. **103:**714-21.

23. **Roop, R. M., J. M. Gee, G. T. Robertson, J. M. Richardson, W. L. Ng, and M. E. Winkler.** 2003. *Brucella* stationary-phase gene expression and virulence. Annu. Rev. Microbiol. **57:**57-76.

24. **Roop, R., B. Bellaire, M. Valderas, and J. Cardelli.** 2004. Adaptation of the *Brucellae* to their intracellular niche. Mol. Microbiol. **52:**621-30.

25. **Sallstrom, B. and S. G. Andersson.** 2005. Genome reduction in the alpha-Proteobacteria. Curr. Opin. Microbiol. **8:**579-85.

26. **Whatmore, A., L. Perrett, and A. MacMillan.** 2007. Characterisation of the genetic diversity of *Brucella* by multilocus sequencing. BMC Microbiol. **7:**34.

27. **Yanisch-Perron, C., J. Vieira, and J. Messing.** 1985. Improved M13 phage cloning vectors and host strains: nucleotide sequences of the M13mp18 and pUC19 vectors. Gene **33:**103-19.